THE EFFECTS OF SELENIUM ON STZ-INDUCED DIABETIC

RAT KIDNEY PLASMA MEMBRANE

A THESIS SUBMITTED TO THE
GRADUATE SCHOOL OF NATURAL AND APPLIED SCIENCES
OF
MIDDLE EAST TECHNICAL UNIVERSITY

BY

RAFIG GURBANOV

IN PARTIAL FULFILLMENT OF THE REQUIREMENTS
FOR
THE DEGREE OF MASTER OF SCIENCE
IN
BIOCHEMISTRY

JANUARY 2010

Approval of the thesis:

THE EFFECTS OF SELENIUM ON STZ-INDUCED DIABETIC
KIDNEY PLASMA MEMBRANE

submitted by **RAFIG GURBANOV** in partial fulfillment of the requirements for the degree of **Master of Science in Biochemistry Department**, **Middle East Technical University** by,

Prof. Dr. Canan Özgen   _____
Dean, Graduate School of **Natural and Applied Sciences**

Prof. Dr. Mesude Işcan   _____
Head of Department, **Biochemistry**

Prof. Dr. Feride Severcan   _____
Supervisor, **Biology Dept., METU**

Assoc.Prof. Dr. Sreeparna Banerjee   _____
Co-Supervisor, **Biology Dept., METU**

Examining Committee Members

Prof. Dr. Faruk Bozoğlu   _____
Food Engineering Dept., METU

Prof. Dr. Feride Severcan   _____
Biology Dept., METU

Prof. Dr. Orhan Adalı   _____
Biology Dept., METU

Assoc. Prof. Dr. Nursen Çoruh   _____
Chemistry Dept., METU

Dr. Sevgi Türker   _____
Biology Dept., Kocaeli University

Date: <u>14.01.2010</u>

I hereby declare that all information in this document has been obtained and presented in accordance with academic rules and ethical conduct. I also declare that, as required by these rules and conduct, I have fully cited and referenced all material and results that are not original to this work.

Name, Last name: Rafig Gurbanov

Signature:

ABSTRACT

THE EFFECTS OF SELENIUM ON STZ-INDUCED DIABETIC RAT KIDNEY PLASMA MEMBRANE

Gurbanov, Rafig

M.Sc., Department of Biochemistry

Supervisor: Prof. Dr. Feride Severcan

Co Supervisor: Assoc. Prof. Dr. Sreeparna Banerjee

January 2010, 129 Pages

The kidney is one of the most affected organs of body from diabetes. Diabetic kidney disease is a complication of diabetes seen in 30-40% of diabetic person.

The aim of this work is to contribute the useful information in the therapy of diabetes. It is very important to know the role of antioxidants at the molecular level during diabetes. The protecting role of antioxidants against lipid peroxidation, the effect of cellular antioxidant enzyme systems, understanding the changes of membrane fluidity, lipid order and protein structure which are resulted from antioxidant treatment, determining the effective therapeutic dose with the help of biochemical methods are very important in order to understand the effect of antioxidants at molecular level.

In this thesis work, the Attenuated Total Reflectance Fourier Transform Infrared Spectroscopy (ATR-FTIR) was used in order to study the diabetic kidney disease at

the molecular level, which is encountered as a complication of diabetes. Furthermore, the protecting and possible therapeutic role of selenium in the course of diabetic kidney disease was investigated.

To conclude, the kidney plasma membranes were severely deteriorated due to diabetes with respect to its lipid, protein and carbohydrate structure and content, which were corrected after selenium treatment. The diabetes causes diminishment of whole membrane fluidity, which was normalized with the selenium administration. This is the first study demonstrating the effect of diabetes on kidney plasma membrane and the effect of selenium on stz-induced diabetic kidney plasma membranes using spectroscopic tools. The study revealed serious therapeutic and preventing capacities of selenium on diabetic kidney plasma membranes which needs confirmation of future researches. Furthermore, the dosage of selenium given to diabetics should be investigated in detail and proved with biochemical and clinical data.

Key Words: Diabetic Nephropathy, Selenium, ATR-FTIR Spectroscopy, Plasma membranes

ÖZ

SELENYUMUN STREPTOZOTOSİN İLE DIYABET OLUŞTURULAN SIÇAN BÖBREK HÜCRE ZARI ÜZERINDEKİ ETKİLERİNİN İNCELENMESİ

Gurbanov, Rafig

Yüksek Lisans, Biyokimya Bölümü
Tez Yöneticisi: Prof. Dr. Feride Severcan
Ortak Tez Yöneticisi: Yrd. Doç. Dr. Sreeparna Banerjee

Ocak 2010, 129 sayfa

Vücutta diyabet hastalığından etkilenen dokular arasında böbrek dokusu da bulunmaktadır. Diyabetik böbrek hastalığı 30-40% diyabet hastalarında görülen bir diyabet komplikasyonudur.

Bu çalışmanın amacı diyabetin komplikasyonlarından biri olarak tanımlanan diyabetik böbrek hastalığının moleküler düzeyde araştırılması, antioksidanların diyabetik böbrek hastalığında tedavi edici rolünü saptamak, özellikle böbrek hücre zarlarındakı yapısal değişikleri moleküler düzeyde incelemek ve sıçanlara selenyum vererek selenyumun diyabetik böbrek dokularındakı iyileştirici rolünü araştırmaktadır.

Bu tez çalışmasında ATR-FTIR specktoskopisi kullanarak, diyabetin böbrek üzerindeki etkileri ortaya çıkarılmaya çalışılmışdır. Ayrıca, selenyumun diyabetin tedavisinde koruyucu ve tedaviedici rolu incelenmiştir.

Sonuc olarak, diyabetin böbrek hücre zarlarında üzerinde önemli değişimlere neden olduğu gözlemlenmiştir. Diyabet, hücre membranın lipit, protein ve karbonhidratının yapı ve miktarlarında değişimlerlere yol açmıştır. Selenyum tedavisi sonucunda bu değişimlerin giderildigi gözlemlenmiştir. Diyabet sonucunda azalmış membrane akışkanlığını selenium uygulanması sonucunda giderilmiştir. Bu ilkin çalışma, diyabetin böbrek hücre zari üzerindeki ve selenyumun diyabetik böbrek hücre zari üzerindeki etkilerini, spektroskopik araçlar kullanılarak ortaya çıkarmıştır. Ayrıca, bu çalışma sonucunda selenyumun diyabetik böbrek hücre zarı üzerinde tedavi edici ve koruyucu özellikleri saptanmıştır. Bu çalışmanı kanıtlamak için gelecek araştırmalara gerek duyulmaktadır. Ayrıca selenyumun diyabetik hastalara uygulana bilecek dozları detaylı şekilde araştırılmalı ve klinik, biyokimyasal verilerle desteklenmelidir.

Anahtar kelimeler: Diyabetik nefropati, Selenyum ATR-FTIR spektroskopisi, Hücre zarı

To My Father,

ACKNOWLEDGEMENTS

TABLE OF CONTENTS

LIST OF FIGURES

FIGURES

LIST OF TABLES

TABLES

CHAPTER 1

INTRODUCTION

In this study the renal brush-border plasma membranes, the effect of streptozotocin induced diabetes on kidney plasma membranes and possible healing effect of trace element selenium (antioxidant) on diabetic kidney plasma membranes were reported via ATR-FTIR spectroscopic techniques. In this chapter a preliminary detailed survey including structure and function of kidneys, diabetes mellitus, the plasma membranes, structural and functional properties of selenium in health and disease and basis of infrared spectroscopy have been conducted.

1.1 Kidneys

1.1.1 External Anatomy of the kidneys

Anatomically kidney is a bean-shaped, reddish organ, 10-12 cm long, 5-7 cm wide, 3 cm thick and have a mass of 135-150 gr. Kidneys are located between the posterior wall of the abdomen and the peritoneum. They are called retroperitoneal organs because they are positioned posterior to the peritoneum of the abdominal cavity (retro means behind). Kidneys proximal and distal sides are commonly at the levels of the 12-th thoracic and 3-rd lumbar vertebrae, respectively. The right kidney is typically located 1-2 cm lower than the left kidney. By the help of the surrounding renal fascia (connective tissue) and renal fat, kidneys are held in position. The lateral side of kidney is convex; however its media surface is concave in shape. The resulting medial depression forms a chamber which is called the renal sinus. The hilum is an entrance of renal sinus. Through the hilum, blood vessels, lymphatic vessels and nerves enter and exit. The ureter also leaves the kidney through the hilum. Kidneys are surrounded by three layers of tissue. The renal capsule is a

deepest layer. It constitutes, smooth, transparent sheet of dense irregular connective tissue. The function of the renal capsule is to protect the kidney against injury and to maintain the shape of organ. The fat tissue surrounding the renal capsule is a middle layer, called adipose capsule. It serves to hold the kidney tightly in place within the cavity of abdomen. The thin outer layer is composed of dense, irregular connective tissue. This layer is called the renal fascia (Jenkins et al., 2007; Hole et al., 1993).

1.1.2   Internal Anatomy of the kidneys

There are two different regions of the kidneys. The red superficial region is called the renal cortex and a deep, reddish-brown region is called the renal medulla. The renal medulla is composed of conical masses of tissue called renal pyramids. The wider end of pyramid faces the renal cortex, the narrow end (apex) points toward the renal hilum. The tissue of the renal cortex dips into the medulla between adjacent renal pyramids, forming renal columns. The renal pyramid, its superficial reg, one of renal cortex and one-half of each adjacent renal column forms renal lobe. Nephrons are the microscopic structures, located inside the renal pyramids and the renal cortex. They are called functional units of kidney and their number is about 1 million. Urine is formed by the nephrons and drains into large papillary ducts. These ducts drain into cuplike units called minor and major calyces (calyx means cup). Each kidney has 8 to18 minor calyces and 2 to 3 major calyces. Urine drains from minor calyces into major calyces and from the major calyces drains into a large cavity called the renal pelvis. From the renal pelvis it infiltrate through the ureter to the urinary bladder. The renal sinus is a cavity, into which the hilum expands. The renal sinus contains the calyces, the branches of the renal bold vessels and nerves and part of the renal pelvis. The positions of these structures are stabilized by the adipose tissue (Jenkins et al., 2007; Hole et al., 1993).
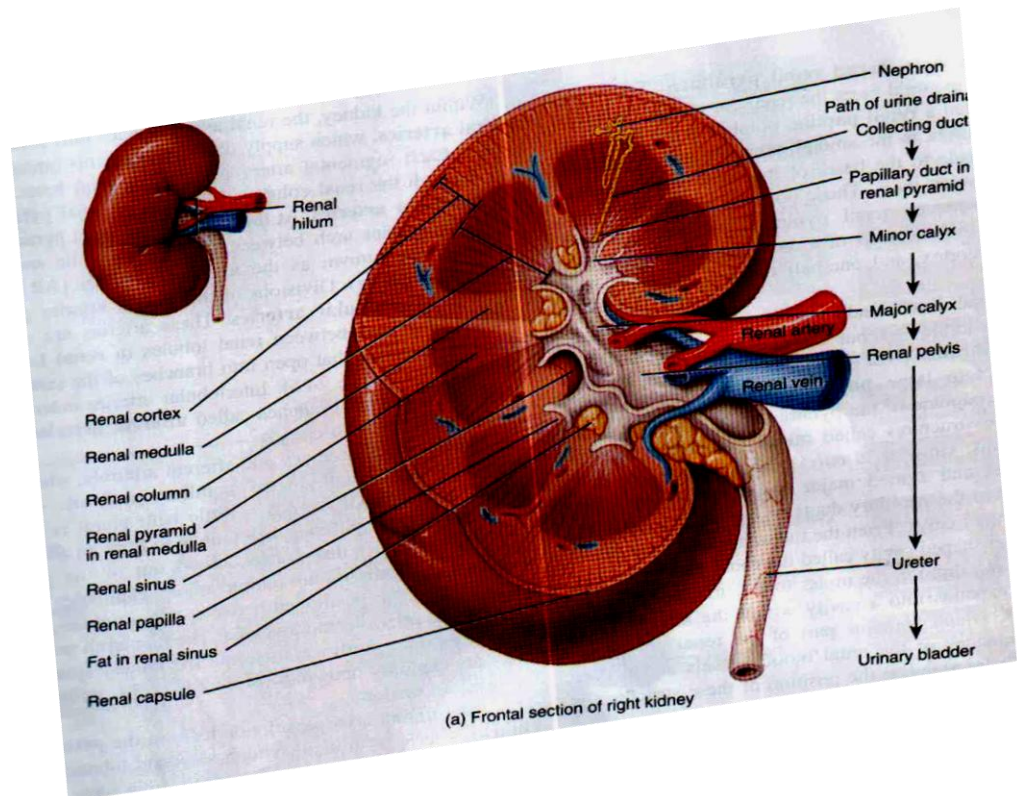
Figure 1. Internal and External Anatomy of Kidneys (Hole et al., 1993).

1.1.3   Blood supply of kidney

The renal artery divides into several segmental arteries within the kidney. Branches of these segmental arteries pass through the renal columns as the interlobar arteries. At the bases of renal pyramids these interlobar arteries give off branches. These branches are called arcuate arteries. Interlobar arteries also enter the renal cortex and divides into branches called afferent arterioles. Nephrons supplied by these afferent arterioles. Within the nephron these arteriole subdivides into a ball-shaped capillary network called the glomerulus (little ball). These capillaries are then combining to form an efferent arteriole that carries out the glomerular blood. The division of the efferent arterioles forms the peritubular capillaries. In the cortex these capillaries surround tubular part of the nephron. Capillaries extending from efferent arterioles

3

are called vasa recta. In the medulla, vasa recta supplies tubular part of the nephron. Peritubular capillaries open to the interlobar veins, and then the blood drains from the arcuate veins to the interlobar veins. Through the kidney vein, the venous blood leaves the kidney, draining into the interior vena cava (Jenkins et al., 2007; Hole et al., 1993).
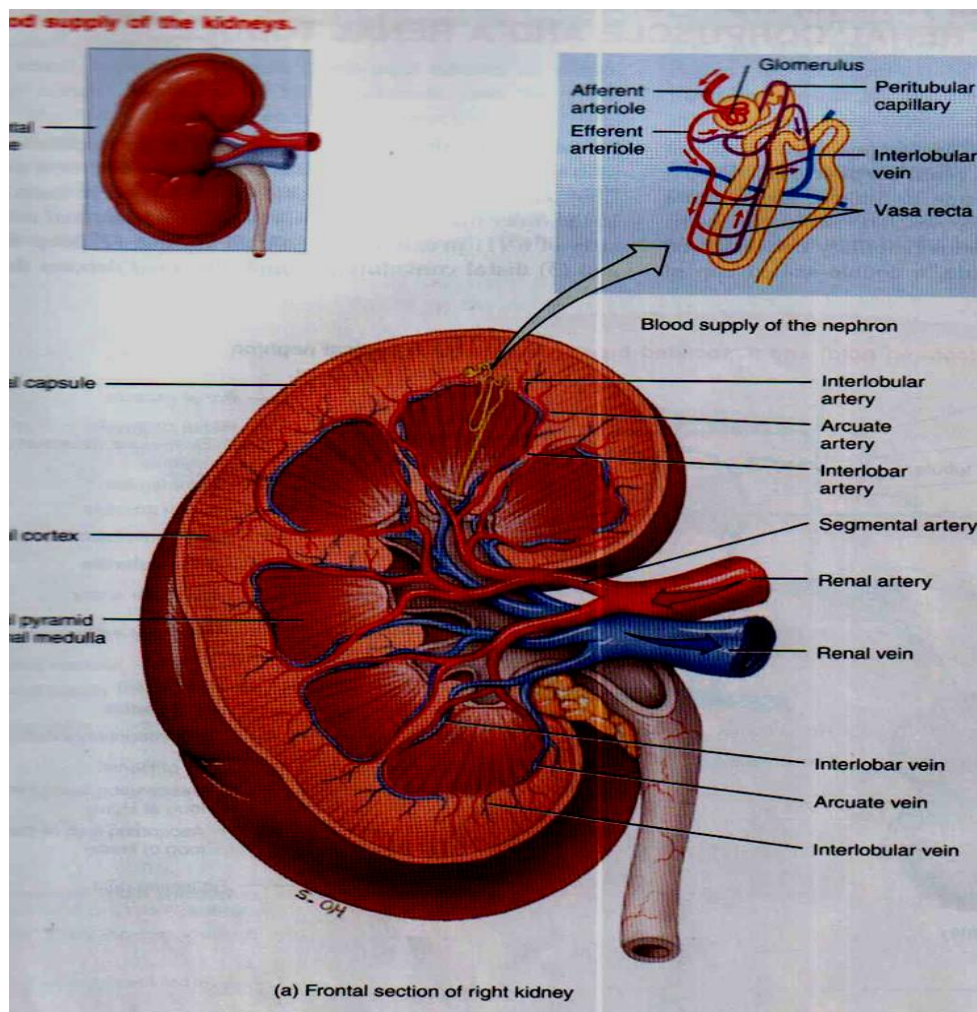
Figure 2. Blood supply of Whole kidney (Hole et. al, 1993).

1.1.4 Nephrons

Nephrons consist of a renal corpuscle and a renal tubule. Blood plasma is filtered in the renal corpuscle, then filtered fluid pass into the renal tubule. The renal corpuscle has two units: glomerulus and glomerular Bowman's capsule. Bowman's capsule is composed of the tissue surrounding the glomerular capillaries. The renal tubule has three parts. The filtered plasma passes through these parts. They are proximal convoluted tubule, distal convoluted tubule and loop of Henle. Convoluted means the tubule is firmly coiled. The convoluted tubules and renal corpuscle located within the cortex; however Henle loop located within the medulla. Proximal and Distal convoluted tubules are connected through the Henle loop.

The first part of the Henle loop starts from the cortex and continues downward to the medulla. In the medulla it is called the descending limb of the Henle loop. Then it turns and returns to the cortex. This part is called ascending limb of the Henle loop. Approximately, 80-85 % of the nephrons are located in the cortex. Remaining 15-20 % are located near the medulla and called juxtamedullary nephrons (juxta means near). Distal convoluted tubules merge into the cortex forming a collecting duct. These ducts then combine to form papillary ducts in the medulla. These papillary ducts open to the minor calyx (Jenkins et al., 2007; Hole et al., 1993).

A thin layer of epithelial cells forms the wall of the glomerular capsule, renal tubule and ducts. Nevertheless, each part has their own histological features. There are two layers of glomerular capsule. The visceral layer composed of podocytes. Projections of these cells form inner wall of Bowman's capsule. The parietal layer composed of simple squamaous epithelium and forms an outer wall of the glomerular capsule. Filtered plasma enters the space between these layers. Simple cuboid epithelial cells with microvillus serve to increase surface area for reabsorption. Ascending limb of Henle loop composed of columnar epithelium. The final part of this ascending limb of Henle loop is rich of the columnar cells. These cells are called macula densa. Alongside of macula densa the wall of the efferent arteriole contains modified smooth muscle fiber called juxtaglomerular cells. Together with macula densa they

5

form the juxtamedullary apparatus. Juxtamedullary apparatus regulates the blood pressure within the kidney. There are two different types of cells that form distal convoluted tubules. Most of them are principal cells, which have receptors for antidiuretic hormone and aldesterone. Small number of intercalated cells regulates the blood homeostasis.
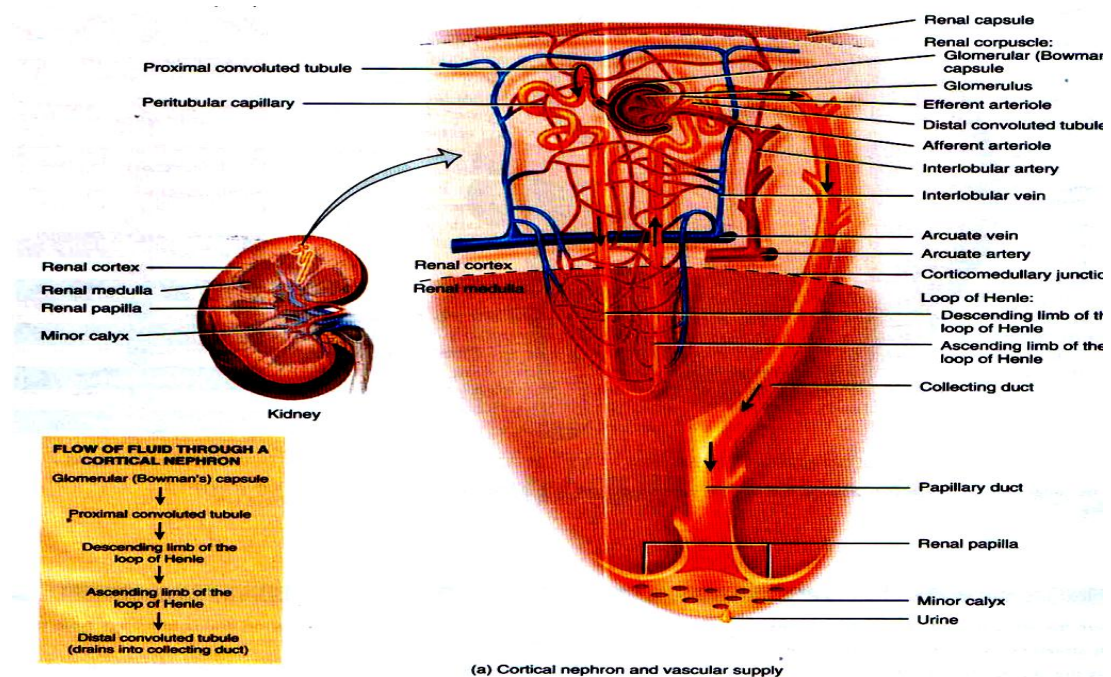
Figure 3. Structure of nephron (Hole et al., 1993)

Nephrons serve to regulate water and electrolyte balance of body and to remove waste products from the organism. Urine is an end product of nephrons work, contains excess electrolytes, water and wastes. In order to produce urine nephrons and collecting ducts perform the following three basic steps. In the first step, fluid moves across the capillaries of glomerulus into the glomerular capsule and then into the renal tubule. This process is called glomerular filtration. As the fluid moves

through the renal tubule and collecting duct, 99% is reabsorbed by the tubule and duct cells. Through the vasa recta and peritubular capillaries the water and solutes return to the blood stream, in order to recycle the useful substances. This process is called tubular reabsorption. As the fluid cross the renal tubule and the collecting duct waste material such as drugs, excess ions are secreted into the fluid, in order to be removed from the body. Solutes in the fluid drain into the renal pelvis and remain in the urine until excretion (Jenkins et al., 2007; Hole et al., 1993).

Endothelial cells of glomerular capillaries and the podocytes surrounding the capillaries form a leaky filter. This filter is called glomerular filtration membrane. The function of filtration membrane is to catch blood cells and plasma proteins. The size of these proteins and cells do not permit them to cross the membrane so they remain in the blood. Furthermore, filtration membrane allows removal of water and small solutes from the blood into the capsular space (Jenkins et al., 2007; Hole et al., 1993).
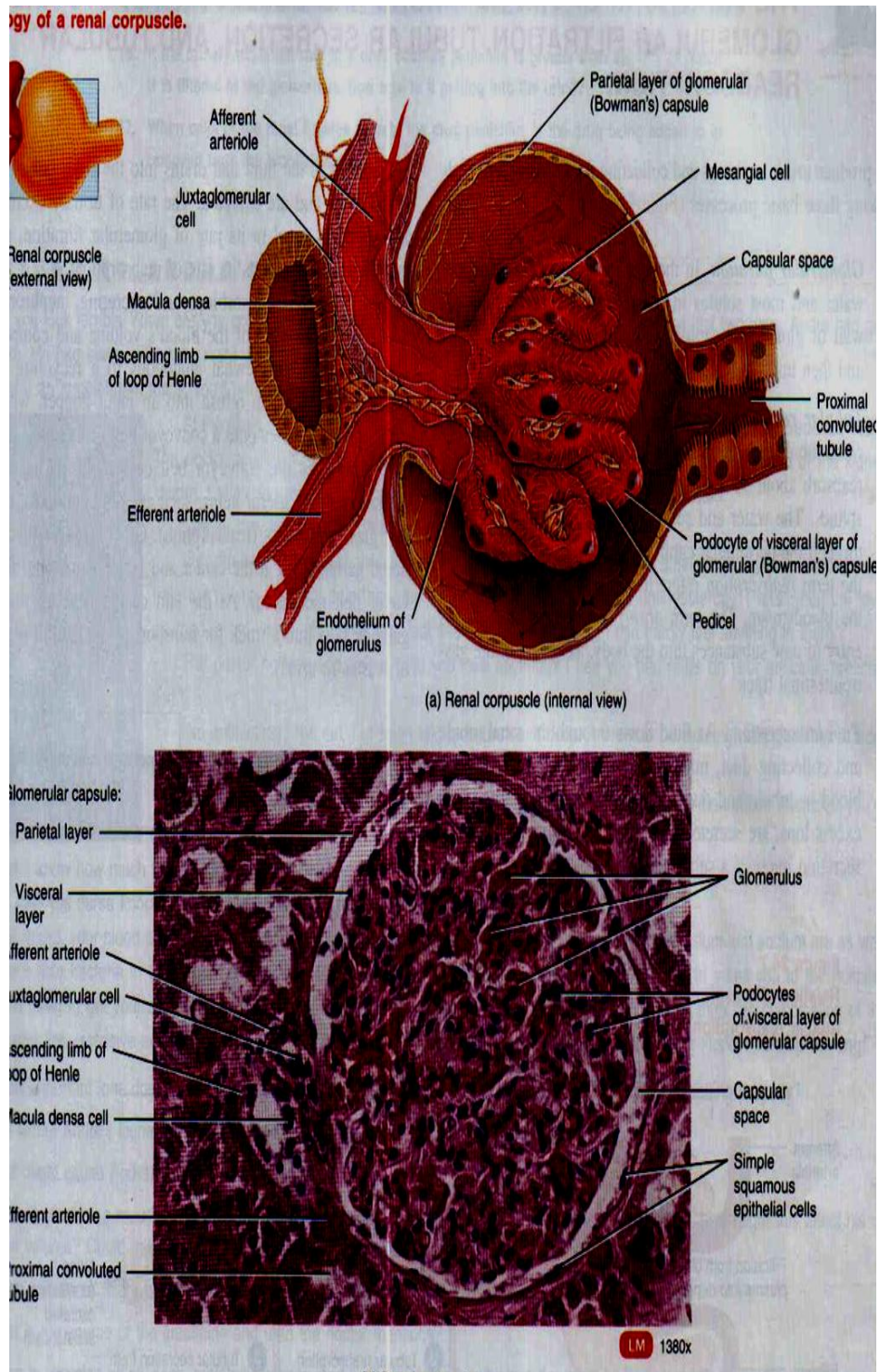
Figure 4. Renal glomerulus (Hole et al. , 1993)

1.2 The Plasma Membranes

The plasma membrane interacts between the cell and its external environment; in addition, it acts on intracellular metabolism. Facilitated diffusion, active transport, endocytosis and exocytosis performed by plasma membrane. It is also a passive diffusion barrier to charged and large molecules. Furthermore this membrane is participated in events that transport a cell from unsafe environment or to a more wealth climate called chemotaxis and locomotion. On a more complex level, for the formation and maintenance of multicellular organisms cells must counteract with other cells. The secretion and reception of hormones, conduction of nerve impulses and direct cellular interactions such as adhesion and contact inhibition all works with the mediation of plasma membrane (Joseph et al., 1973). Finally, the assembly of multi-protein complexes, signal transduction, wastes and metabolite exchange are the main functions of plasma membrane. For this reason, the two leaflets of the membrane bilayer each have their specific lipid composition (Bevers et al., 1999). It has been encountered that membrane microdomains enriched in glycosphingolipids and cholesterol and containing glycosylphosphatidylinositol (GPI) anchored proteins is a lateral structural components of the plasma membrane (Simons and Ikonen, 1997).
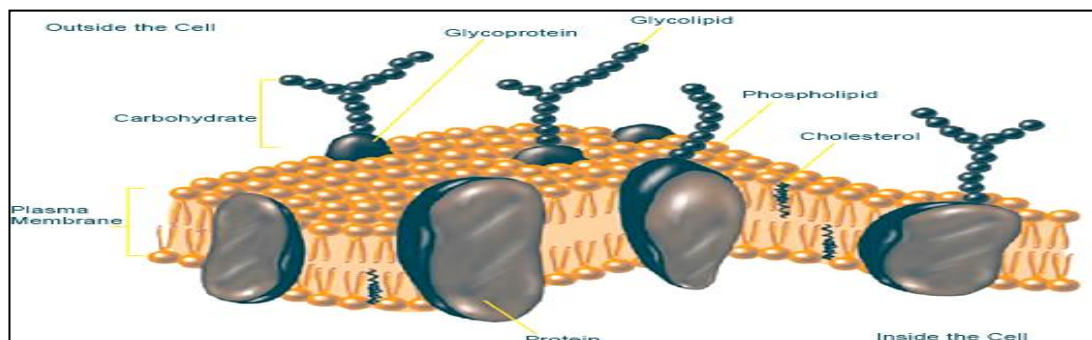
Figure 5. The Schematic view of Plasma Membrane (From theWebSite of National Institutes of Health, Bethesda, MD Revised 2006).

9

1.2.1 The Plasma Membranes of Kidney

Proximal tubule cells, a specialized and relatively homogeneous type of renal epithelial cell found in the first part of the nephron in the kidney. It is the most abundant cell type existed in the renal cortex and reabsorbs the small molecules filtered at the glomerulus. Transcellular transport in renal tubules involves the movements of solutes between three compartments: luminal, intracellular and peritubular. They are separated by two barriers: the apical (luminal, brush border) and the basolateral (contra luminal, per tubular, serosal) plasma membranes (Murer et al., 1986). Like all epithelial cells, proximal cells are polarized, such that their apical (brush-bordered) and basolateral membranes are separated by tight junctions and have different structures and corresponding transport functions (Martin et al., 2000).

The functional polarity of the cell is required for vectorial transport of solutes so the transport properties of the apical and the basolateral membrane must be different. Morphology, enzyme content, protein, lipid, and carbohydrate composition hormone receptors and transport properties of these two membranes are distinct in almost every respect and these distinctions are used in the procedures for membrane separation.

Differences in enzyme activities provide the criteria for identification of the separated membranes. In addition, differences in lipid to protein ratios and carbohydrate contents result in distinct physical properties of the two membranes. The physical properties such as density and surface charge, license for their separation by density gradient centrifugation, phase partitioning, differential precipitation and electrophoresis (Heine Murer and Piotr Gmaj, 1986; Aronson, 1981; Kinne et al., 1980).

1.2.2   The Brush-Border Plasma Membrane

The Brush-Border Plasma Membrane means the part of plasma membrane that close to lumen of the kidneys. So this part of plasma membrane plays an important role in the filtering and reabsorption processes in the kidney. The apical membrane has a brush border, which increases the surface area available for reabsorption of the glomerular filtrate. Channel and transport proteins located at the apical membrane (brush border membrane, BBM), performs reabsorbtion of solutes present in this filtrate (tubular fluid). Many of these transport proteins are coupled indirectly to the gradient for Na+ due to the low intracellular Na+ concentration maintained by the 'sodium pump'(Na+, K+ -ATPase) located in basolateral membrane (BLM). The other transport proteins are also expressed at the BLM that transfer solutes from inside the cell to the interstitial space and peritubular capillary blood (Martin et al., 2000).

1.3 Diabetes Mellitus

Diabetes Mellitus is a disease of metabolism affecting the great amount of world's population, accompanied with long-term hyperglycemic condition, in which fat, protein and carbohydrate metabolism is severely affected by deficient insulin secretion or function. General signs of diabetes are loss of weight, frequent thirst, polyuria, polyphagia and impairment of eyes. Ketoasetosis also may develop as a result of accummulation of ketone bodies in severe forms of disease leading to glycemic come and even to death. Chronic diabetes open way to the complications of illness by damaging perivascular and cardiovascular system. These include, retinopathy, nephropathy, neuropathy and cardivascular disorders (Albert and Zimmet, 1998).

There are two general forms of Diabetes. First one, is insulin dependent diabetes mellitus (IDDM) called Type I, results from autoimmune degradation of ß cells of pancrease producing insulin. Second one, is non-insulin dependent DM (NIDDM) called Type II. In this form insulin concentration in blood almost cannot be detected or detected in very low amounts. In Type 2 insulin secretion or function is affected by loss of cell responces to insulin secretion (Stapleton et al. , 2000).

1.3.1   Type 1 Diabetes Mellitus (IDDM)

In Type I DM immune system cells attack to the pancreatic ß cells producing insulin, because the body recognizes islet cells as antigens (Bardsley et al. , 2004). CD+4, CD+8 T cells, B cells, macrophages and cytokines accumulate in the area of lesion but they are not destructive (Pietropaolo et al. , 2007; Lee et al., 1988; Kawasaki et al., 1999; Pearl-Yafe et al., 2007). The processes how autoantibodies are synthesized against islet cells are well studied but the onset of trigger is still unknown. About 90 % of islet cells should be destroyed in order to see clinical picture of the diabetes (Kawasaki et al., 1999). During the pathogenesis of Type I diabetes many autoimmune processes involved. Concentration of autoantigens and autoantibodies increases as a disease progresses. Insulin, islet-cell antigen-2 and glutamic acid decarboxylase (GAD) are well investigated autoantigens triggering immune response (Atkinson et al., 2001). Studies showed that insulin is a first autoantigen found in the early diabetes, later as a disease progresses other antigens also exist in the laceration area (Hutton et al., 2007).

Only two chromosomal regions are found to be related to autoimmune diabetes. They are human leukocyte antigen (HLA) region on chromosome 6p21 and the insulin gene region on chromosome 11p15 (Nepom et al., 1995). Genetic factors seem to be more important to cause islet autoimmunity than environmental factors (Redondo et al., 2004). Environmental factors also play a role as a possible trigger of autoimmune diabetes (Akerblom et al., 1998). Viruses are the most potent environmental triggers for Type I diabetes, because of their capability to produce severe immune response when entered to the body.

Potential viral triggers are adenoviruses, coxsachkie B virus, enteroviruses, retroviruses, cytomegaloviruses and etc (Yoon et al. , 1991 ; Varela-Calvino et al. , 2003; Green et al. , 2004 ; Barbu et al. , 2005 ; Chen et al. , 2005; Jun et al. , 2002). Viruses can change host cell environment in such a way that, immune cells recognize them as a potent antigens and destruct them. Furthermore, viruses produce proteins similar to host proteins. Consequently, the host cell proteins can be encountered as viral proteins by antibodies (Akerbhlom et al., 1998; Jun et al., 2002).

1.3.2 Type 2 Diabetes Mellitus (NIDDM)

Most common form of diabetes mellitus is Type II. It is a multifactorial metabolic illness characterized by the elevation of blood glucose concentrations. There is an interaction between defects of insulin secretion and peripheral insulin resistance. Due to this interaction insulin deficiency and impairment of glucose tolerance occurs. Typically type II diabetes patients have high insulin levels which do not completely compensate for insulin resistance. Later, gradually developing ß cell dysfunction causes disruption of this compensation that leads to deficiency of insulin secretion (Stern et al., 2000). Underlying causes of ß cell dysfunction and insulin resistance can be genetic predisposition, obesity, chemical exposure, physical inactivity and etc.
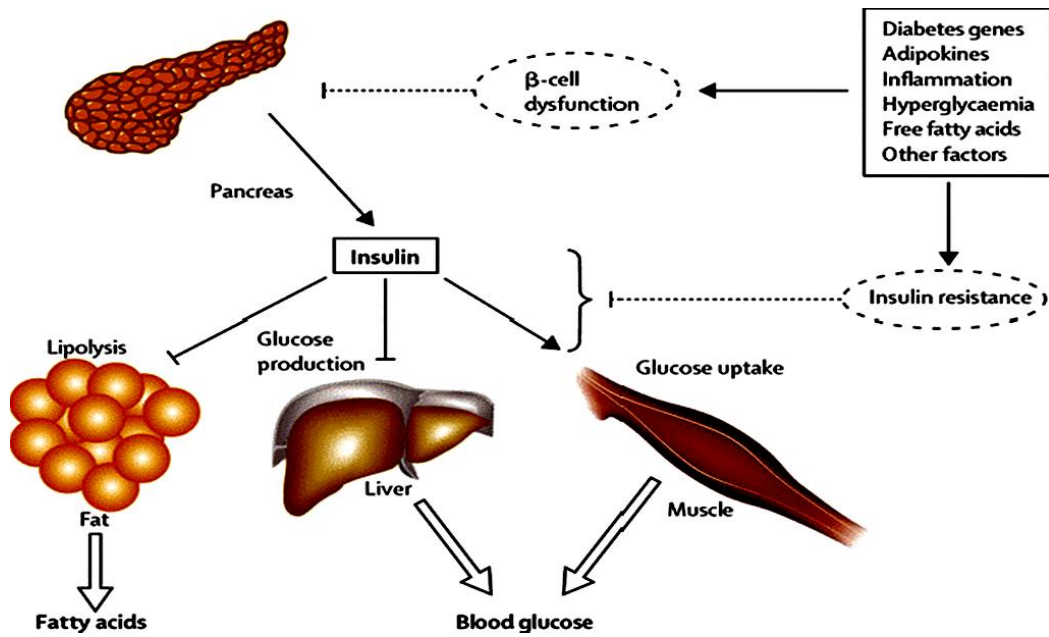
Fig 6. Abnormalities in type 2 diabetes that contribute to hyperglycemia (Lancet et al., 2005)

When insulin cannot bind to its receptors located on liver and muscle tissues insulin resistance may develop. Furthermore, impairments of post receptor coupling pathway can lead to IR, respectively. As a result, glucose is overproduced by the cells at the same time; inhibition of glucose clearance occurs (Kelley et al., 1996; Cline et al., 1999).

Impairments of insulin receptor signaling pathway can cause IR. Normally, phosphorylation of insulin receptor substrate proteins is activated by insulin receptor. These proteins interact with phosphatidylinasitol kinase which causes activation of Akt-2/ PKBb pathway. Akt-2/ PKBb plays a crucial role in the insulin initiated transportation of the glucose transporter 4 (GLUT 4) through cell membrane in order to eliminate high levels of glucose from blood (Younger et al., 2007). Impairment of any step of insulin signal transduction leads to IR (Surampudi et al., 2009). Among the causes inducing IR, inflammation is an important one. TNF-α is a main cytokine secreted during inflammatory processes. Adipocyte lipolysis is intensified by TNF-α, which causes increase of the concentration of nonesterified FFAs. These FFAs can cause IR by exerting negative effects on insulin signaling pathway (Schulman et al.,

14

1999; Bergman et al., 2000). In skeletal muscle, elevated levels of free fatty acids can affect insulin signaling pathway which leads to IR (Guillermo et al., 2008).

When blood glucose concentration increases GLUT 2 transporters enter the ß cells of pancreas and elevate the ATP/ ADP ratio. Increase of ATP/ ADP ratio causes depolarization of cell membrane, Ca ion influx increases and insulin secretes from insulin granules. In Type II DM the secretion of insulin is disrupted as a result of ß cell dysfunction. ß cell mass can be reduced (20% - 50%) in long-term type II DM. This reduction is caused by apoptosis of ß cells (Porte et. al, 2001). The loss of ß cells can be hereditary either acquired. High amounts of FFAs and glucose badly affects ß cell function through various pathways such as, defects of metabolic mechanisms, generation of reactive oxygen species (ROS), elevation of intracellular Ca levels and interaction with membrane potassium channels (Surampudi et al. , 2009) .

1.3.3   Complications of Diabetes Mellitus

Chronic diabetes often damages the renal glomerulus, the retina and peripheral nerves. All these microvascular diseases are associated with chronic hyperglycemic state. Atherosclerosis also may develop as s consequence of diabetes, which leads to microvascular heart problems (Lancet et al., 1998). Similar pathological mechanisms are observed in all diabetic complications. In the early diabetes, vascular permeability and increased blood flow are observed, caused by hyperglycemia. Increased amount of extracellular matrix components result irreversible increased vascular permeability. Over time, microvascular cell loss and capillary occlusion occurs.

These abnormalities cause ischemia, edema and hypoxia induced neurovasculization in the retina. Glomerulosclerosis, proteinuria and meshangial matrix expansion in the

kidney and multiple degenerative lesions in axonal peripheral nerves happen (Brownlee M., 2001).

There are four main mechanisms explaining the molecular pathogenesis of diabetic complications. These mechanisms are increased polyol pathway flux, increased hexosamine pathway, increased formation of advanced glycation end products (AGEs) and activation of protein kinase C (PKC) pathway. Particularly, increased ROS production as a consequence of diabetes alters the enzymes and molecules of above mentioned pathways opening way to new diseases besides diabetes. These disorders are called diabetic complications.

The main enzyme of the polyol pathway is an aldose reductase which inactivates alcohols by decreasing the amount of toxic aldehydes. Aldose reductase reduces glucose to sorbitol during hyperglycemic state. Sorbitol oxidized to fructose by using cofactor NADPH. NADPH is an essential cofactor regenerating reduced glutathione. Glutathione is an essential intracellular antioxidant. The polyol pathway rise susceptibility to intracellular oxidative damage by decreasing the concentration of reduced glutathione (Lee et al., 1999; Brownlee M., 2005).

Hexosamine pathway also induces diabetic complications. During normal conditions glucose is converted into glucose-6 phosphate and later to fructose-6 phosphate. When hyperglycemia develops, enzyme glutamine fructose-6-phosphate amidotransferase metabolizes F6P into glucosamine-6 phosphate and later to uridine diphosphate N-acetyl glucosamine (Brownlee M., 2005). Serine and threonine residues of transcription factors interact with N-acetyl glucosamine and this reaction leads to pathological disturbances in expression of genes (Wells L. et al., 2003). Increased gene expression include, increase of plasminogen activator inhibitor^{-1} and transforming growth factor-β1 (Du et al., 2000).

Diacylglycerol is an important cofactor activating PKC-α, PKC-β and PKC-δ. During hyperglycemia elevation of diacylglycerol occurs (Facchini et. al, 2000; Mueller CF et al., 2005). In diabetes induced microvascular diseases, such as

ischemia and neovascularization, PKC-β isoform is especially activated (Idris et al., 2006).

Activation of PKC causes changes in gene expression such as inhibition of antiatheroschlerotic factors (eNOS inhibition) and activation of proatherogenic factors (endothelin[-1], TGF-β) (Idris et al., 2006; Wagner et al., 2007). In addition PKC activates NF-kβ in endothelial cells (Pieper et al., 1997).

The enzymatic interaction of glucose with extracellular proteins causes the formation of advanced glycation end products (AGEs). When hyperglycemia occurs, the rate of AGEs formation also increases (Degenhardt et al., 1998). During diabetic complications AGEs damage the cells by three mechanisms. First, AGEs cause conformational changes in extracellular protein structure thus altering their functional capabilities. Second, modified plasma proteins react with AGE receptors on endothelial cells and macrophages and as a result, reactive oxygen species (ROS) are generated. AGE receptor binding also activates NF-kβ transforming factor which leads to altered gene expression. Third, extracellular matrix proteins modified by AGEs abnormally binds to receptors of matrix components (integrins) on cells and to matrix components themselves (Brownlee M., 2001).
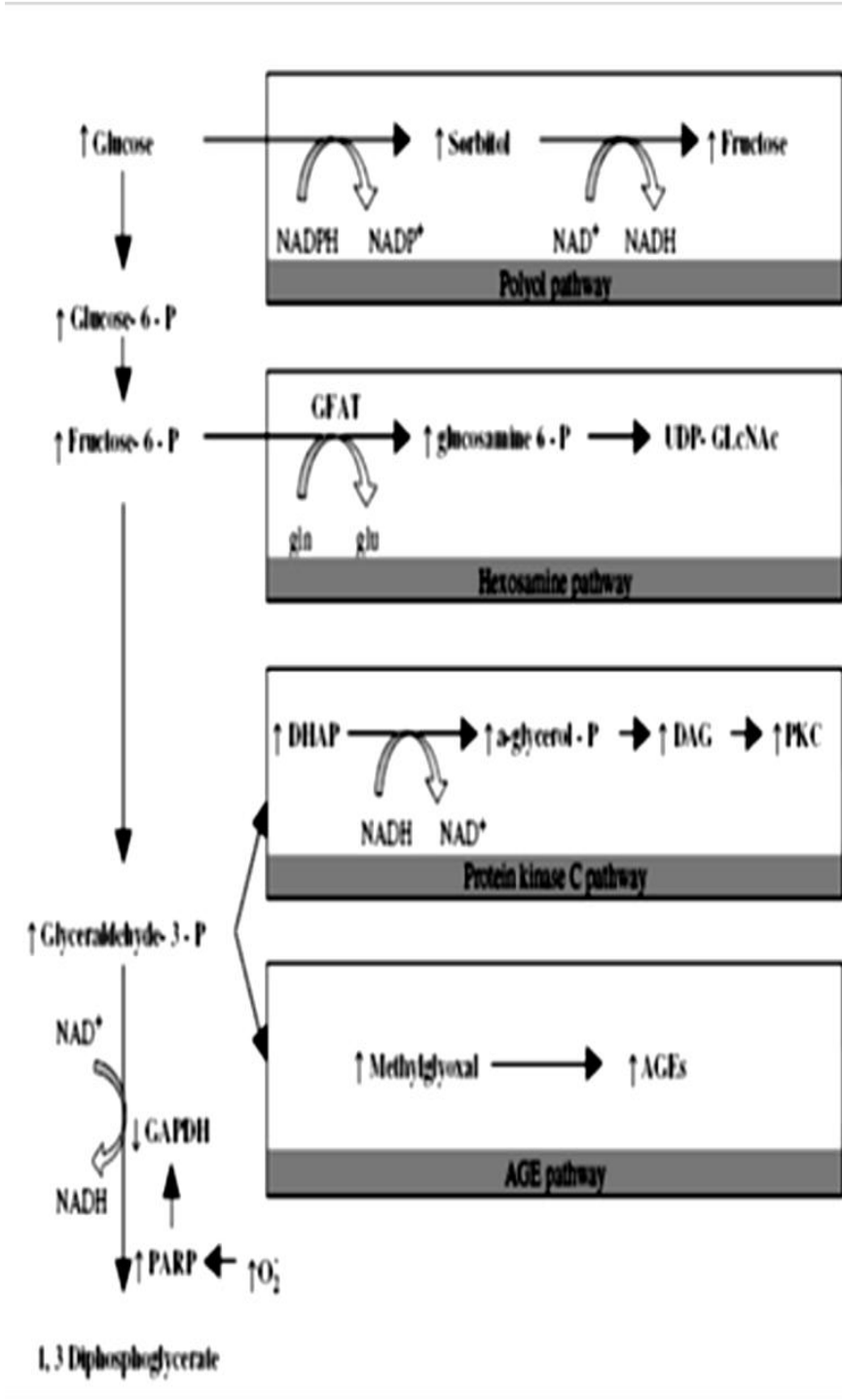
Figure 7.Illustration of the pathways leading to diabetic complications. (Brownlee M., 2001).

1.3.4 Oxidative Stress and Diabetes

Accumulation of oxidants (ROS) causes oxidative stress in many diseases, particularly in diabetes. Disturbances of cellular homeostasis and alterations of vascular function are the resulted damages of ROS. Oxygenated free radicals block the synthesis and action of nitric oxide and activate the NF-kβ. Furthermore the strong interaction takes place between AGEs and ROS, since AGEs are involved in complications of diabetes and also they can produce free radicals by themselves. In the pathogenesis of diabetic nephropathy ROS and AGEs are especially involved (Bonne font et al., 2000).

The elevation and accumulation of ROS leads to the activation of NF-kβ and PARP. NF-kβ is a transforming factor that activates proinflammatory and proadhesive pathways. Activation of this factor causes synthesis of substances such as cytokines, prothrombotic and vasoconstrictive gene products, AGE and their receptors (RAGE) (Barnes et al., 1997; Li et al., 1997). Furthermore, apoptotic genes such as Bcl-2and BCL-XL also activated through NF-kβ synthesis (Li et al., 1997). In addition, ROS damages the cell by activating polyadenyl ribose polymerase. PARP accelerates breakdown of reduced NADH and ATP depletion. In general, inhibition of glycolysis occurs through activation of PARP. As a result C3 and C6 intermediates of glucose metabolism accumulate causing diacylglycerol formation and subsequently PKC pathway is activated (Soriano et al., 2001). Finally, C6 intermediates promote polyol and hexosamine pathways which lead to diabetic complications (Wells et al., 2003; Du et al., 2000). To conclude, the ROS accumulation activates the complex interaction of molecular pathways involved in diabetes and its complications.

1.3.5 Experimental Models of Diabetes Mellitus

Investigation of pathogenetic mechanisms, diagnosis and treatment strategies of various diseases require experimental animal models. There are some advantages of using experimental models:

a) Researcher can control experimental alterations in model study more easily,

b) Researcher can produce designed number of animal models to obtain significant statistical results,

c) Other undesired factors that may affect the result of a study can be removed out in experimental models in order to see the results of specific factor.

In order to investigate molecular basis of diabetes experimental models are widely used. The experimental models also allow studying effect of environmental factors on diabetes. These factors include drugs, toxins, viruses, physical activity, diet and etc. Nowadays there are so many experimental models of diabetes, however none of them completely correspondence to human diabetes (Irer and Alper G., 2003).

The experimental models of diabetes include chemical diabetes (streptozotocin and alloxan), surgical diabetes, diet (high fatty and high carbohydrate diet), hormones and etc.

*Surgical diabetes.*Removal of 90% of pancreatic tissue is needed to see stable increase of glycemia. This process is called pancreaectomy. Technically, very difficult and is rarely used in our days (Pickup et al., 2002). When exposed to electrical shock in the ventromedial and paraventricular regions of the hypothalamus, lesions are formed. These lesions cause hyperphagia, hyperinsulinemia and obesity in animal models (Pickup et al., 2002).

*Viral diabetes.*The most investigated diabetes related virus is M variant of encephalomyocarditis virus which belongs to picarnoviruses family. Its injection to rats causes insulinitis, hyperglycemia, glucose intolerance, ketoacidosis and death. Another most studied virus is Kilham rat virus (KRV). It causes autoimmune

diabetes in rats. Other diabetes related viruses are rubella, reovirus, coxsachie B, cytomegalovirus (CMV) and Venezuelan guinea encephalitis viruses (Pickup et al., 2002; Jun et al., 2001).

*Chemical diabetes.*Chemically induced diabetic models include streptozotocin and alloxan induced experimental diabetes. Alloxan is an antienoplastic agent and metabolite of uric acid. Alloxan inhibits the glucose induced insulin secretion and at high doses, induces necrosis of β cells. Another mechanism of action of alloxan is inhibition of mitochondrial transport chain system which leads to elevation of intracellular pH levels and cell death (Bell et al., 1983). Pathological changes in chemically induced diabetic nephropathy are very similar to pathological changes of human diabetic kidney disease (Brown DM., 1982).

1.3.5.1 Streptozotocin Induced Diabetes

Streptozotocin is a chemical with diabetogenic, carcinogenic and antibiotoical properties. It is a large-spectrum antibiotic which is the metabolite of *streptomyces griseus*. STZ is very toxic to β cells of pancreas. The mechanism of action is through the binding to glucoreceptors of cell membrane. While it has glucose molecule in its structure, the glucose receptors on cell membrane accept STZ as glucose molecule and finally blocking of insulin secretion occurs. Furthermore, it affects the nuclear DNA. Inside the cell STZ decomposes and reactive carbonium ions forms causing alkylation of DNA bases. In addition, STZ has oxidant properties. It decreases superoxide dismutase levels in red blood cells and glutathione concentrations in β cells (Bell et al., 1983; Szkudelski et al., 2001; Crouch et al., 1978; Irer SV and Alper G, 2004).

STZ has negative effect not only to pancreas but also to liver and kidneys. In order to produce diabetes STZ should be injected IV or IP in $50^{-1}00$ mg / kg single dose or during 5-6 days with small doses (5 mg / kg). Blood clearance is about 15 minute (Schein et al., 1973; Rossini et al., 1976; Irer and Alper G, 2004).

The effect of STZ on diabetes is dose-dependent. In mild diabetes 35 mg / kg dose leads to acute ketoacidosis, while 100 mg /kg dose leads to death in 2-3 days. Moderate doses (55-65 mg /kg) causes elevation of blood glucose levels 3-4 fold and weight losses (Tomlinson et al., 1992).

1.3.6 Diabetic Kidney disease

Kidneys are damaged extensively due to hyperglycemic state. The disease of a kidney caused by diabetes is called diabetic nephropathy. In diabetic nephropathy, a structural alteration in kidney tissue is observed. These alterations are commonly podocyte loss, thickening of glomerular basement membrane, dysfunction of a glomerular endothelium and deposition of extracellular matrix components in the mesangial area (Wolf et al., 2005). In the development of diabetic nephropathy genetic and environmental factors play an important role. Factors such as hyperlipidemia, proteinuria and hyperglycemia can cause renal damage during diabetes. In addition, this condition is supported by genetic predispositions to diabetes, as the diabetic nephropathy frequently seen in some ethnicities and siblings (DCCT group, 1995).

Epidemiological studies showed that control of a metabolism of diabetes and diabetic nephropathy does not differ, predicting involvement of a genetic susceptibility to diabetes (Klein et. al, 1984). The results of familial cluster studies revealed that there is a four times more risk of developing diabetic nephropathy in relatives of diabetic and diabetic nephropathy patients (Seaquist et al., 1989). As several races are more susceptible to diabetic nephropathy than others, one can propose an importance of ethnic background of diabetic nephropathy. Studies revealed that the rate of progression of end-stage renal disease in siblings of type II black diabetic patients is 5 times more than white ones (Freidman et al., 1993). In Pime Indians, high prevalence of diabetic nephropathy in type II diabetic families is observed. The

variations between races may be provoked by clustering of different loci of genes, leading to genetic predisposition to the diabetic nephropathy (Schena et al., 2005).

*Pathogenesis.*During the early stage of diabetes (1-2 years), extracellular matrix protein synthesis and damage of protein degradation develops. It results in increase of collagen IV leading to glomerular basement membrane thickening (Wolf et al., 2007). Elevation of Collagen IV level causes pores in the structure of GBM that permits protein loss from this barrier (Isogai et al., 1999). In the late period of diabetic nephropathy decrease of negatively charged proteoglycans within the GBM occurs, leading to protein leakage (Adler et al., 1994). Proteoglycans are synthesized in all glomerular cells but major fractions are produced in podocytes (Wolf et al., 2005).

The major proteoglycans within the GBM are agrin and perlecan. When hyperglycemia develops agrin production is modified. In addition, angiotensin II also has contributions to modification of agrin synthesis (Yard et al., 2001; Brinkkoetter et al., 2004).

The hallmark of diabetic kidney disease is a proteinuria caused by density decrease of podocytes (Pagtalunan et al., 1997). In normal conditions, podocytes are attached firmly to the GBM by the foot processes and the gap between these feet processes are occupied by a porous membrane. This membrane filters is permeable to water and small solutes but highly impermeable to proteins (Tsilibary et al., 2003; Kreitzer et al., 2002). Transmembrane protein nephrin is a major component of porous membrane. It is bounded to filaments of podocytes. Decrease in number of nephrins cause damage to glomerulus. Furthermore, nephrin plays a role in podocyte integrity, so nephrin reduction causes podocytopenia (Saleem et al., 2002; Doublier et al., 2003; Patari et al., 2003).

Glomeruloschlerosis may develop as a result of apoptosis of podocytes by formation of synechiae (attachment of tissues to each other) among the erosed GBM and Bowman's capsule (Pavenstadf et al., 2003). Podocyte loss is probably caused by Ang II, the effect of which is mediated by TGF-β (Ding et al., 2002). Elevation of

ROS levels, increase the angiotensinogen suppression and subsequently podocyte apoptosis happens (Kojima et al., 2000). Some growth factors and cytokines also play a crucial role in the development of diabetic kidney disease. Vascular endothelial growth factor (VEGF) stimulates NOS and increased GBM permeability to proteins develops (Schrijvers et al., 2004). Especially during diabetes VEGF originates from podocytes (Cooper et al., 1999; Wendt et al., 2003). In addition, VEGF synthesis is upregulated by AGEs. TGF-β and VEGF increase is observed during excessive expression of AGE receptors (RAGE) in podocytes (Wendt et al., 2003). Also during diabetes, increased production of α3 chains of collagen IV is observed due to VEGF stimulation of podocytes. Stimulation of podocytes by VEGF causes GBM thickening (Chen et al., 2004).

Cytokine that is expressed excessively in kidneys during diabetes is TGF-β1. It causes mesangial expansion, fibrosis, proteinuria and renal insufficiency during diabetic nephropathy (Kern et al., 1996). In the formation of new blood vessels angiopoetins are participated. Ang-I promotes the formation of non-leaky vessels (Suri et al., 1996). It is antagonized by Ang-II and Ang-II together with VEGF stimulates angiogenesis. Upregulation of Ang-II in diabetic nephropathy may cause increase of angiogenesis, formation of immature vessels and increase of protein leakage (Hammes et al., 2004; Ichinose et al., 2007).
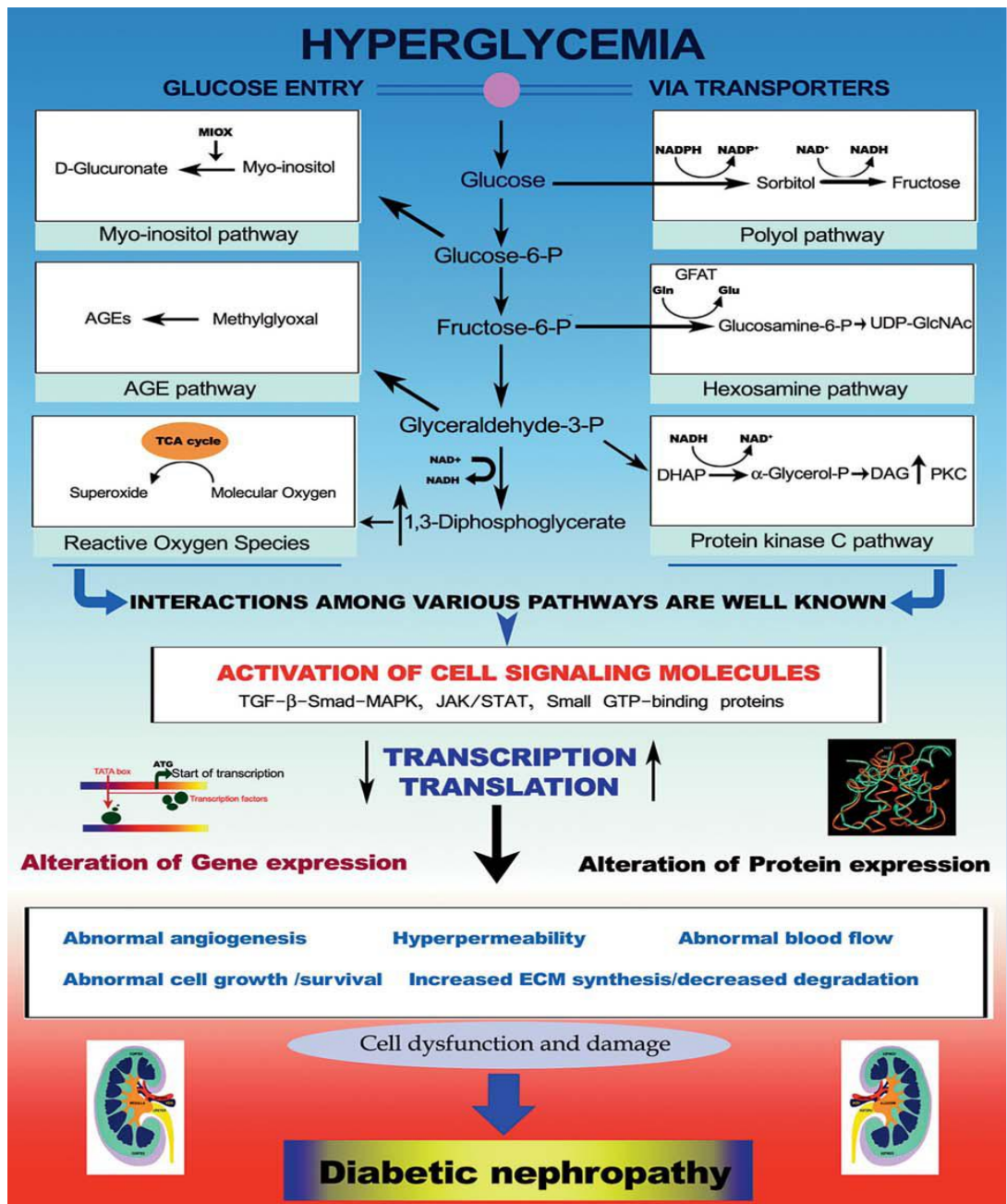
Figure 8. From hyperglycemia to diabetic nephropathy (Kanwar et al., 2005)

1.4 Selenium

Selenium is an essential metalloid trace element for mammalians because it is a component of two main body enzymes, glutathione peroxides and iodothyroine 5 '-de-iodinase (Arthur et. al., 1993). Selenium positioned among sulphur and tellurium

in group VI A and between arsenic and bromine in period IV of the periodic table. Atomic weight is 79 (Tinggi, 2003). Atomic weight, bond energies and electron energy changes are very similar to sulphur, however selenium happens as reduced quadrivalent form. Selenium may exist in different oxidative shapes which allow it to exist in several organic selenium compounds and in amino acids content (Tinggi, 2002). Selenium is a component of enzyme, glutathione peroxides, characterized as a tetramer protein with 4 atoms of selenium per molecule (Rotruck et al., 1973). Glutathione peroxides provide intracellular defense mechanisms against oxidative stress (Ursini and Bindoli, 1987). In addition, Se is a component of enzyme iodothyronine deiodonase which protects from abnormal hormone metabolism (Foster and Sumar, 1997; Arthur et al., 1993). In fishes, high selenium levels provides against Hg toxicity (Curvinaralar and Furness, 1991).

1.4.1   Selenium Deficiency and Toxicity

Experimentally, selenium deficiency are developed in group of people receiving parenteral nutrition without selenium for long period (Brown et al., 1986 ; Kien et al., 1983 ; Lockitch et al., 1990 ; Van Rij et al., 1979) . Recommended selenium supplementation doses for adults are 20-60 microgram per day (Levander et al., 2003). Excretion path is through the kidneys, therefore low doses should be given if person have already developed renal disorders (Greene et al., 1988).

Keshan disease was developed in the mountain regions of the China. In these regions, cultivated soya was lacking proper amounts of selenium leading to selenium deficiency related Keshan disease. Keshan disease is characterized as cardiovascular myopathy (Yang et al., 1987). In addition, coxsackieviruses play an important role as a potential cofactor in the etiology of the selenium responsive cardiomyopathy (Beck. et al., 1994).

It is possible that, avirulent coxsakievirus B3 viral genome acquires virulence during selenium deficiency (Beck et al., 1995).   In the regions where soil selenium

concentrations are low (Allander et al., 1994) Keshan-Beck disease development was reported. Signs of this disease include, joint swelling, short stature, pain, general malaise and arthritis (WHO, 1990). Hyperthyroidism and selenium deficiency have associated with the acuteness of myxoedemetous cretinism in the iodine-deficient region of central Africa. Selenium deficiency appears to protect against iodine deficiency (Vanderpas et al., 1990; Contempre et al., 1991). In the second generation of selenium deficient diet rats, the development of growth retardation was reported (Hurt et al., 1971; Ewan et al., 1976; Thompson et al., 1995).

The most widespread Selenium toxicity was occurred in between 1961 and 1964 in China. In this country, corn and vegetables grown in soil that contained high amounts of selenium was eaten by people and developed classical symptoms of Se toxicity such as, red, blistered skin, discolored nail and hair, hairiness and dysfunction of nervous system (Yang et al., 1983). Severe intoxication of Selenium affects mainly the nervous system causing peripheral anesthesia, paralysis, convulsions, ataxia and depression. Other signs of Selenium intoxication are anorexia, diarrhea, fatigue, pulmonary edema, liver and kidney necrosis, blindness and respiratory distress (Fan AM. et al., 1990; Helzlsouer et al., 1985).

Recently, the effect of dietary selenium on the biochemical properties of rat bone was reported using FTIR and X-ray diffraction analysis. Biomechanical data was supported the results of above mentioned techniques. Selenium and vitamin E deficient and excess selenium and vitamin E diet lead to decreased crystalline and mineral content diminish in the tibiae and femora of the rats. The authors suggest that the bones affected seriously from intoxication and deficiency syndromes. The underlying mechanism of action has not been clarified (B. Turan et al., 2000).

Despite the fact that human environmental poisoning with Selenium is rare there are a numerous accidents in which acute and sub acute Selenium intoxication happened. Until now, molecular mechanism of Se toxicity is not completely studied. However, interaction of glutathione with Selenium forms selenotrisulphides.

The selenotrisulphides produces toxic super oxides and hydrogen peroxide that may lead to Selenium poisoning (Spallahlz, 1994). Usage of Selenium as dietary supplement should be approached carefully because no complete knowledge exists about its exact effect. Furthermore, there are other factors influencing Selenium toxicity such as age, physiological state, mutation, route of administration and etc.

1.4.2 Selenoproteins

Proteins containing selecysteine in their structure are called selenoproteins. Until now 11 total selenoproteins are identified (Stadtman, 1996; Takahashi et al., 1987).

Glutathione peroxides. There are four distinct types of glutathione peroxides, catalyzing the reduction of peroxides which damage the cells. Selenium as a component of this enzyme is considered as antioxidant. Selenium prevents ROS formation that leads to severe diseases, by damaging DNA, proteins, lipids and carbohydrates (Holben et al., 1999).

Cellular glutathione peroxides found in all cells and reduces hydrogen peroxide and free organic hydro peroxides to water and alcohol (Hoekstra WG, 1975). This enzyme is depository for selenium and activity is decreased with Se deficiency (Rea HM et al., 1978).

Plasma glutathione peroxides found in human milk and plasma produces in the proximal tubule cells of the kidney (Bhattachorya et al., 1988; Avissar et al., 1994). Phospholipids hydro peroxide glutathione peroxides reduces esterified fatty acid hydro peroxides (Ursini et al., 1985). In membranes and in low density lipoproteins (LDL) it reduces cholesterol hydro peroxides and cholesterol esters. It functions to prevent the organism against lipid peroxidation (Thomas et al., 1990; Ursine et al., 1987; Ursini and Bindoli, 1987). Prevention of LDL oxidation is important because oxidized LDL can be taken by macrophages and endothelial cells in the arterial walls initiating atherosclerosis (Holovet and Collen, 1994). Gastrointestinal glutathione

peroxides plays an important role in preventing organism from toxicity of ingested lipid hydro peroxides.

Selenoprotein P. Hypothetically it has role in transport and oxidant protection but the exact function in body are not studied yet. Glutathione peroxides and selenoprotein P are the only known plasma selenoproteins (Burk and Hill, 1994; Burk and Hill, 1991). Studies demonstrated that liver necrosis and lipid per oxidation were inhibited with increase of selenoprotein P levels in Se-deficient rats that were administered Se (Burk and Hilli, 1991; Burk et al., 1995). In addition, delivery of Selenium to the testes in Se-deficient rats with the help of selenoprotein P was observed (Wilson and Tappel, 1993).

Thyroid hormone deiodinases function in the formation and regulation of active thyroid hormone triiodothyronine (T3). It catalyses the deiodination of thyroxin(T4) to T3. Types 1, 2 and 3 of this enzyme contain selenium. Consequently, selenium is found to be participated in growth and metabolism. It was reported that during Se deficiency 15-20% decrease in T3 and T4 levels happens (Larsen and Berry, 1995; Arthur et al., 1993).

Selenoprotein W associated with white muscle disease which is a metabolic disorder characterized by calcified skeletal muscle tissue. Selenium supplementation alleviates the disease state (Vendeland et al., 1993; Schubert et al., 1961).

1.4.3   The effect of Selenium on Glucose metabolism and Diabetes

Several chronic diseases are related to diminished selenium levels in body. These diseases include cancer, cirrhosis, heart diseases, renal diseases and diabetes. Changes of homeostasis of Selenium have been associated to diabetes and its complications (Simonoff, 1991). The serum and red blood cell concentrations of selenium as well as enzyme activities are decreased during diabetes. These enzymes include, superoxide dismutase's (SOD) and glutathione peroxides. Controversies

exist in literature about plasma selenium concentrations of diabetic patients. Some studies revealed Selenium decreases in diabetic patients while others observed no change in Se levels versus controls (Simonoff, 1991 ; Schlienger et al. , 1988 ; Tawardowska-Saucha et al. ,1994 ; Navarro-Alarcon et al. , 1999 ; Klapec et al. ,1998 ; Wang et al. , 1995 ; Armstrong et al. , 1996) . Some researchers even found significant increases in serum selenium levels in diabetic persons (Gebre-Medhin et al., 1984; Cser et al., 1993).

Studies revealed that selenate stimulates glucose transport activity in a dose-dependent manner in isolated rat adiposities. Increased glucose transport activity was due to translocation of glucose transporters (GLUT1 and GLUT2) to the membrane surface (Ezaki et al., 1990). Furthermore selenite acts as insulin-mimetic in whole animal diabetic models. Insulin-mimetic effect of Selenium causes decrease of blood glucose level. In addition, Se stimulates glycolysis, fatty acid synthesis and glucagon production. The increase of ability of these pathways blocks the glucose increase via the increased expression of key enzymes of these pathways. These enzymes are glycogen syntheses', glucokinase, phospho-enolpyrivatecarboxykinase (PEPCK), fatty acid syntheses' (FAS) and glucose-6-phosphate dehydrogenase. In addition, Selenite activates insulin signaling pathway which controls important key enzymes metabolism and expression (Stapleton, 2000).

The effect of Selenium on diabetic complications was observed through many studies. Selenate administration to diabetic rats normalized heart functions compared to control group (Bartell et al., 1998). Selenium diminishes the diabetic platelet hyperactivity involved in thrombosis. Thrombosis is one of the most important factors leading to diabetic cardiovascular disorders (Douillet et al., 1996).

In the diabetic rats the modified antioxidant enzymes activities were recovered as a result of sodium selenite administration. Contraction-relaxation functions of thoracic aorta were altered by an oxidant shift of cellular thiolic reserves. The study suggests that, selenium restores the modified contraction-relaxation activities of thoracic aorta through acting on glutathione redox cycle during diabetic state. So, selenium

administration diminishes the oxidative stress in diabetes. As a conclusion, they propose that the small doses of selenium may be useful as an adjunctive therapy in the treatment of human diabetes (Turan et al., 2007).

Selenium or Selenomethionine supplementations increased Se concentrations in plasma and in kidneys further improving glycemic state, increased arachidonic acid levels in diabetic kidneys, normalized renal hyper filtration and diabetic renal lesions. The beneficial effect of selenium on renal lesions could be explained as insulin-like effect of selenium. The authors of study suggest that selenium supplementation should be used as additive therapy to delay diabetic nephropathy (Douillet et al., 1999; Stachouse et al., 1990).

Recently it was demonstrated that Selenium deficiency induces albuminuria, glomerular sclerosis and hyperglycemia in normal and diabetic rats. Furthermore, the lumen size of interlobular artery was decreased as a result of Se-deficient diet. Researchers suggest that selenium deficient diet may induce renal oxidative stress and damage via the action of TGF-β1 in normal and diabetic rats (Reddi et al., 2001). In addition, it was reported that selenium deficient diet induces proteinuria and glucosuria with renal calcifications of kidney in rats. The mechanism by which selenium deficient diet causes renal calcifications is not known, however, the calcification may be induced by lipid peroxidation damaging proximal tubular cells. These findings suggest that proximal tubule cells are most vulnerable targets of oxidative stress or selenium deficiency may influence other factors, such as renal hemodynamic. Study also revealed that selenium deficiency is the primary factor affecting glutathione peroxides activity since glutathione peroxides activity markedly decreased during 2 weeks of selenium deficient diet (Mikija Fujieda et al., 2006).

Selenium also improves lipid levels in rats. It was reported that, liver lipid levels especially triglycerides was decreased in diabetic rats without supplements compared to controls. However selenium supplements normalized liver triglyceride levels. In situ selenium supplements modulated fatty acid composition in kidney, heart and aorta maintaining normal tissue functions (Douillet et al., 1998).

Recently the alterations of the rat heart tissues caused by selenium treatment were reported. The study revealed that selenium caused increase of both saturated and unsaturated lipid content in rat heart tissues. In addition the protein profile was changed with decreased α-helix and increased ß-sheet structure in the rat heart and vein tissues using FTIR micro spectroscopy. The authors suggest that the dose of selenium used in this study (5 μmol / kg) might be slight subtoxic for healthy rat heart, which has known as non-toxic dose (N. Toyran et al., 2007). Another study of same authors demonstrated that the lipid, glycogen and glycolipid contents were increased during early diabetes in rats. Also an altered protein profile with a decrease in α-helix and an increase in β-sheet structure in all the diabetic groups was demonstrated (N. Toyran et al. , 2006) .

1.5 Fundamentals of Spectroscopy

According to Maxwell's theory, radiation is considered as two perpendicular electric and magnetic fields oscillating in single planes at right angles to each other. The magnitudes of the electric and magnetic vectors are represented by E and B respectively as shown in figure 8 (Stuart, 2004).
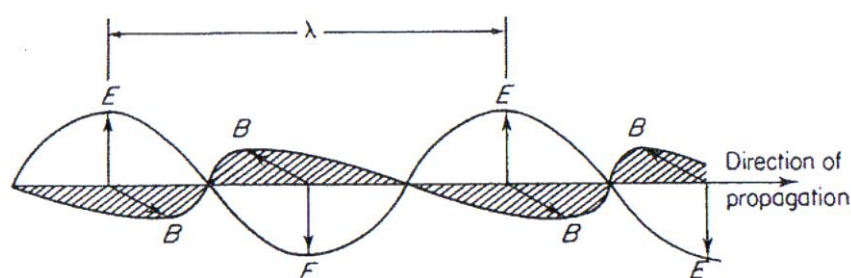
Figure 9. An electromagnetic wave

When a wave encounters a molecule it can be scattered (direction of propagation changes) or absorbed (its energy is transferred to the molecule). When electromagnetic energy of the light is absorbed the molecule is said to be excited. An excited molecule can possess any one of a set of discrete amounts of energy. These amounts are called the energy levels of the molecule. The major energy levels are determined by the possible spatial distributions of the electrons and are called electronic energy levels. Usually, electronic energy levels are shown by an energy-level diagram in figure 9. The lowest energy level is called the ground state and all others are excited states.
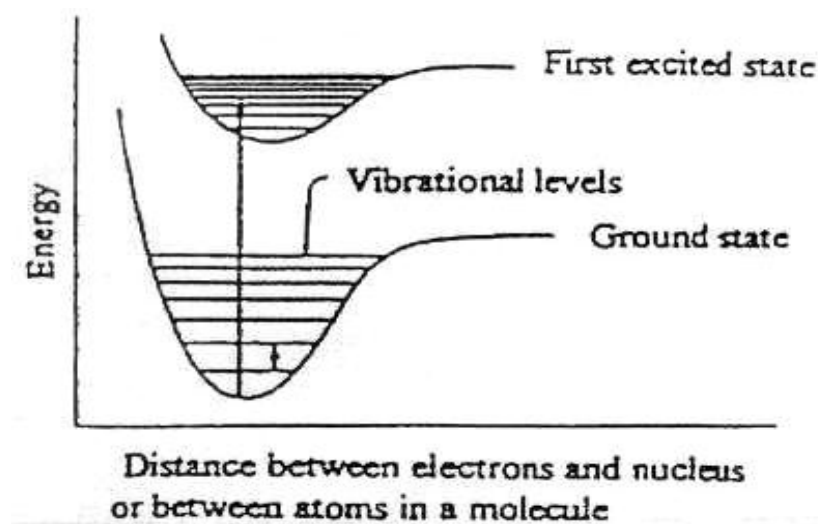
Figure 10.Typical energy-level diagrams showing the ground state and the first excited state.

Vibration levels are shown as thin horizontal lines. A possible electronic transition between the ground state and the fourth vibration level of the first excited state is indicated by the long arrow. A vibration transition within the ground state is indicated by the short arrow (Freifelder, 1982).

The absorption of energy is most probable, only if the amount absorbed corresponds to the difference between energy levels. This can be expressed by stating that light of wavelength λ can be absorbed only if $\lambda = \dfrac{HC}{E2-E1}$. In which, E is the energy level of the molecule before absorption and E_2 is an energy level reached by absorption. A change between energy levels is called a transition (Freifelder, 1982). It is convenient to treat a molecule as if it possesses several distinct reservoirs of energy. Total energy is described by equation: T_{otal} = $Tr_{ansition}$ +$R_{otation}$+ $V_{ibration}$+ $E_{lectronic}$+ $E_{lectron\ spin\ orientation}$ + $N_{uclear\ spin\ orientation}$ (Campbell and Dwerk et al., 1984).

Spectroscopy is the study of the interaction of radiation with matter. Radiation is characterized by its energy E which is linked to the frequency ν or wavelength λ of the radiation by him Planck relationship: $E = h\nu = hc/\lambda$

To investigate biological systems spectroscopy is a powerful technique, providing a convenient opportunity for analysis of proteins, nucleic acids and metabolites. Furthermore, the detailed structural information about molecule and action mechanism can be obtained (Hammes, 2005). Figure 11 represents many of the important regions of the electromagnetic spectrum.
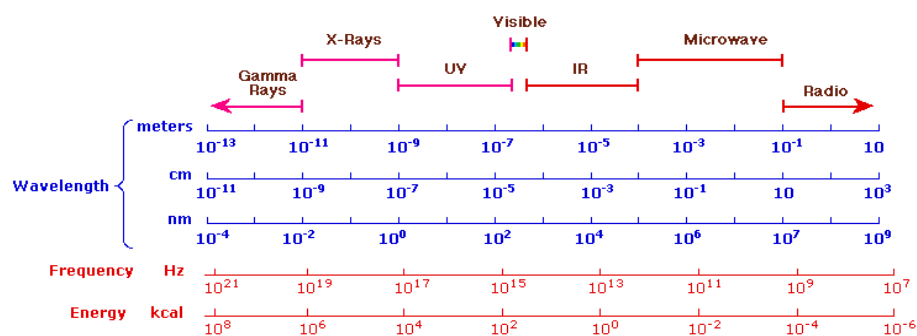
Figure 11.The Electromagnetic spectrum

1.5.1   Infrared Spectroscopy

Transitions between vibration levels of the ground state of a molecule result from the absorption of light in the infrared region. Infrared spectra are generated by the characteristic motions of various functional groups. The modes of vibration of each group are very sensitive to changes in chemical structure, conformation and environment making infrared spectra valuable for analysis (Freifelder, 1982).

The term "infrared" covers the range of the electromagnetic spectrum between 0.78 and 1000 μm. In the context of infrared spy, wavelength is measured in "wave number". Infrared (IR) region is divided into three sub regions (Smith, 1999):

Region	Wave number range (cm^{-1})
Near	14000-4000
Middle	4000-400
Far	400-4

Infrared spectroscopy is based on the transitions between vibration energy levels of the atoms of a molecule. Spectrum is obtained by passing radiation through a sample and determining what fraction of the incident radiation is absorbed at a particular energy. The energy at which any peak in an absorption spectrum corresponds to the frequency of a vibration of a part of a sample molecule (Stuart, 1996). The atoms in molecules can move relative to one other, that is, bond lengths can vary or one atom can move out of its present plane. This is a description of stretching and bending movements that are collectively referred to as vibrations (Stuart, 2004). Figure 12 schematically shows main types of vibrations.
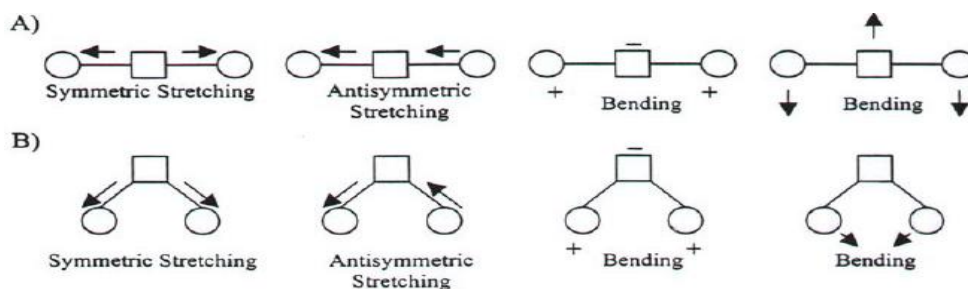
Figure 12.The schematic representation of some molecular vibrations in linear triatomic molecules (A) and non-linear triatomic molecules (B). +; - symbols represent atomic displacement out of page plane (Arrondo et. al., 1993).

For a molecule to demonstrate infrared absorptions it must possess an electric dipole moment that changes during the vibrations. Vibrations can involve either a change in bond length (stretching) or bond angle (bending). Some bonds can stretch in-phase (symmetrical stretching) of out-phase (asymmetrical stretching). Bending vibrations also contribute to infrared spectra and these are summarized in Figure 13. The types of bending vibrations are deformation, rocking, wagging and twisting motions.
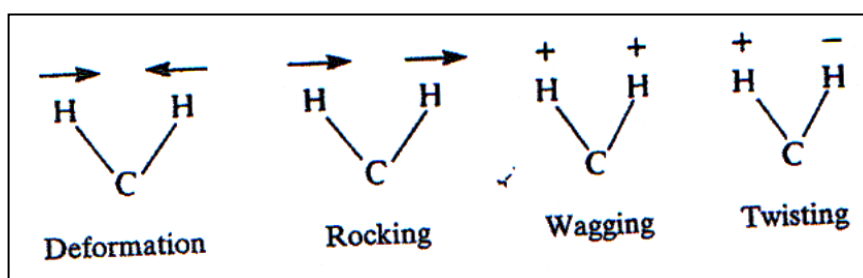
Figure 13. Types of bending vibrations

Symmetrical molecules will have fewer '' infrared-active '' vibrations than asymmetric molecules. To conclude, asymmetric vibrations will be stronger than symmetric ones,   since the symmetric vibrations will not lead to a change in dipole

36

moment. There are also skeletal vibrations associated with whole skeleton of the molecule rather than a specific group within the molecule (Stuart, 2004).

1.5.2   The Advantages of Infrared Spectroscopy

✓ It is a universal technique. Solid, liquids, gases, semi-solids, powders and polymers are all can be analyzed.

✓ Infrared spectra are very informative. The peak positions, intensities, widths and shapes in a spectrum all gives useful information.

✓ An infrared spectrum is a relatively fast and easy technique. The majority of samples can be prepared, scanned and the results plotted in less than five minutes.

✓ It is sensitive method. By interfacing an infrared spectrometer to a gas chromatograph, the infrared spectrum of as little as 5 nanograms of material can be obtained. Micrograms of material can be detected routinely.

✓ Infrared instruments are relatively inexpensive laboratory equipments.

✓ The different functional groups belonging to the macromolecules in the biological system can be monitored simultaneously from the same spectrum.

1.5.3   Fourier- Transform Infrared Spectrometers (FT-IR)

The basic principle of FTIR spectroscopy is the interference of radiation among two beams yielding an interferogram. Interferogram is a signal generated as a function of the change of path length among the two beams. The Figure 14 schematically represents an FTIR spectrometer.
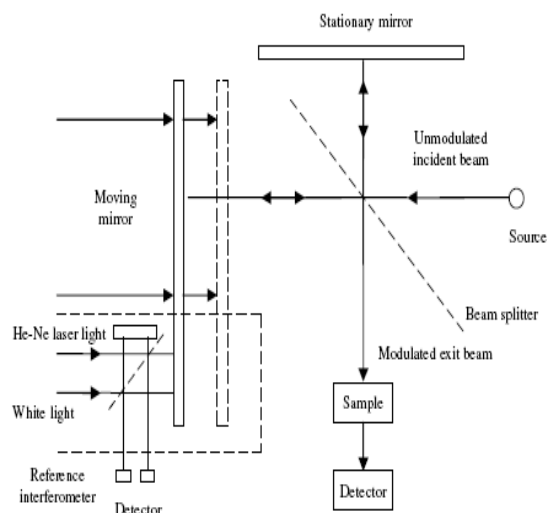
Figure 14. Schematic of Michelson interferometer.

The emerged radiation from the source is passed through an interferometer to the sample before reaching a detector. The high-frequency contributions have been removed by the filter when signal is amplified. Then by the help of analog-to-digital converter, the data are transformed to digital form and passed on to the computer for Fourier-transformation.

Michelson interferometer is the most used interferometer, consists of two perpendicular plane mirrors. One mirror can move in direction perpendicular to the plane. The beam splitter intersects the planes of two mirrors. The transmitted beam emerges from interferometer at 90∘ to the input beam. In FTIR spectrometry this beam is detected.

In order to investigate mid-infrared region of FTIR spectrometer, Globar or Nernst source is used. High-pressure mercury lamps are used for far-infrared region and tungsten-halogen lamps used for near-infrared region as sources.

There are two type of detectors used for mid-infrared region. The normal pyrolectric device (deuterium tryglycine sulfate (DTGS)) routinely used in a temperature-

resistant alkali halide window. The mercury cadmium telluride (MCT) detectors used for sensitive studies. MCT requires to be cooled to liquid nitrogen temperatures (Stuart, 2004).

The Advantages of FT-IR Spectrometers

Fellgett advantage is due to an improvement in the SNR per unit time, proportional to the square root of the number of resolution elements being monitored. This results from the large number of resolution elements being monitored simultaneously.

Jacquinot's advantage is due to the substantial gain in energy at the detector hence translating to higher signals and improved SNRs. Because FTIR spectrometry does not require the use of a slit or other restricting device, the total source output can be passed through the sample continuously.

Speed advantage. The mirror has the ability to move short distances quite rapidly and this, together with the SNR improvements make it possible to obtain spectra on a millisecond timescale (Stuart, 1997).

1.5.4   Attenuated Total Reflectance Spectroscopy (ATR)

ATR spectroscopy uses the total internal reflection phenomena. A radiation beam penetrating into the crystal undergoes total internal reflection when the angle of incidence at the interface among the crystal and sample is greater than the critical angle. The critical angle is the function of the refractive indices of the two surfaces. The beam enters a fraction of a wavelength beyond the reflecting surface. When a material that selectively absorbs radiation is in close contact with the reflecting surface, the beam loses energy at the wavelength where the material absorbs.

The resultant attenuated radiation is detected and plotted as a function of wavelength by the spectrometer and gives rise to the absorption spectral characteristics of the sample.
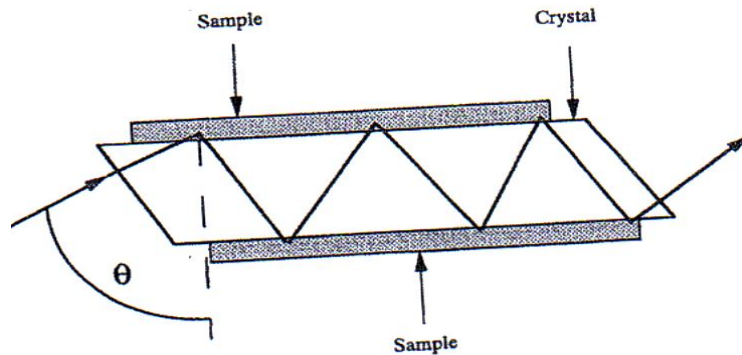
Figure 15.Typical attenuated total reflectance cell.

The crystals used in ATR cells are made from materials that are low soluble in water and are have very high refractive index. The commonly used materials are zinc-selenide (ZnSe), thallium-iodide (KRS-5) and germanium (Ge). Both solid and liquid samples can be analyzed in ATR cells. Furthermore, it is possible to set up a flow of sample through ATR cell which allows monitoring of spectral changes with time (Stuart, 2004).

The advantages of ATR-FTIR spectroscopy are the following:

1. The samples can be directly investigated without extensive drying

2. The results are not affected from the width of the samples. As a result more reliable results can be obtained for quantitative measurements.

1.6   Aim of the Study

Diabetes Mellitus is a disease of metabolism affecting the great amount of world's population. Protein, fat and carbohydrate metabolism are severely affected during diabetes. Complications of diabetes affect mostly retina, nerves and kidneys. The kidney is one of the most damaged organs in diabetes. Diabetes-induced kidney disease is the complications of diabetes mellitus affecting 30-40 % of diabetic patients. Diabetic kidney disease is characterized by micro and macroangiopathy in kidney cortex leading to glomerulosclerosis, proteinuria and meshangial matrix expansion. If untreated, these pathologies cause renal insufficiency and even death. Hyperglycemia is a main factor causing diabetes and diabetic kidney disease. As kidneys have serious functions such as regulation of water and electrolyte balance in the body, it is very important to diagnose and apply proper treatment during diabetic kidney disease.

In this study we made an attempt to explain the structural and functional alterations involved in diabetic kidney disease via infrared spectroscopic techniques, using rat animal model. We have used three different dose of selenium as low, medium and high, to discover the optimal curing dose of selenium for the diabetes-induced disorders.

Oxidative stress may cause diabetes and diabetic complications through various pathways. To sum up, in the pathogenesis of diabetic nephropathy ROS production can extensively damage the kidneys. Nowadays, the usage of antioxidants in the treatment of diabetes is also a promising strategy for diabetic complications (Guvenc Gorgulu, 2004). Selenium is a metal cofactor of antioxidant enzyme glutathione peroxides which is an important enzyme removing free radicals from the body. Furthermore, Selenium exerts antioxidant effects and also demonstrates insulin-like properties in animal studies. However, the exact mechanism of action of selenium is not known, yet.

The literature survey reveals the interesting results about the effect of selenium on diabetes and diabetic complications. Most studies show that selenium exerts healing effect on diabetes and diabetic complications (Ezaki et al. , 1990 ; Gebre-Medhin et al. , 1984 ; Cser et al. , 1993 ; Stapleton, 2000 ; Turan et al. , 2007). We conducted this study in order to investigate biological action of selenium in diabetic kidney disease via ATR-FTIR spectroscopy in rat animal model.

To conclude, the aim of this study is to investigate the diabetes-induced structural and functional changes of rat kidney tissue, especially alterations of kidney brush-border plasma membrane using ATR-FTIR spectroscopy. Furthermore, the best of our knowledge it is the first study investigating the structural properties of the macromolecules of kidney plasma membrane. In addition, the structural alterations of kidney brush-border plasma membrane caused by selenium supplementation on diabetes induced damages were studied, for the first time. Finally, the possible recovery effect of selenium as an antioxidant on diabetic kidney disease state was investigated via ATR-FTIR spectroscopy.

CHAPTER 2

MATERIALS AND METHODS

2.1 Reagents

Mannitol, Trisma Base, HEPES, Calcium Chloride, Stretozotocin (STZ) and Sodium Selenite used in this study were obtained from Sigma at the high grade of purity.

2.2 Animals and Feedings

Male adult Wistar rats (250-300 gr) 12-14 weeks old were obtained from Experimental Center of Adnan Menderes University. Animals were fed with standard diet with water and libitum. All experimental procedures were approved by the ethics committee of Adnan Menderes University.

The animals were divided randomly, into 5 groups as control (n=10), diabetic (n=8), low dose selenium treated diabetic (n=8), medium dose selenium treated diabetic (n=8) and high dose selenium treated diabetic group (n=5).

2.2.1 Formation of Control group

Animals were injected 0.05 M Citrate buffer (PH-4.5) intraperitonally as a single dose. Also physiological saline solution was injected daily for 5 weeks. All the

animals were fed without any restriction for 5 weeks. At the end of 5 the week they were decapitated, kidneys were removed and stored at -80 C until use.

2.2.2 Formation of Diabetic group

Diabetes was induced with intraperitonal injection of streptozotocin (50 mg/ kg) dissolved in 0.05 M Citrate buffer. Animals received 5 % dextrose solution in order to prevent death due to hyperglycemic shock. After 4 days of STZ injection blood glucose levels were measured using a glucometer (One Touch Horizon Blood Glucose Monitoring System/ Glucometer, USA). Blood glucose levels higher than 250 mg/ dl were encountered as diabetic. During 5 weeks the animals were fed with standard diet without any restriction and at the end of 5 th week they were decapitated, kidneys were removed and stored at -80 °C for experimental purposes.

2.2.3 Formation of Selenium treated Diabetic groups

Diabetes was induced with intraperitonal injection of streptozotocin (50 mg/ kg) dissolved in 0.05 M Citrate buffer as described previously. Diabetic rats were divided into three groups. Low dose (1µmol/ kg), medium dose (5µmol/ kg) and high dose (25 µmol/ kg) sodium selenite were injected daily for 5 weeks into rat's intraperitonally. At the end of 5 th week they were decapitated, kidneys were removed and stored at -80 °C till usage.

2.3 Isolation of Rat Kidney Brush Border Plasma membrane vesicles using Calcium precipitation method.

The renal brush-border plasma membranes were isolated using Calcium precipitation method with some modifications (Evers et al., 1978). The fatty tissue surrounding kidneys was removed and kidneys were dissected and the cortex part was obtained. Tissue was weighted and homogenized as 10% w/ w suspension with mannitol buffer

(10 mM Mannitol, 2mM Tris-Hcl) for 2 min. The tissue was homogenized using Potter-Elvehjem glass homogenizer packed in crush ice, coupled motor – driven (Black & Decker, V850, multispeed drill) Teflon at 2400 rpm for 3 X 20 sec. 10 mM $CaCl_2$ was added to final concentration. All procedures was carried out at 0- 4 ^{o}C. After 15 min the homogenate was diluted 1:1 with a buffer containing10 mM Mannitol, 2mM Tris-Hcl and 10 mM $CaCl_2$. The homogenate was centrifuged at 500 g for 12 min and pellet was discarded. The supernatant was centrifuged at 15. 000 g for 12 min. The resulting supernatant was discarded and pellet was resuspended with 4 ml Mannitol buffer (10 mM Mannitol, 2mM Tris-Hcl). 10 mM $CaCl_2$ was added to final concentration. After 15 minute the homogenate was diluted 1:1 with a buffer containing10 mM Mannitol, 2mM Tris-Hcl and 10 mM $CaCl_2$. The homogenate was centrifuged at 750 g for 12 min and pellet was discarded. The supernatant was centrifuged at 15.000 g for 12 min and resulting supernatant was discarded. The pellet was resuspended in 15 ml of buffer containing 10 mM Mannitol, 20mM Tris-Hcl and 20 mM HEPES and centrifuged at 48. 000 g for 20 min. The supernatant was discarded and the pellet was homogenized with 1.5 ml of buffer containing 10 mM Mannitol, 20mM Tris-Hcl and 20 mM HEPES by sucking the suspension 10 times through a steel needle into a plastic syringe. The homogenate was centrifuged at 2000 g for 5 min and the pellet was discarded. The supernatant was centrifuged at 48.000 g for 20 min. The resulting pellet was final brush-bordered plasma membrane vesicles. The pellet was resuspended with 0.25 ml of final supernatant in order to transfer to eppendorf tubes and centrifuged at 14.000 rpm for 10 minute. The supernatant was discarded and pellet was used for ATR-FTIR experiments.

2.4 ATR-FTIR study

The infrared spectra of kidney brush border plasma membrane samples were collected in the one-bounce ATR mode in a Spectrum 100 FTIR spectrometer (Perkin- Elmer Inc., Norwalk, CT, USA) equipped with a Universal ATR accessory. The air was scanned and spectrum was used as a reference. The samples (10 μl) were placed on a Diamond/ ZnSe crystal plate (PerkinElmer) with a micropipette. The samples were scanned from 4000 to 650 cm^{-1} for 200 scans with a resolution of 4 cm^{-1} at room temperature. Since the membrane contains water, the last buffer used during membrane isolation was scanned and subtracted manually from the samples using Spectrum 100 software. Collections of spectra and data manipulations were carried out using Spectrum 100 software (Perkin-Elmer). The band positions were measured using the frequency corresponding to the center of weight. Using the same software, the spectra were first smoothed with thirteen-point Savitsky-Golay smooth function to remove the noise. Then the spectra were baseline corrected. The spectra were normalized with respect to specific bands for visual demonstration. The purpose of the normalization is to remove differences in peak heights between the spectra acquired under different conditions. It allows a point-to-point comparison to be made (Smith, 1999). The ratios of the intensities and shifting of the frequencies were examined before the normalization process. Band areas were calculated from smoothed and baseline corrected spectra using Spectrum 100 software. The bandwidth values of specific bands were calculated as the width at 0.75 x height of the signal in terms of cm^{-1}.

air spectrum
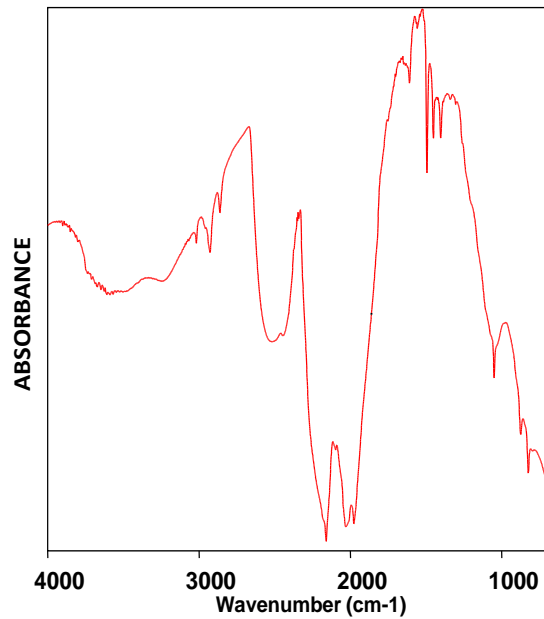
Figure 16. The reference spectrum of air

2.5 Cluster Analysis

For the observation of the spectral differentiation among experimental groups, cluster analysis was applied by using OPUS 5.5 software (Bruker Optics, GmbH). For cluster analysis, first derivative of each sample was taken in 3020-950 cm $^{-1}$ region and subsequently vector normalization was applied over the investigated frequency range. As input data for this analysis, spectral distances were calculated between pairs of spectra as Pearson's correlation coefficients. Cluster analysis for the separation of control versus other groups was based on the Euclidean distances. Ward's algorithm was used to construct dendrograms.

2.6 Structural Analysis of Main Protein (Amide I) Band

OPUS 5. 5 software (Bruker Optics, GmbH) was used in order to analyze main protein band. Vector normalized second derivatives was used to determine the spectral differences of Amide I band (1700-1600 cm^{-1}) among all groups. Minimum positions were used for the comparisons in the second derivative spectra because absorption maxima displayed as minima in the second derivatives (Ozek et al., 2009).

Concentration sensitive alterations in the constituents of amide I band were observed by using these spectra because peak height is very sensitive to alterations of FWHH (full width at half height) of the FTIR bands in the second derivative spectra. Finally, the qualitative and quantitative evaluation of protein secondary structure components was acquired, detailly in addition to the determination of band frequencies.

2.7 Statistical Analysis

The results were expressed as ± standard error of mean (SEM) . Control vs diabetic group, diabetic versus selenium treated groups (low dose, medium dose and high dose group) data were analyzed statistically using non-parametric Mann–Whitney U test. A 'p' value less than or equal to 0.05 was considered as statistically significant. The degree of significance was denoted as less than or equal to $p < 0.05$ *, ‡ , $p < 0.01$ **, ‡‡ $p < 0.001$ ***, ‡‡‡ .

CHAPTER 3

RESULTS

3.1 General ATR-FTIR Spectrum and Band Assignment of Rat Kidney Plasma Membranes

Current research was conducted using 5 (five) groups of wistar rat, namely control (n=10) , diabetic (n=8), treated groups at high selenium dose (n=5), medium dose (n=8) and low dose (n=8) to reveal the effect of diabetes on kidney brush-border cell membranes and ffurthermore, the role of of selenium as an antioxidant on the diabetes-induced damages. In this study, ATR-FTIR spectroscopy was used as a basic informative method. Through the use of this spectroscopic method the structural and compositional alterations such as protein and lipid concentration, lipid / protein ratio, lipid peroxidation, acyl chain flexibility and membrane dynamics were compared among healthy (control group), diabetic and selenium treated diabetic animals. In addition, the secondary structural changes of membrane proteins were also revealed.

In order to investigate the aqueous system in FTIR spectroscopy, water must be subtracted from the system, because water is a strong infrared absorber (Mantsch, 1984). In infrared spectroscopy, water gives strong bands around 3409 cm^{-1} and 1645 cm^{-1} regions that overlap the C-H stretching modes of lipids in the 3000-2800 cm-1 region and the C=O stretching's belonging to tryglicerides, cholesterol esters and protein (amide I) bands located around 1730 cm^{-1} and 1650 cm^{-1} (amide II) respectively.

In this work, the spectrum of buffer used in last step of membrane isolation was subtracted from the system using appropriate software. The experimental conditions such as amount of sample scan number and temperature of buffer (water) was exactly same for all samples. Mainly two regions of the spectra were analyzed in details because there are too many bands belonging to different functional groups of proteins, lipids and polysaccharides. These regions namely are the C-H stretching region (3030 cm^{-1} - 2800 cm^{-1}) and the finger-print region (1800 cm^{-1} – 950 cm^{-1}).

Figure 17 shows representative overall spectra of kidney brush-border cell membrane in $3030\text{-}950 \text{ cm}^{-1}$ region. The bands were assigned on the basis of this work together with citations of other studies from literature (Rigas et al. , 1990 ; Wong et al. , 1991 ; Takahashi et al. , 1991 ; Wang et al. , 1997 ; Jamin et al. , 1998 ; Melin et al. , 2000 ; Jackson et al. , 1998 ; Lyman et al. , 1999 ; Chiriboga et al. , 2000 ; Cakmak et.al , 2003 ; Banyay et al. , 2003 ; Toyran et al. , 2006 ; Cakmak et al. , 2006) . The assigned bands were summarized in Table 1.
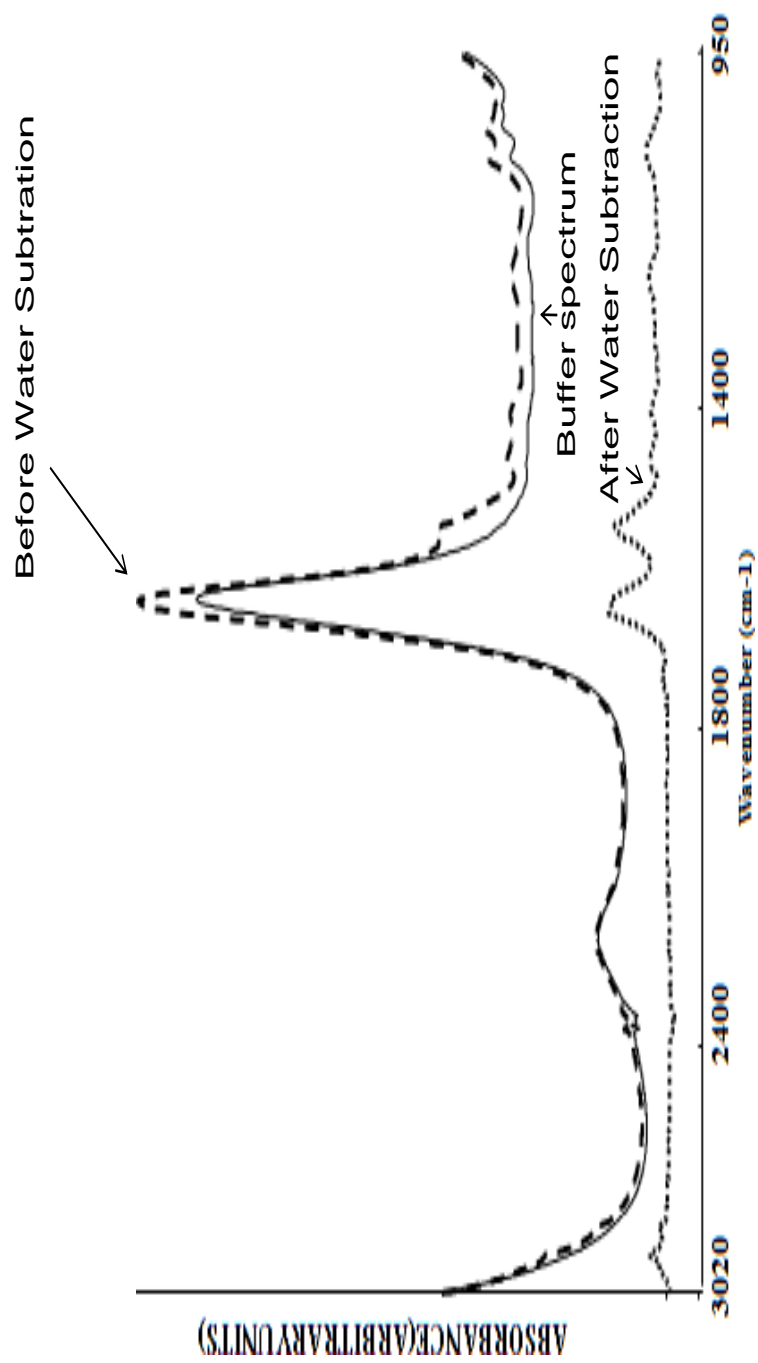
Figure 17.The representative ATR-FTIR spectra of rat kidney brush-border plasma membranes before and after water subtraction in the region between $3020 - 950$ cm^{-1}. The buffer spectrum was also shown as solid line.
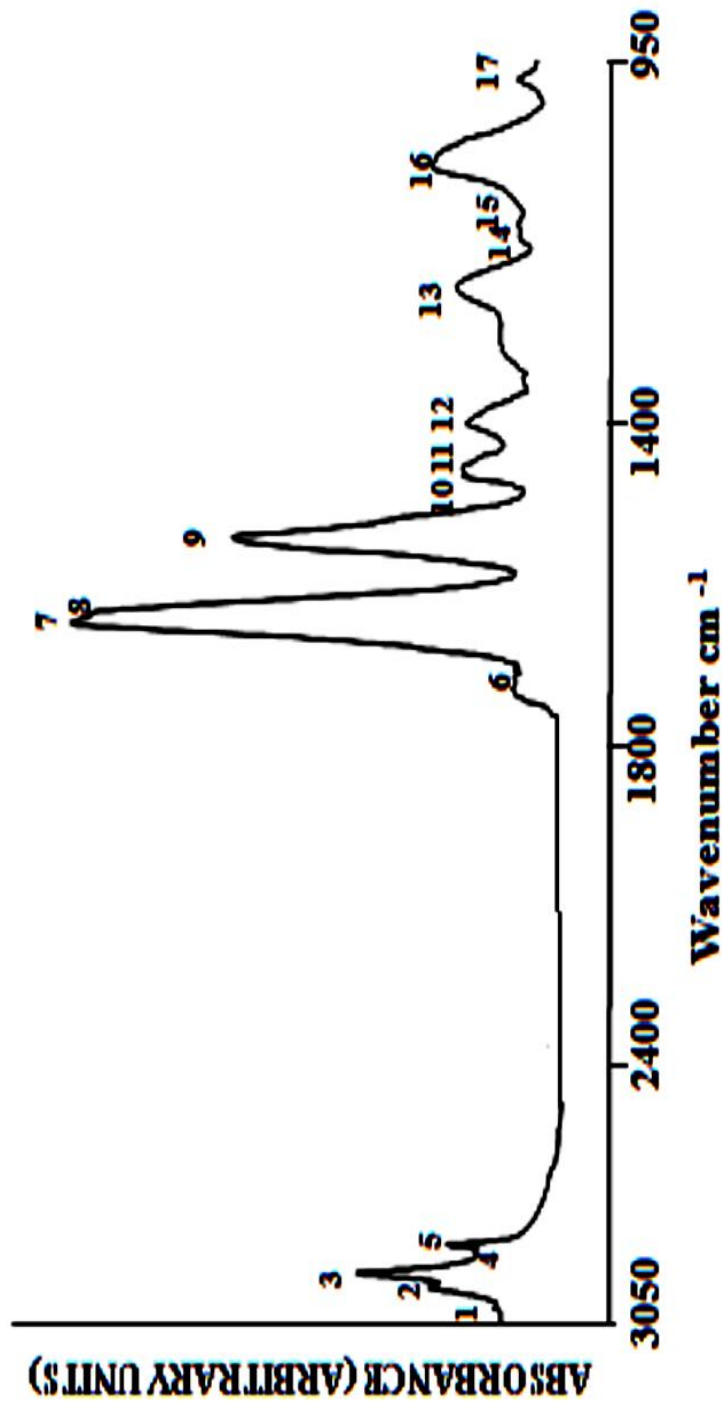
Figure 18.The representative spectra of control rat kidney brush-border plasma membrane in the 3020- 957 cm^{-1} region. The emerging bands are numerized respectively.The definition of numerized bands are illustrated in Table 1.

Table 1.FT-IR spectral band assignments of rat kidney brush-border plasma membrane in the region of 3030- 950 cm^{-1} (Mantsch, 1984 ; Toyran and Severcan et al. , 2004 ; Severcan et al. , 2000) .

#	Wavenumber (cm$^{-1)}$)	Definition of Assignment
1	3011	Olefinic = CH unsaturated Lipids
2	2962	CH$_3$ asymmetric stretching: lipids
3	2923	CH$_2$ asymmetric stretching: lipids
4	2873	CH$_3$ symmetric stretching: mainly proteins with some contributions of lipids
5	2853	CH$_2$ symmetric stretching: lipids
6	1731	Saturated ester C= O stretch : phospholipids, cholesterol esters and hemicelluloses
7	1652	Amide I (protein C=O stretching)
8	1636	
9	1546	Amide II (protein N-H bend, C-N stretch)
10	1468	CH$_2$ scissoring: lipids
11	1455	CH$_2$ Bending: mostly lipids, with some contribution from proteins
12	1400	COO- symmetric stretching (fatty acids)
13	1233	PO$_2$ asymmetric stretching (phospholipids)
14	1171	CO-O-C asymmetric stretching : glycogen
15	1084	PO$_2$ symmetric stretching : phospholipids
16	1045	C-O stretch : polysaccharides, glycolipids
17	972	C-N+ - C stretch : Phosphate Monoesters

Table 2.Numerical summary of the detailed differences in the band frequencies of the control, diabetic and treated groups. The values are the means ± SEM for each group. Man-Whitney U-test was used to compare the groups. The degree of significance was donated as *, ‡ P < 0.05; **, ‡‡ P < 0. 01 and ***, ‡‡‡ P < 0.001. The upward arrow indicates an increase and the downward arrow indicates a decrease. The ddiabetic group was compared with respect to the control group. The Selenium treated groups were compared with respect to the diabetic group.

#	Control (n=10)	Diabetic (n=8)	HDSe(n=5)	MDSe (n=8)	LDSe (n=8)
1.	3011.66 ± 1.5	3013.25 ± 2.32 ↑	3012.62 ± 2.19 ↓	3017 ± 0.07 ‡ ↑	3011.81 ± 0.9 ↓
2.	2962.6 ± 1.95	2959.84 ± 2.46 ↓	2960.78 ± 2.1 ↑	2958.6 ± 0.12 ↓	2960.3 ± 2.87 ↑
3.	2923.74 ± 1.15	2923.49 ± 0.91 ↓	2924.15 ± 0.93 ↑	2924.08 ± 0.24 ↑	2924.39 ± 0.4 ‡ ↑
4.	2873.072± 0.37	2873.23 ± 1.76 ↑	2872.28 ± 0.11 ↓	2872.84 ± 0.42↓	2872.7 ± 0.43 ↓
5.	2853.05 ± 0.37	2852.2 ± 0.5 ** ↓	2853.4 ± 0.4 ‡ ↑	2853.36± 0.24 ‡ ↑	2853.66 ± 0.3 ‡ ↑
6.	1731.86 ± 0.31	1732.25 ± 0.4 ↑	1730.34±0.8 ‡↓	1730.84 ± 2.4 ↑	1731.24 ± 2.01 ↓
7.	1652.29 ± 0.73	1651.59 ± 0.4 ↓	1651.67 ± 0.5 ↑	1652.97 ± 0.08 ‡ ↑	1651.95 ± 0.84 ↑
8.	1636.05 ± 0.7	1635.34 ± 0.92↓	1637.68 ± 0.7 ‡ ↑	1636.13 ± 0.51‡ ↑	1636.48 ± 1.08 ↑
9.	1546.37 ± 0.3	1546.03 ± 0.2 * ↓	1542.6 ± 0.67 ‡ ↓	1546.4 ± 0.47 ‡ ↑	1546.68 ± 0.5 ‡ ↑
10.	1468.88 ± 0.78	1469.47 ± 0.19 ↑	1468.28 ± 0.1 ‡ ↓	1468.13 ± 0.11 ‡ ↓	1469.16 ± 0.5 ↓
11.	1455.38 ± 2.07	1455.06 ± 0.31 ↓	1453.87 ± 0.9 ‡ ↓	1458.1 ± 0.4 ‡ ↑	1454.97 ± 0.76 ↓
12.	1400.061± 2.15	1398.92 ± 1.86 ↓	1399.4 ± 1.99 ↑	1400.34 ±1.93 ‡ ↑	1401.74 ±1.37 ‡ ↑
13.	1233.3 ± 2.09	1233.59 ± 1.17 ↑	1226.7 ± 2.77 ‡↓	1231.87 ±0.82 ‡ ↓	1233.13 ± 1.09 ↓
14.	1171.55 ± 0.69	1172.34 ± 0.43 ↑	1172.23 ± 0.37 ↓	1172.95 ±0.64 ‡ ↑	1171.67 ±0.29 ‡ ↓
15.	1084.95 ± 0.75	1085.82 ± 0.96 * ↑	1082.15 ± 0.14 ‡↓	1085.79 ± 0.6 ↓	1085.47 ± 2.09 ↓
16.	1045.83 ± 0.21	1045.78 ± 0.18 ↓	1040.68 ± 1.1 ‡ ↓	1045.39 ±0.26 ‡ ↓	1045.63 ± 0.2 ↓
17.	972.255 ± 0.568	972.45 ± 1.13 ↑	972.91 ± 0.9 ↑	972.74 ± 0.4 ↓	971.88 ± 0.48 ↓

Table 3.Numerical summary of the detailed differences in the band areas of the control, diabetic and treated groups. The values are the means ± SEM for each group. Man-Whitney U-test was used to compare the groups. The degree of significance was donated as *, ‡ P < 0.05; ** , ‡‡ P < 0.01 and ***, ‡‡‡ P < 0.001. The upward arrow indicates an increase and the downward arrow indicates a decrease. The diabetic group was compared with respect to the control group. The Selenium treated groups were compared with respect to the diabetic group.

#	Control (n=10)	Diabetic (n=8)	HDSE (n=5)	MDSE (n=8)	LDSE (n=8)
1.	0.0034 ± 0.002	0.007 ± 0.01 ↑ ***	0.009 ± 0.004 ‡‡ ↑	0.012 ± 0.003 ‡ ↑	0.0067 ± 0.001 ‡ ↓
2.	0.0282 ± 0.009	0.022 ± 0.006 ↓	0.16 ± 0.1 ↑	0.06 ± 0.01 ‡↑	0.035±0.01 ‡↑
3.	0.215 ± 0.006	0.06 ±0.03 *** ↓	0.88 ± 0.45 ‡ ↑	0.16 ± 0.04 ‡↑	0.16 ± 0.04 ‡ ↑
4.	0.0029 ± 0.009	0.02±0.017 *** ↑	0.29 ± 0.15 ‡ ↑	0.063 ± 0.012 ‡ ↑	0.03 ± 0.007 ‡ ↑
5.	0.039 ± 0.01	0.02 ± 0.007 *** ↓	0.37 ± 0.19 ‡ ↑	0.074 ± 0.02 ‡ ↑	0.04 ± 0.01 ‡ ↑
6.	0.006 ± 0.001	0.006 ± 0.001	0,03 ± 0,008 ‡ ↑	0.007 ± 0.002 ‡↑	0.01 ± 0.002 ‡ ↑
7.	0,71 ± 0,34	0.88 ± 0.1 ↑	6.7 ± 3,29 ‡‡‡ ↑	0,83 ± 0,22 ↓	0,95 ± 0,23 ↑
8.	0.21 ± 0.05	0.21 ± 0.03	1.23 ± 0.6 ‡ ↑	0.19 ± 0.05 ↓	0.028 ± 0.07 ‡ ↓
9.	0.82 ± 0.19	0.06 ± 0.01 *** ↓	1.44 ± 0.66 ‡ ↑	0.15 ± 0.03 ‡ ↑	0.86 ± 0.23 ‡ ↑
10.	0.025 ± 0.006	0.02 ± 0.004 ↓	0.21 ± 0.09 ‡ ↑	0.04 ± 0.009 ‡↑	0.04 ± 0.01 ‡ ↑
11.	0.027 ± 0.022	0.02 ± 0.003 ↓	0.21 ± 0.1 ‡ ↑	0.03 ± 0.007 ‡ ↑	0.03 ± 0.01 ‡ ↑
12.	0.02 ± 0.006	0.02 ± 0.003	0.29 ± 0.12 ‡ ↑	0.03 ± 0.008 ‡ ↑	0.026 ± 0.008 ↑
13.	0.12 ± 0.04	0.15 ± 0.016 ↑	0.28 ± 0.17 ‡ ↑	0.04 ± 0.01 ‡ ↓	0.18 ± 0.04 ‡ ↑
14.	0.006 ± 0.001	0.006 ± 0.001	0.17 ± 0.088 ↑	0.005 ± 0.004 ↓	0.005 ± 0.001 ↓
15.	0.08 ± 0.03	0.068 ± 0.01↓	1.46 ± 0.66 ‡ ↑	0.11 ± 0.04 ‡ ↑	0.07 ± 0.02 ↑
16.	0.032 ± 0.008	0.06 ± 0.017 ** ↑	1.3 ± 0.6 ‡ ↑	0.06 ± 0.02 ↑	0.09 ± 0.13 ↑
17.	0.02 ± 0.02	0.01 ± 0.002 ↓	0.086 ± 0.05 ‡ ↑	0.02 ± 0.003 ‡↑	0.011 ± 0.001 ↑

Table 4.Numerical summary of the detailed differences in the bandwidths of control and treated groups. The values are the means ± SEM for each group. Man-Whitney U-test was used to compare the groups. The degree of significance was donated as *, ‡ P < 0.05; **, ‡‡ P < 0.01 and ***, ‡‡‡ P < 0.001. The upward arrow indicates an increase and the downward arrow indicates a decrease. The ddiabetic group were compared with respect to the control group. The Selenium treated groups were compared with respect to the diabetic group.

Bands	Control (n=10	Diabetic (n=7)	HDSE (n=5)	MDSE (n=8)	LDSE (n=8)
CH$_2$ ASYM	9,44 ± 3,03	8,89 ± 3,68 ↓	7,61 ± 3,69 ↓	9,07 ± 3,46 ↑	9,08 ± 3,07 ↑
CH$_2$ SYM	9,64 ± 3,89	6.97 ± 1,73 ↓ *	10,13 ± 0,6 ↑ ‡‡	9,08 ± 0.2 ↑ ‡‡	11,68 ± 4,4 ↑ ‡‡‡

Table 5.The summary of the differences in lipid to protein ratios between the control, diabetic and treated groups for kidney brush-border plasma membranes. The values are the means ± SEM for each group. Man-Whitney U-test was used to compare the groups. The degree of significance was donated as *, ‡ $P < 0.05$; **, ‡‡ $P < 0.01$ and ***, ‡‡‡ $P < 0.001$. The upward arrow indicates an increase and the downward arrow indicates a decrease. The ddiabetic group was compared with respect to the control group. Selenium treated groups were compared with respect to the diabetic group.

Ratio of Peak Areas (Lipid to Protein)	Control (n=10)	Diabetic (n=8)	HDSe (n=5)	MDSE (n=8)	LDSe (n=8)
CH$_2$SYM / CH$_3$SYM	1,35 ± 0,12	1,26 ± 0,45 ↓	1,25 ± 0,03 ↓	1,18 ± 0,15 ↓	1,73 ± 0,1 ↑ ‡‡‡
CH$_2$ ASYM / CH$_3$ SYM	7,52 ± 0,5	4,46 ± 0,5 ↓ ***	2,94 ± 0,1 ↓ ‡‡	2,62 ± 0,22 ↓ ‡‡‡	6,19 ± 0,23 ↑ ‡‡‡
CH$_2$ASYM + CH$_2$SYM / CH$_3$SYM	8,67 ± 0,82	5,85 ± 0,72 ↓ ***	4,19 ± 0,13 ↓ ‡‡	3,8 ± 0,3 ↓ ‡‡‡	7,92 ± 0,32 ↑ ‡‡‡

Table 6.The summary of the differences in lipid to protein ratios between the control, diabetic and treated groups for kidney brush-border plasma membranes. The values are the means ± SEM for each group. Man-Whitney U-test was used to compare the groups. The degree of significance was donated as *, ‡ P < 0.05; **, ‡‡ P < 0.01 and ***, ‡‡‡ P < 0.001. The upward arrow indicates an increase and the downward arrow indicates a decrease. The ddiabetic group was compared with respect to the control group. The Selenium treated groups were compared with respect to the diabetic group.

Ratio of Peak Areas (Lipid to Protein)	Control (n= 8)	Diabetic (n=8)	HDSe (n=5)	MDSE (n=8)	LDSe (n=8)
CH2 ASYM + CH2 SYM / AMIDE I	1,65 ± 0,37	0,08 ± 0,03 ↓ ***	0,74 ± 0,13 ↑ ‡‡	1,39 ± 0,12 ↑ ‡‡‡	0,9 ± 0,16 ↑ ‡‡‡

Furthermore, cluster analysis was presented to observe the differences among all groups. The results are given in figure 19.

Finally, the second derivative structural analysis of main protein band was presented in order to show structural modifications of diabetic and selenium treated groups.

58
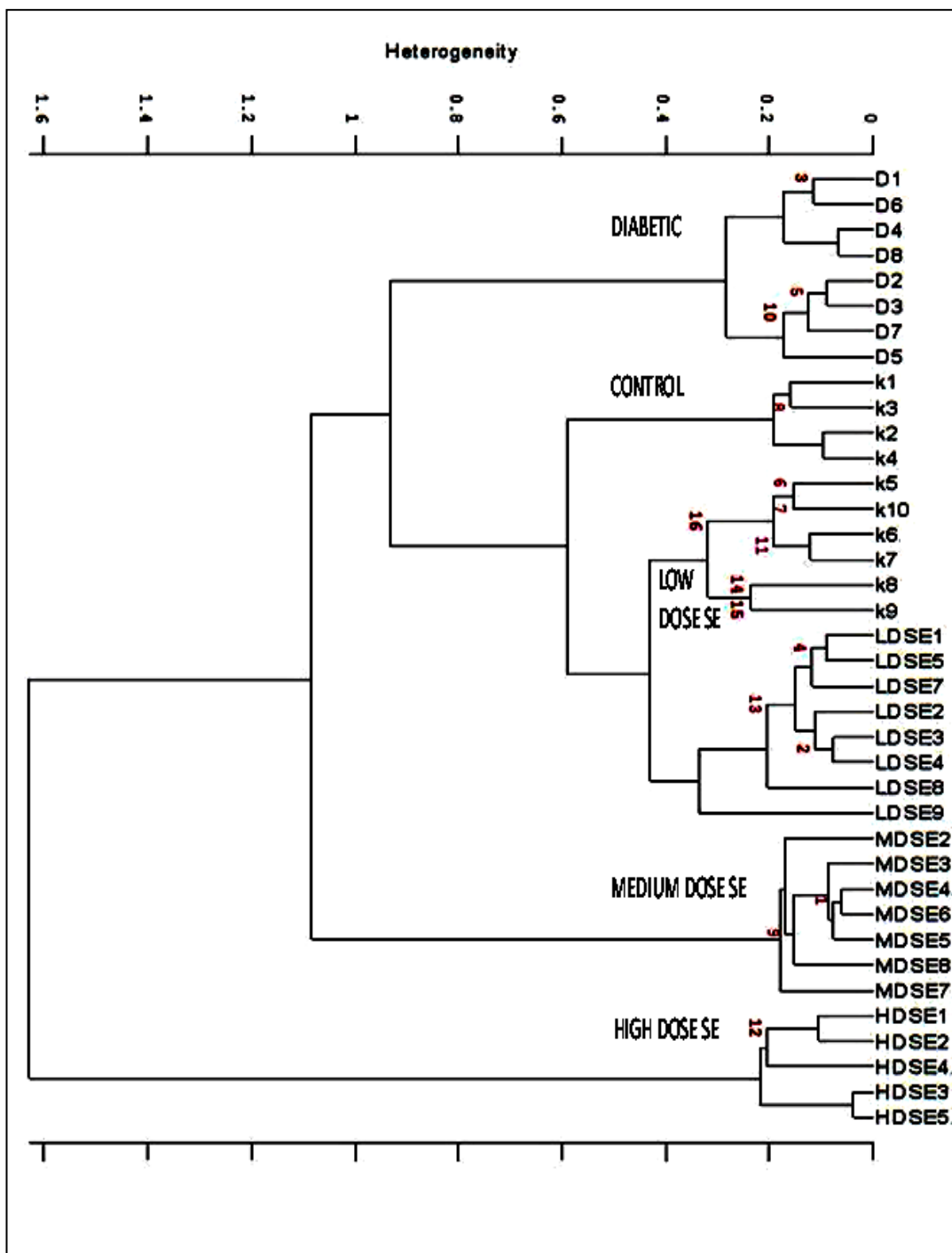
Figure 19.Hierarchical clustering of all groups of kidney cell membrane using second derivative spectra (spectral range: 3020- 950 cm^{-1}).

3.2 Effect of Diabetes on Rat Kidney Plasma Membranes

In order to see the effect of diabetes on kidney cell membranes, the band frequency, band area and bandwidth value changes of normal and diabetic samples will be discussed in detail in this part of research. Table 2, 3 and 4 summarized all obtained data.

3.2.1 Effect of Diabetes on Rat Kidney Plasma Membranes in the C-H Region (3020-2800 cm^{-1})

As can be seen from the Figure 20 the diabetes induced several alterations in the spectral bands in the 3020 cm^{-1} - 2800 cm^{-1} region. These regions represent mainly lipids of cell membrane, more precisely, the C-H stretching vibrational modes of fatty acyl chains of lipids. The spectra were normalized with respect to the CH$_2$ asymmetric stretching band.
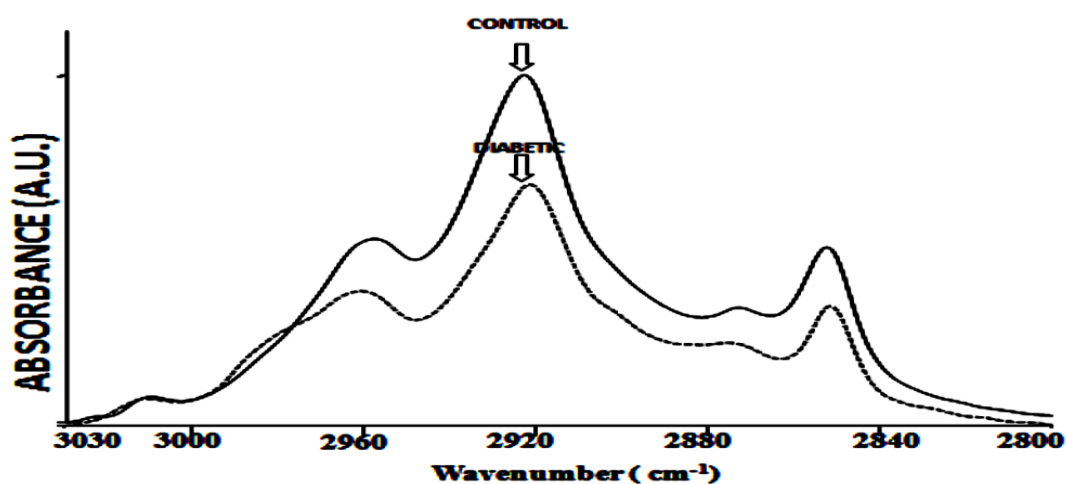
Figure 20.The representative infrared spectra of control and diabetic kidney brush-border plasma membranes in the 3030-2800 cm^{-1} region (The spectra were normalized with respect to the olefinic = CH band at 3011 cm^{-1}).

The band positioned at 3011 cm^{-1} represents H-C=C-H vibrational stretching's of lipid molecules. The bands centered at 2962 cm^{-1}, 2923 cm^{-1}, 2873 cm^{-1} and 2853 cm^{-1} monitor CH$_3$ asymmetric, CH$_2$ asymmetric, CH$_3$ symmetric and CH$_2$ symmetric stretching vibrations, respectively (Melin et al. , 2000 ; Chang and Tavaka, 2002 ; Cakmak et al. , 2003 ; Severcan et al. , 2003 ; Cakmak et al. , 2006). Phospholipids acyl chain unsaturation can be monitored by evaluation of the intensity value of 3011 cm^{-1} band.   No significant variations wea observed in the frequency of this band due to diabetes. The area of olefinic band was increased significantly in diabetic group (P < 0.001) (see the figure 21).

The degree of conformational modifications is closely related to the frequency shifts of the CH$_2$ stretching vibrational modes. For this purpose, the CH$_2$ stretching vibrations in the system can assist to obtain trans/gauche isomerization in the lipid acyl chain. (Mantsch et al., 1984; Severcan, 1997; Bizeau et al., 2000). An increase in the frequency of the CH$_2$ stretching band implies an increase in the number of gauche conformers in the fatty acyl chains (Severcan 1997 ; Rana et al. , 1990 ; Schultz et al. , 1991 ; Melin et al. , 2000 ; Cakmak et al. , 2003 ; Cakmak et al. , 2006).

The CH$_3$ asymmetric, CH$_2$ asymmetric, CH$_2$ symmetric stretching bands arise from the vibration of the related functional groups in lipid molecules. However, CH$_3$ symmetric stretching band monitors proteins (Mantsch, 1984 ; Severcan et al. , 1997 ; Severcan et al. , 2000 ; Severcan et al. , 2003 , Cakmak et al. , 2006) .

The area under the CH$_3$ asymmetric band decreased insignificantly, but the CH$_2$ asymmetric band area decreased significantly (p < 0.001 ***) (see the Figure 22). The peak area of thee CH$_3$ symmetric stretching band increased significantly (p < 0.001 ***). The CH$_2$ symmetric band frequency and band area were both decreased significantly in diabetic group (p < 0.001 ***).
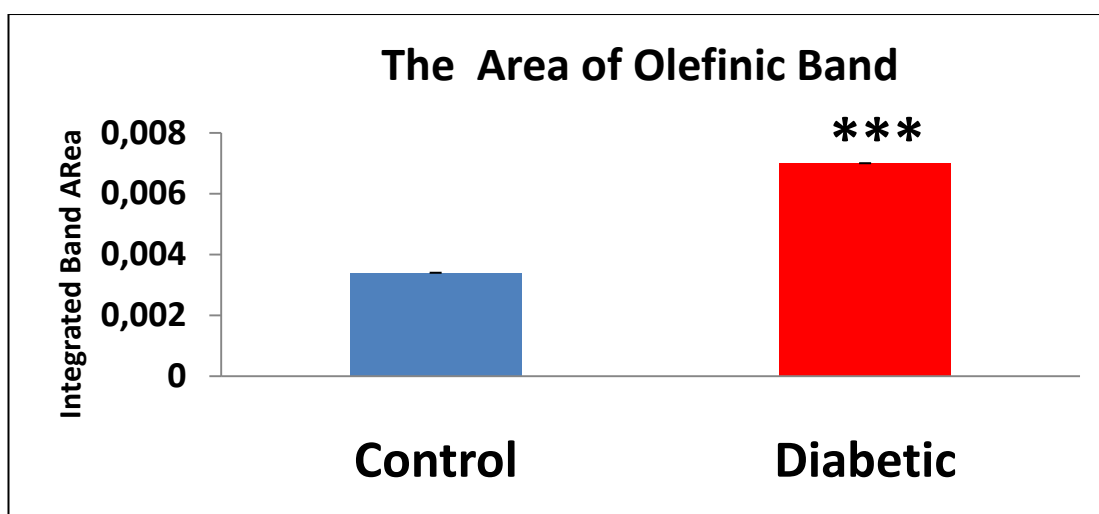
Figure 21.The comparison of Olefinic band area (3011 cm^{-1}) between the control and diabetic groups. * show significances p < 0. 05, *** show significance p < 0.001.
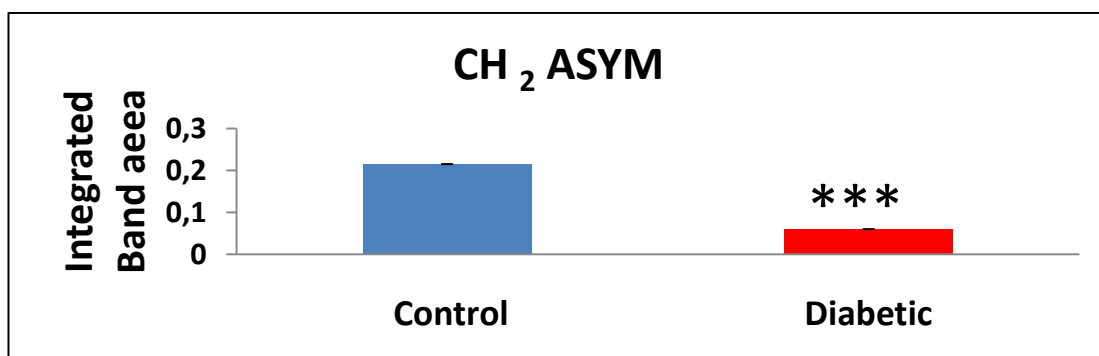
Figure 22.The comparison of CH$_2$ asymmetric band area (2923 cm^{-1}) between the control and diabetic groups. * show significances p< 0.05 *** show significance p<0.001.

The bandwidth values give information about membrane dynamics. The bandwidth value of the CH$_2$ asymmetric band diminished insignificantly during diabetes. However, the bandwidth value of the CH$_2$ symmetric band decreased significantly during diabetes as represented in figure 23 and Table 4.
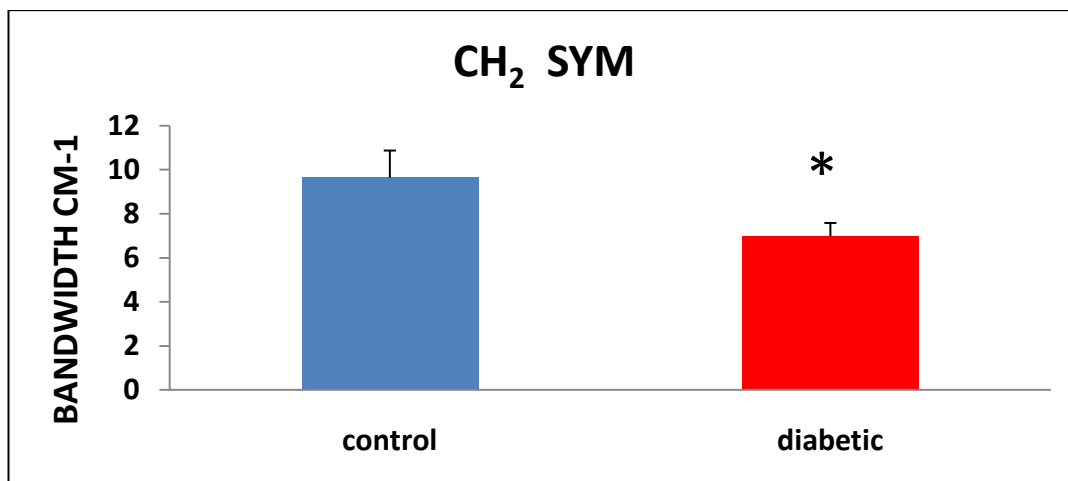
Figure 23.The comparison of bandwidth value of the CH_2 symmetric band between control and diabetic groups. The values are the means ± SEM for each group. Man-Whitney U-test was used to compare the groups. The degree of significance was donated as * $P < 0.05$. The ddiabetic group was compared with respect to control group.

In order to see accurately spectral differences between the control and diabetic group the results of cluster analysis was demonstrated in Figure 24.
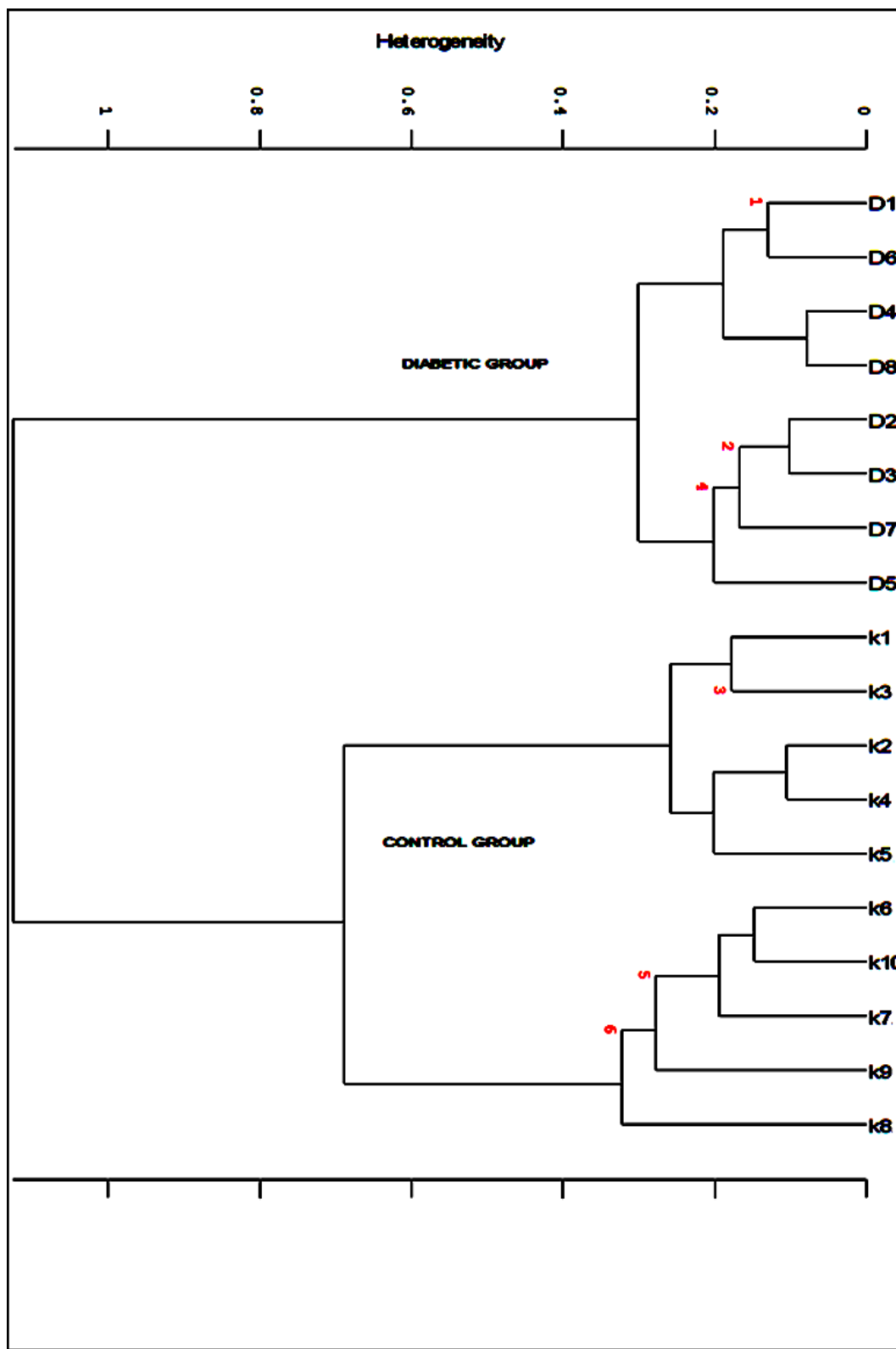
Figure 24.Hierarchical clustering of control and diabetic groups of kidney
Cell membrane using second derivative spectra (spectral range: 3020-950 cm^{-1}).

As seen from the figure diabetic group was succesfully differentiated from the control group with high success (8 / 8 for diabetic, 10 / 10 for control) .

One of the important factor that alters the membrane structure and dynamics is the concentration of proteins and lipids of the membranes (Szalontai et al. , 2000) . A lipid to protein ratios can be calculated precisely by measuring the ratio of the band areas emerging from proteins and lipids. From the Figure 25, 26, 27 and 28 one can see that the band area of the CH_2 asymmetric (lipids) band to CH_3 symmetric (proteins) band and the sum of the areas of these bands to the area of CH_3 symmetric band were calculated. Furthermore, the ratio of the area of the CH_2 symmetric stretchings to the CH_3 symmetric stretchings was calculated. Finally the sum of the areas of the CH_2 asymmetric and symmetric bands to the area of amide I band was calculated (Figure 29, 30 and Table 6) . The results show significant decrease in the lipid to protein ratios, for diabetic state ($p < 0.001$ ***) .
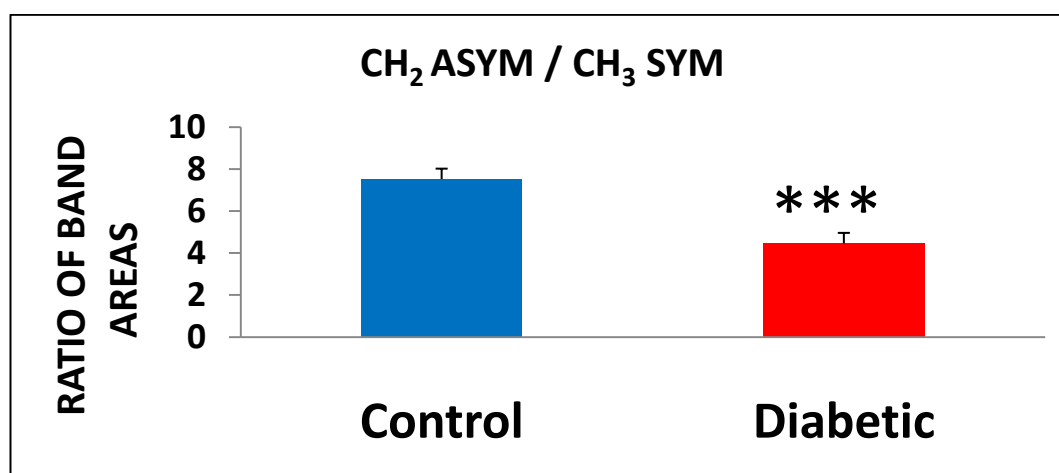
Figure 25.Comparison of band area ratios of the CH_2 asymmetric band to the CH_3 symmetric band among the control and diabetic groups. * show significances $p < 0.001$.
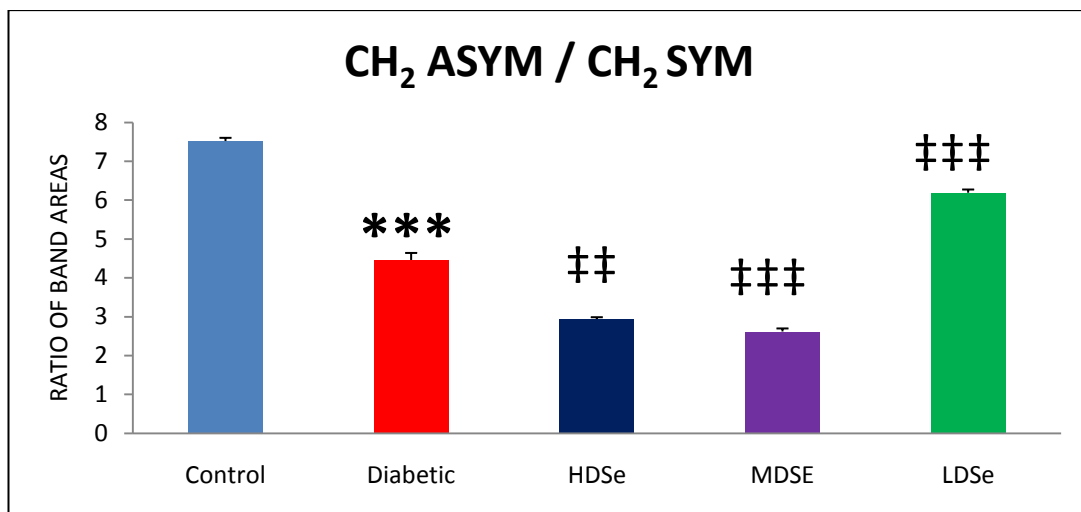
Figure 26.Comparison of band area ratios of the CH_2 asymmetric band to the CH_3 symmetric band among the control, diabetic and selenium treated groups. *, ‡ show significances p < 0.001.
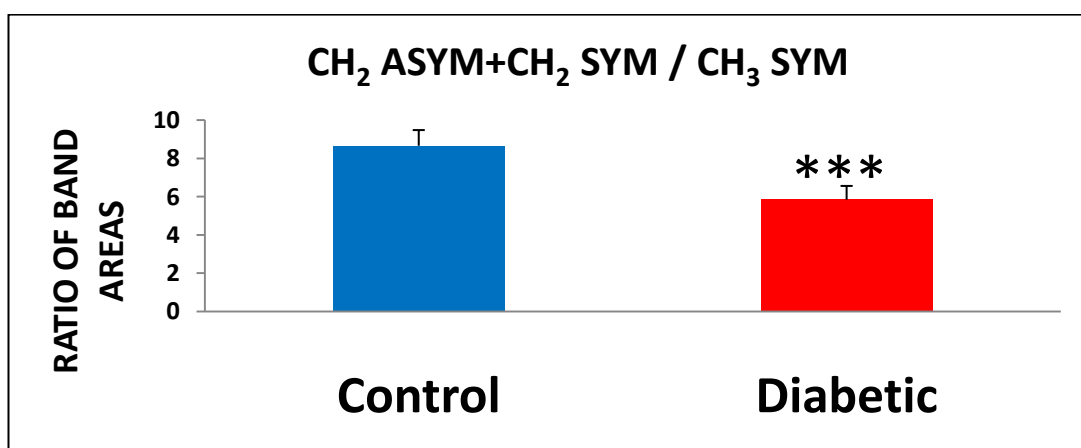
Figure 27.Comparison of band area ratios of the sum of the CH_2 asymmetric and the CH_2 symmetric bands to the CH_3 symmetric band among the control and diabetic groups. (* show significances of p < 0.001)
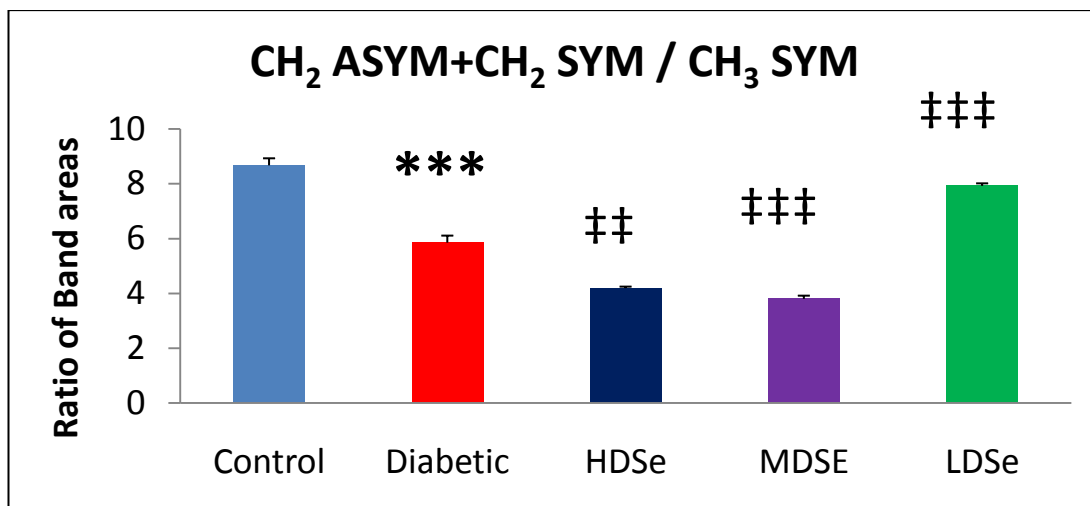
Figure 28. Comparison of band area ratios of the sum of the CH_2 asymmetric and the CH_2 symmetric bands to the CH_3 symmetric band among the control, diabetic and selenium treated groups. The degree of significance was donated as **, ‡‡ $P < 0.01$ and ***, ‡‡‡ $P < 0.001$.
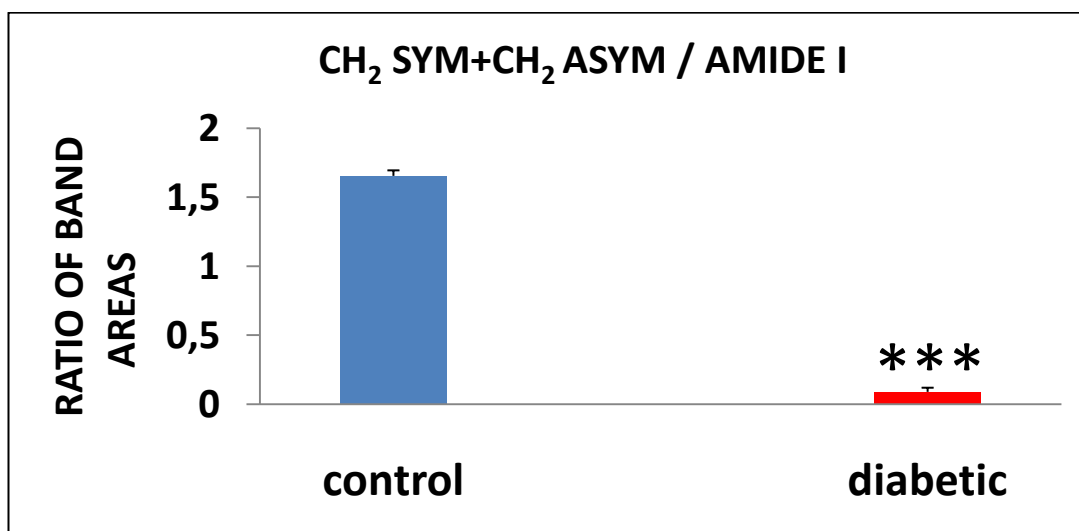
Figure 29. Comparison of band area ratios of the sum of the CH_2 asymmetric and the CH_2 symmetric bands to the amide I band among the control and diabetic groups. The degree of significance was donated as *** $P < 0.001$.
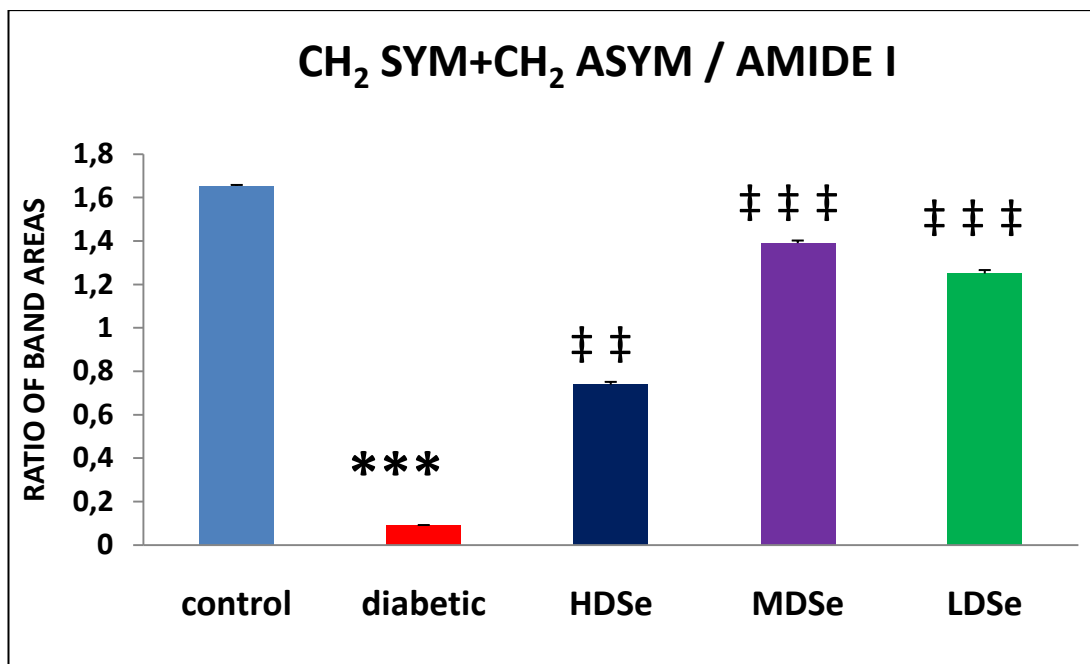
Figure 30.Comparison of band area ratios of the sum of the CH_2 asymmetric and the CH_2 symmetric bands to the amide I band among all groups. The degree of significance was donated **, ‡‡P < 0.01 and ***, ‡‡‡ P < 0.001.

3.2.2 Effect of Diabetes on Rat Kidney Plasma Membranes in the Finger-Print Region (1750-950 cm^{-1}).

The each fingerprint region of spectra was normalized according to amade I band. The results are compared statistically using Mann-Whitney U test. As shown in the Figure 31, there are several peaks arising from different macromolecules in this region. The bands giving important information will be discussed in this part of the research.
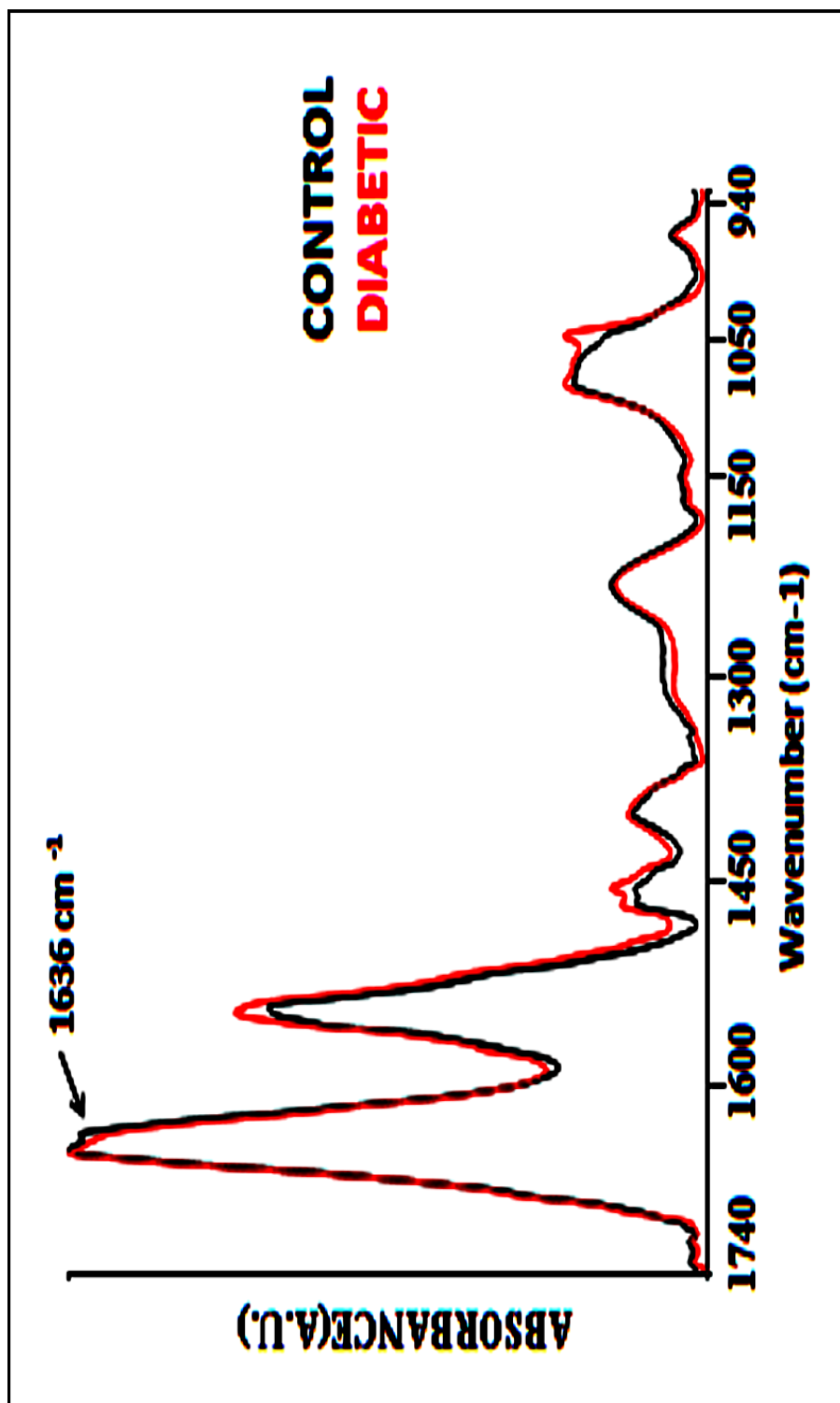
Figure 31.The representative infrared spectra of the control and diabetic kidney brush-border plasma membranes in the 1750-950 cm^{-1} region (The spectra were normalized with respect to the amade I band at 1652 cm^{-1}).

The band at 1731 cm^{-1} is due to the C=O stretching vibrations of esters of phospholipids, cholesterol and hemicelluloses (Dighton, 2001; Melin et al., 2000). In diabetic group no significant shift was observed in the frequency of this band.

The band centered at 1652 cm^{-1} was assigned as amide I which is the main protein band. No significant changes occured in this band during diabetes. We observed another band at 1636 cm^{-1} position in the amide I, but no significant changes occured in this band during diabetes (Figure 31).

The band at 1546 cm^{-1} was assigned as amide II. During diabetes, the frequency of amide II shifted to lower value from 1546.37 ± 0.3 to 1546.03 ± 0.2 significantly ($p < 0.05$ *). Peak area of this band decreased significantly ($p < 0.001$ ***) (see the Figure 42).

The band at 1468 cm^{-1} was assigned as CH$_2$ scissoring mode of lipids. The band centered at 1455 cm^{-1} was considered to be arisen from CH$_2$ bending vibration modes of lipids with little participation of proteins (Manoharan et al., 1993; Cakmak et al., 2003). No significant spectral changes were observed for these bands in diabetic group.

The band positioned at 1400 cm^{-1} was assigned to the COO- symmetric stretching vibrations of fatty acids and amino acids side chains (Jackson et al ., 1998 ; Cakmak et al ., 2003 ; Cakmak et al ., 2006 ; Ozek et al ., 2009). The band located at 1233 cm-1 was considered as hydrogen-bonded PO$_2$- asymmetric stretching groups of phospholipids (Rigas et al., 1990; Wong et al., 1991). No significant alterations were observed for these bands, in diabetic group.

The band centered at 1085 cm^{-1} was assigned to PO$_2$- symmetric stretching vibrations of phospholipids (Ozek et al ., 2009 ; Lyman et al ., 2001 ; Banyan et al ., 2003) . The band frequency significantly shifted to higher value from $1084.95 \pm$

0,75 cm^{-1} to 1085.82 ± 0.96 cm^{-1} (p < 0.05*). The band area decreased insignificantly.

The band at 1045 cm^{-1} was considered as C-O stretching vibration modes of polysaccharides (Melin et al., 2000; Toyran et al., 2006; Cakmak et al., 2006). The frequency of this band shifted to a lower value insignificantly. However, the area under this band increased significantly (p < 0.001 ***).

The band located at 972 cm^{-1} was assigned to symmetric stretching's of dianionic phosphate monoesters (Ci et al ,1999 ; Chiriboga et al. , 2000 ; Cakmak et al. , 2003) and ribose-phosphate main chain vibrations of the RNA backbone (Banyay et al. , 2003, Tsuboi et al. ,1969). No significant variations were observed for this band in diabetic group.

3.3 Effect of Selenium on Diabetic Rat Kidney Plasma Membranes

We have discussed the effect of diabetes on healthy kidney plasma membranes in previous parts of the study. The alterations of the diabetic kidney cell membranes caused by Selenium will be summarized in this part. The changes in the band frequency, band area and bandwidth values of selenium treated diabetic groups against diabetic group will be discussed in detail. Table 2, 3 and 4 include all data.

3.3.1 The Effect of Selenium on Diabetic Rat Kidney Plasma membranes in the C-H region

The figure 32 represents comparison of spectra among all groups in the C-H strectling region. The frequency of olefin band slightly shifted to lower value in both high selenium treated and low selenium treated diabetic groups with respect to diabetic group. However, the frequency of selenium treated group at medium dose shifted significantly to high value from 3013.25 ± 2.32 cm^{-1} to 3017 ± 0, 007 cm^{-1} (p <0.05 ‡). The band area of this band increased significantly in high and medium dose

71

selenium treated groups ($p < 0.05$ ‡; $p < 0.01$ ‡‡). We found that the band area of this band was decreased significantly in low dose selenium treated group (Figure 33). The frequency of the CH_3 asymmetric stretching band slightly shifted to higher value in both high selenium treated and low selenium treated diabetic groups with respect to diabetic group. The band area of this band decreased significantly in low dose selenium treated diabetic groups ($p < 0.05$ ‡). However, the area of olefinic band was increased significantly in high dose and medium dose selenium treated diabetic groups.

The frequency of the CH_2 asymmetric stretching band significantly shifted to higher value in both low and high selenium treated diabetic groups with respect to diabetic group ($p < 0.05$ ‡). However it shifted to lower value in the selenium treated diabetic group at medium dose. The area under this band increased drastically in all selenium treated diabetic groups ($p < 0.05$ ‡) (see the Figure 34). The frequency of the CH_3 symmetric stretching band slightly shifted to lower value in all selenium treated diabetic groups with respect to diabetic group. The band area was increased significantly in all selenium treated diabetic groups ($p < 0.05$ ‡).

The frequency of CH_2 symmetric stretching band significantly shifted to higher value in all selenium treated diabetic groups with respect to diabetic group (see the Figure 35). The band area was increased significantly in all selenium treated diabetic groups ($p < 0.05$ ‡) (see the Figure 36). The bandwidth of CH_2 symmetric stretching band increased significantly in all selenium treated groups (Figure 37 and Table 4).
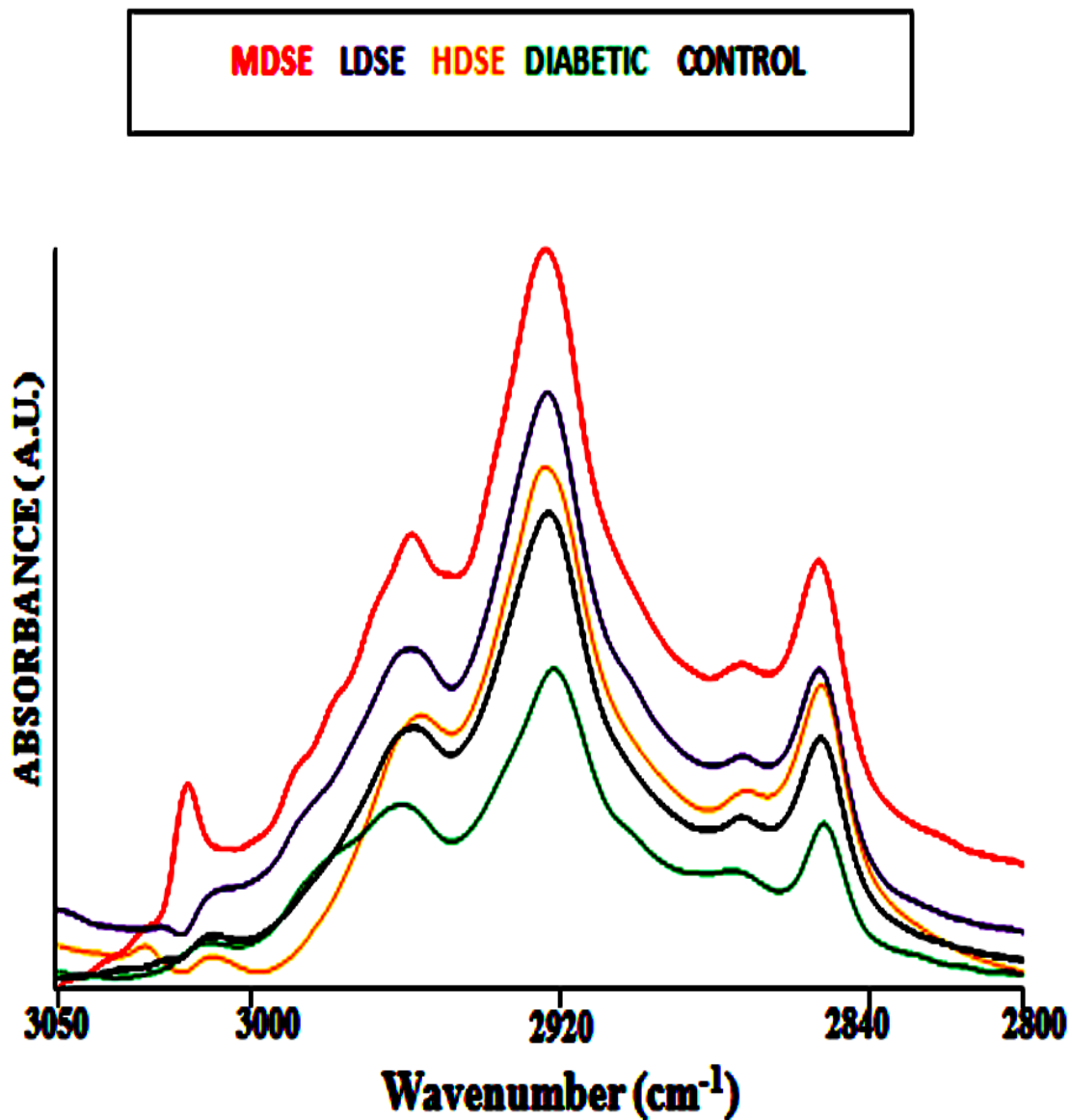
Figure 32.The representative comparison of the Control, Diabetic and Selenium treated diabetic groups of rat kidney plasma membrane at the C-H region (3020-2800 cm $^{-1}$) .
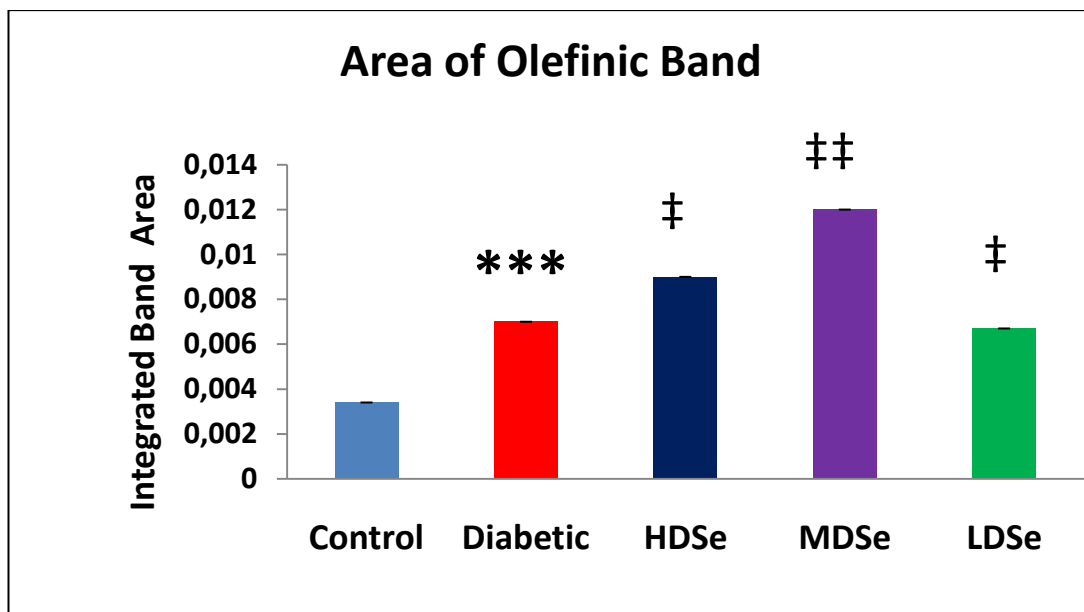
Figure 33.The comparison of Olefinic band area (3011 cm$^{-1)}$) between the control, diabetic and selenium treated groups. *, ‡ show significances of p < 0.05, ***, ‡‡‡ show significance of p < 0.001.
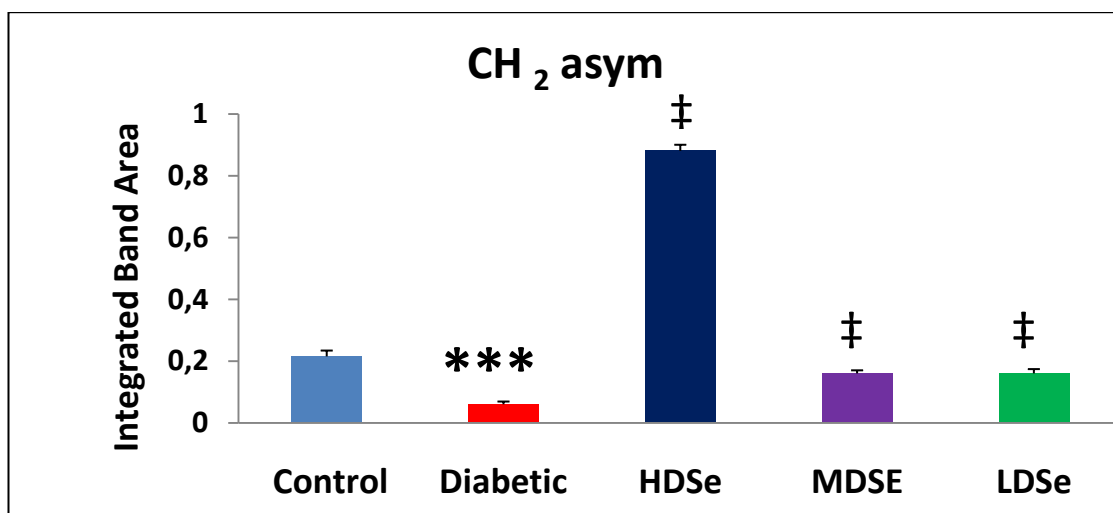
Figure 34.The comparison of CH$_2$ asymmetric stretching band area (2923 cm$^{-1)}$) between the control, diabetic and selenium treated groups. The degree of significance was donated as *, ‡ P < 0, 05. The Selenium treated groups were compared with respect to diabetic group.

Table 4.Numerical summary of the detailed differences in the bandwidths of the control and treated groups. The values are the means ± SEM for each group. Man-Whitney U-test was used to compare the groups. The degree of significance was donated as *, ‡ P < 0.05; **, ‡‡ P < 0.01 and ***, ‡‡‡ P < 0.001. The upward arrow indicates an increase and the downward arrow indicates a decrease. Diabetic group was compared with respect to the control group. Selenium treated groups were compared with respect to the diabetic group.

Bands	Control (n=10)	Diabetic (n=7)	HDSE (n=5)	MDSE (n=8)	LDSE (n=8)
CH_2 ASYM	9,44 ± 3,03	8,89 ± 3,68 ↓	7,61 ± 3,69 ↓	9,07 ± 3,46 ↑	9,08 ± 3,07 ↑
CH_2 SYM	9,64 ± 3,89	6.97 ± 1,73 ↓ *	10,13 ± 0,6 ↑ ‡‡	9,08±0.2 ↑ ‡‡	11,68 ± 4,4 ↑ ‡‡‡

Figure 35.The comparison of the CH_2 symmetric stretching band frequency between all groups. The degree of significance was donated as *, ‡ P < 0.05. The Selenium treated groups were compared with respect to diabetic group.
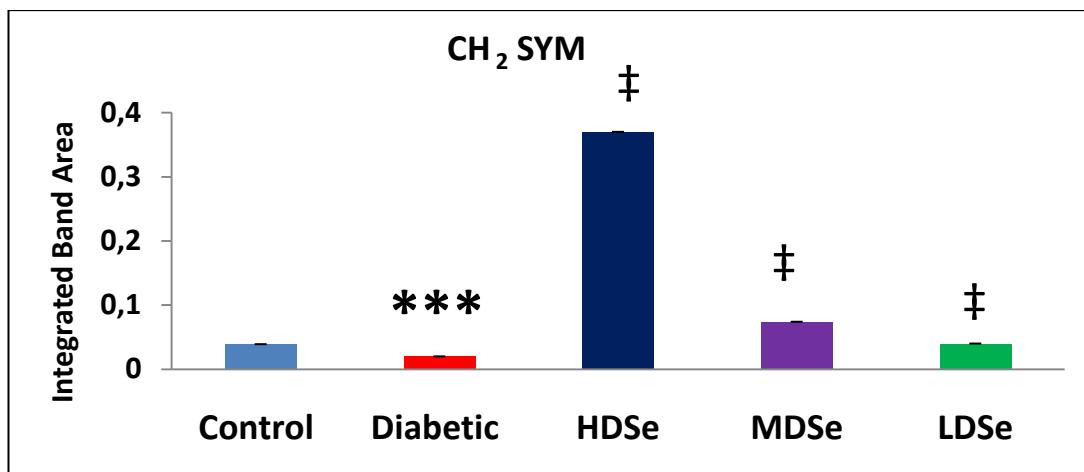
Figure 36. The comparison of the CH_2 symmetric stretching band area between all groups. The degree of significance was donated as *, ‡ $P < 0.05$; **, ‡‡ $P < 0.01$ and ***, ‡‡‡ $P < 0.001$. The Selenium treated groups were compared with respect to diabetic group.
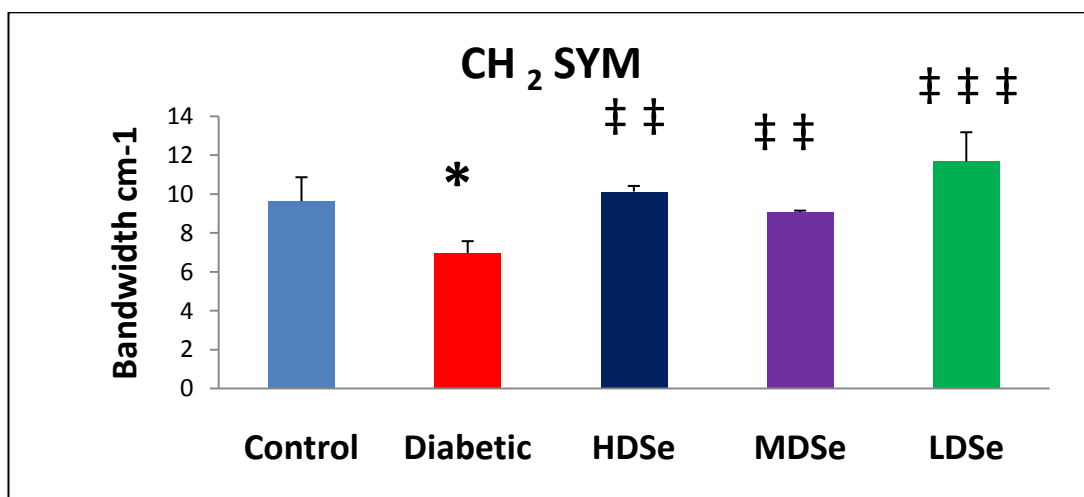
Figure 37.The comparison of bandwidth values of the CH_2 symmetric bands among the control diabetic and selenium treated groups. Man-Whitney U-test was used to compare the groups. The degree of significance was donated as *, ‡ $P < 0.05$; **, ‡‡ $P < 0.01$ and ***, ‡‡‡ $P < 0.001$. The Selenium treated groups were compared with respect to the diabetic group.

The ratio of the CH_2 symmetric band area to the CH_3 symmetric band area was decreased in high and mmedium dose groups. Whilst, it increased significantly in the low dose group ($p < 0.001$ ‡‡‡). The ratio of the CH_2 asymmetric band area to the CH_3 symmetric band area significantly decreased in high and medium dose groups (p

< 0.001 ‡‡‡). However, it increased significantly in low dose group (p < 0.001 ‡‡‡) (Figure 26).

The ratio of the areas of the CH_2 asymmetric and symmetric bands to the area of the CH_3 symmetric band decreased significantly in high and mmedium dose groups (p < 0.001) .We observed a significant increase in this ratio in low dose group (p < 0.001 ‡‡‡) when compared to the diabetic group (Figure 28).

From the Figure 30 and Table 6 we can see that the lipid to protein ratios significantly increased in all selenium treated groups (P < 0.01 and P < 0.001) .

Table 5.The summary of the differences of lipid-to-protein ratios between the control, diabetic and treated groups for kidney brush-border plasma membranes. The values are the means ± SEM for each group. Man-Whitney U-test was used to compare the groups. The degree of significance was donated as *, ‡ P < 0.05; **, ‡‡ P < 0.01 and ***, ‡‡‡ P < 0.001. The upward arrow indicates an increase and the downward arrow indicates a decrease. The diabetic group was compared with respect to the control group. The Selenium treated groups were compared with respect to the diabetic group

Ratio of Peak Areas (Lipid to Protein)	Control (n=10)	Diabetic (n=8)	HDSe (n=5)	MDSE (n=8)	LDSe (n=8)
CH₂SYM / CH₃SYM	$1,35 \pm 0,12$	$1,26 \pm 0,45 \downarrow$	$1,25 \pm 0,03 \downarrow$	$1,18 \pm 0,15 \downarrow$	$1,73 \pm 0,1 \uparrow$ ‡‡‡
CH₂ ASYM / CH₃ SYM	$7,52 \pm 0,5$	$4,46 \pm 0,5 \downarrow$ ***	$2,94 \pm 0,1 \downarrow$ ‡‡	$2,62 \pm 0,22 \downarrow$ ‡‡‡	$6,19 \pm 0,23 \uparrow$ ‡‡‡
CH₂ASYM + CH₂SYM / CH₃SYM	$8,67 \pm 0,82$	$5,85 \pm 0,72 \downarrow$ ***	$4,19 \pm 0,13 \downarrow$ ‡‡	$3,8 \pm 0,3 \downarrow$ ‡‡‡	$7,92 \pm 0,32 \uparrow$ ‡‡‡

Table 6.The summary of the differences of lipid-to-protein ratios between the control, diabetic and treated groups for kidney brush-border plasma membranes. The values are the means ± SEM for each group. Man-Whitney U-test was used to compare the groups. The degree of significance was donated as *, ‡ $P < 0.05$; **, ‡‡ $P < 0.01$ and ***, ‡‡‡ $P < 0.001$. The upward arrow indicates an increase and the downward arrow indicates a decrease. Diabetic group was compared with respect to control group. The Selenium treated groups were compared with respect to the diabetic group.

Ratio of Peak Areas (Lipid to Protein)	**Control** **(n= 8)**	**Diabetic** **(n=8)**	**HDSe** **(n=5)**	**MDSE** **(n=8)**	**LDSe** **(n=8)**
CH_2 ASYM + CH_2SYM /AMIDE I	$1,65 \pm 0,37$	$0,08 \pm 0,03$ ↓ ***	$0,74 \pm 0,13$ ↑ ‡‡	$1,39 \pm 0,12$ ↑ ‡‡‡	$0,9 \pm 0,16$ ↑ ‡‡‡

Based on these spectral differences cluster analysis was performed to see spectral differences of the C-H region of all groups as displayed in figure 38.
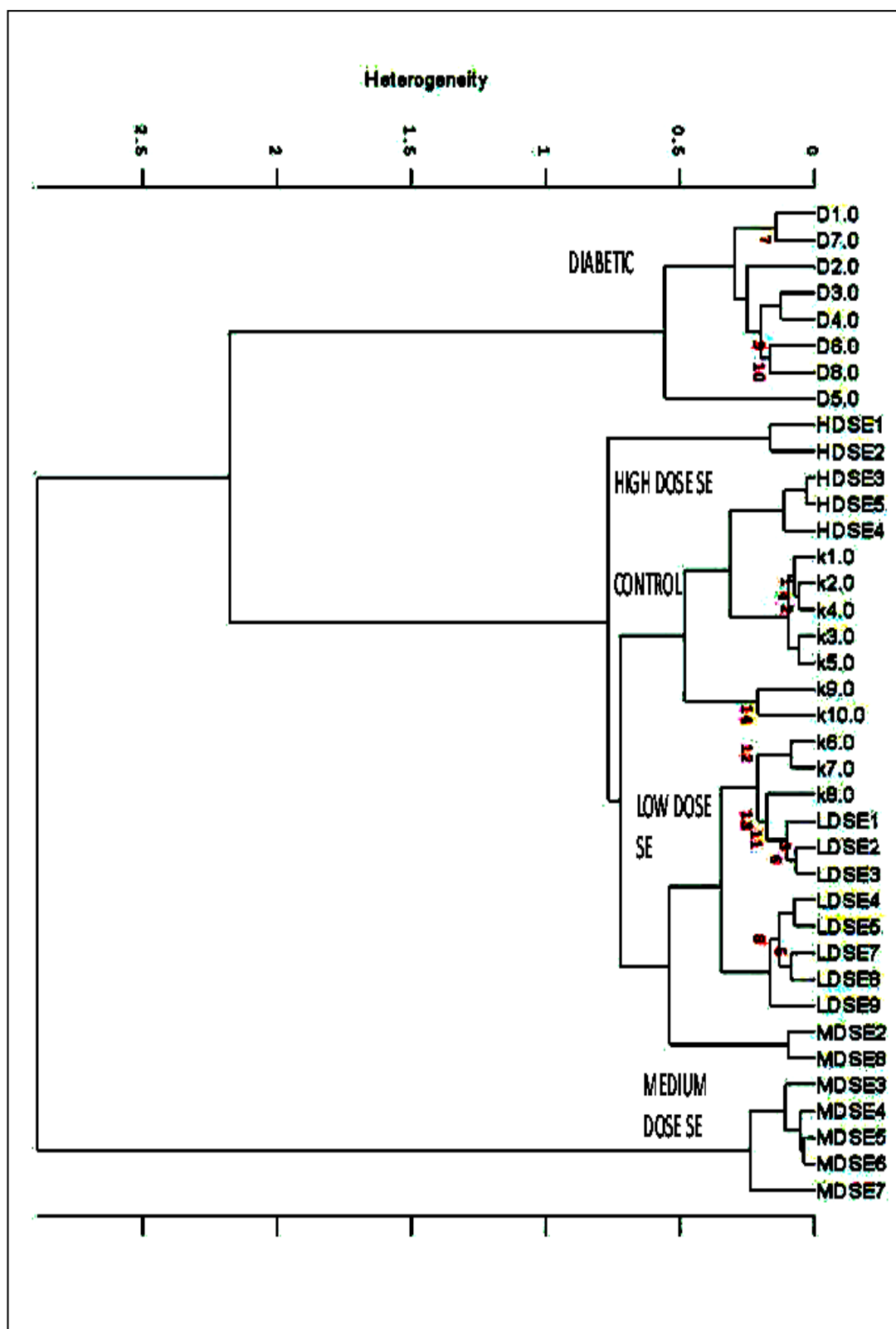
Figure 38.Hierarchical clustering of all groups of kidney cell membrane using second derivative spectra (spectral range: 3020- 2800 cm^{-1}).

As seen from this figure succesful separation of all groups was obtained.

3.3.2. The Effect of Selenium on Diabetic Rat Kidney Plasma membranes in the Finger-Print region

The figure 39 represents comparison of spectra among all groups. The band at 1731 cm $^{-1}$ significantly shifted to lower value from 1732.25 ± 0.4 cm $^{-1}$ to 1730.34 ± 0.8 cm $^{-1}$ in selenium treated diabetic group at high dose ($p < 0.05$). The area under this band significantly increased in all selenium treated groups ($p < 0.05$).

The bands located between 1700- 1600 cm $^{-1}$ correspond to amide I band. Under this band, two peaks located at 1652 cm $^{-1}$ and 1636 cm $^{-1}$ were observed (Figure 40).

The frequency of amide I band significantly shifted to higher wavenumber values from 1651.59 ± 0.4 cm $^{-1}$ to 1652.97 ± 0.008 cm $^{-1}$ in the medium dose selenium group. The band area increased dramatically in high dose selenium group ($p < 0.005$) however, the insignificant changes were observed in both the medium and low dose selenium groups (figure 41).

The frequency of the band at 1636 cm $^{-1}$ increased significantly in all selenium treated groups ($p < 0.05$ *) (Table 2 and 3). The area under this band diminished in both medium and low dose selenium groups ($p < 0.05$), however it increased in the selenium group at high dose ($p < 0.05$) (see the Figure 40).
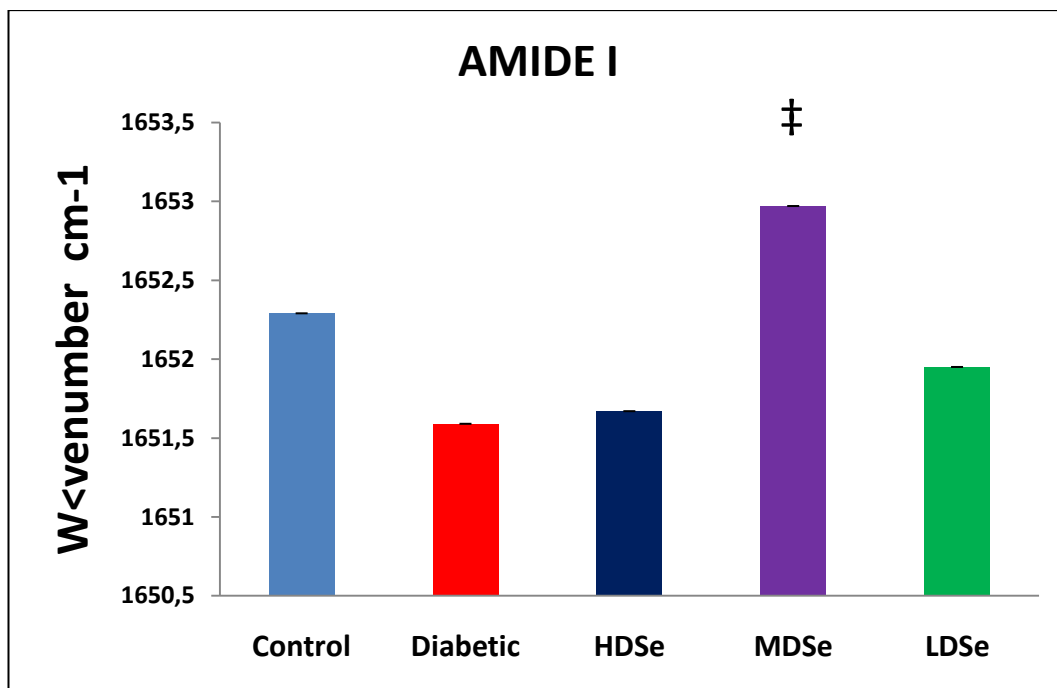
Figure 41.The comparison of amide I band area between the diabetic and selenium treated groups. ‡ show significances $p < 0.05$. The Selenium treated groups were compared with respect to the diabetic group.
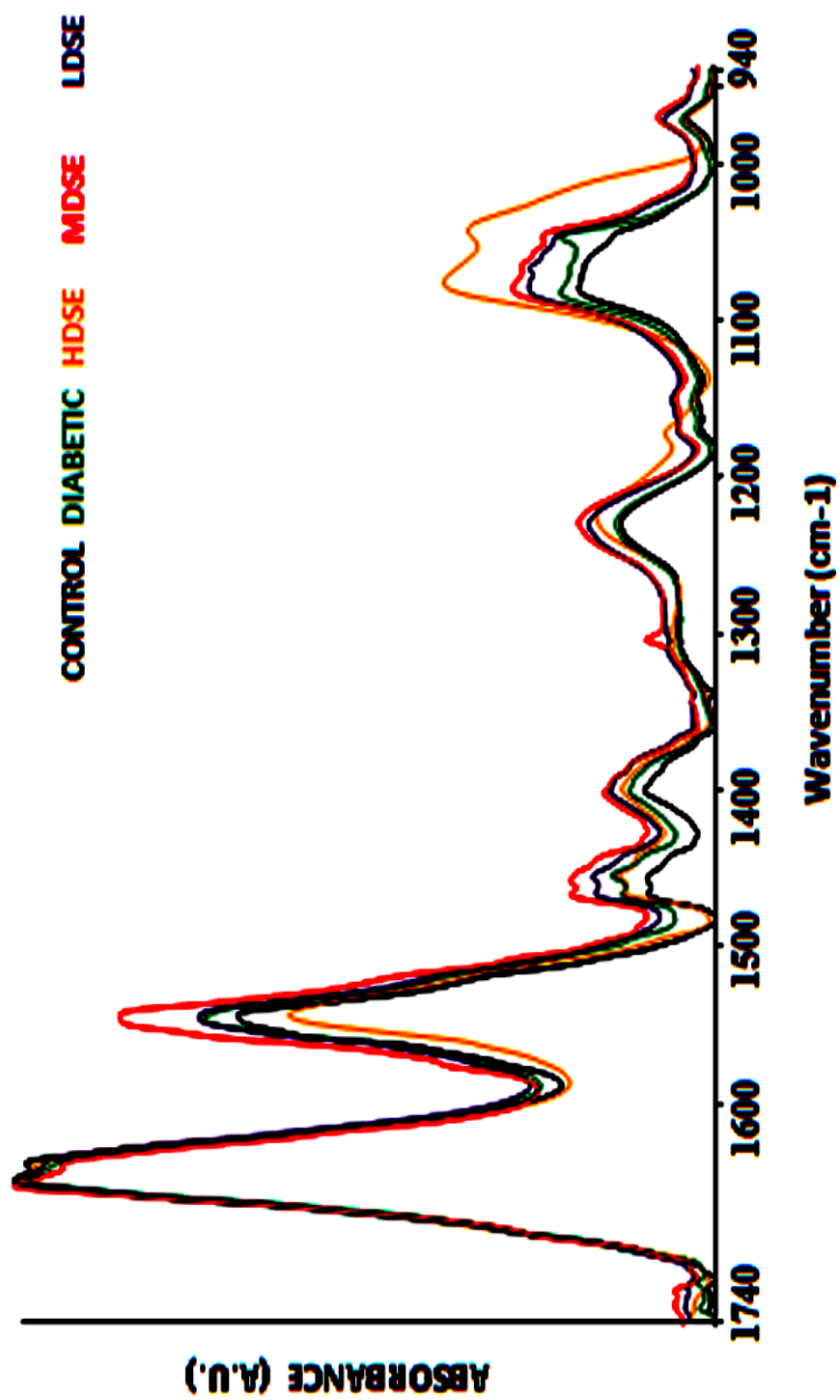
Figure 39.The representative comparison of the infrared sepctra of Control, Diabetic and Selenium treated diabetic groups of rat kidney plasma membrane at Finger-Print region.

83
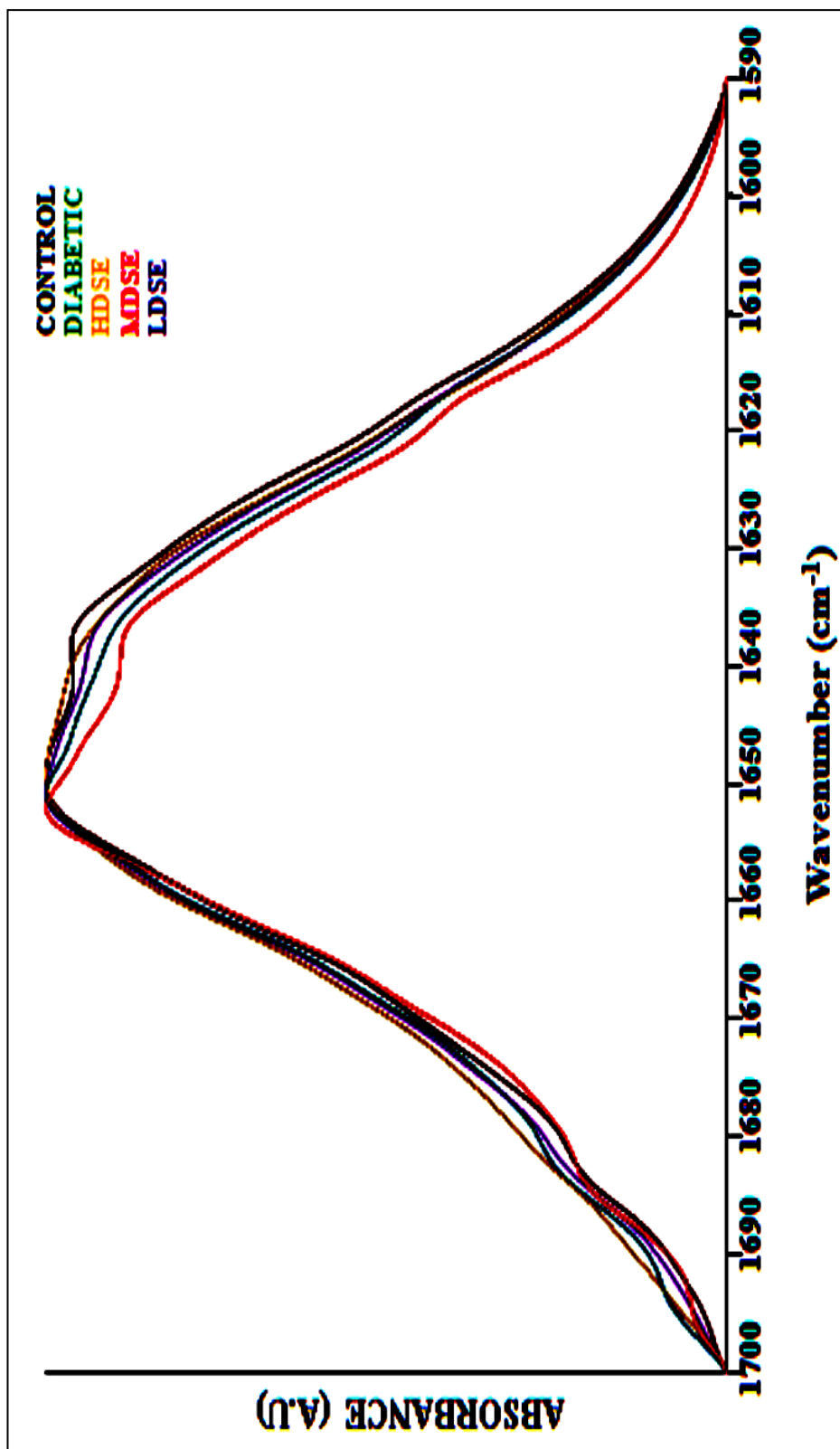
Figure 40.The representative comparison of the infrared spectra of amide I band between all groups.
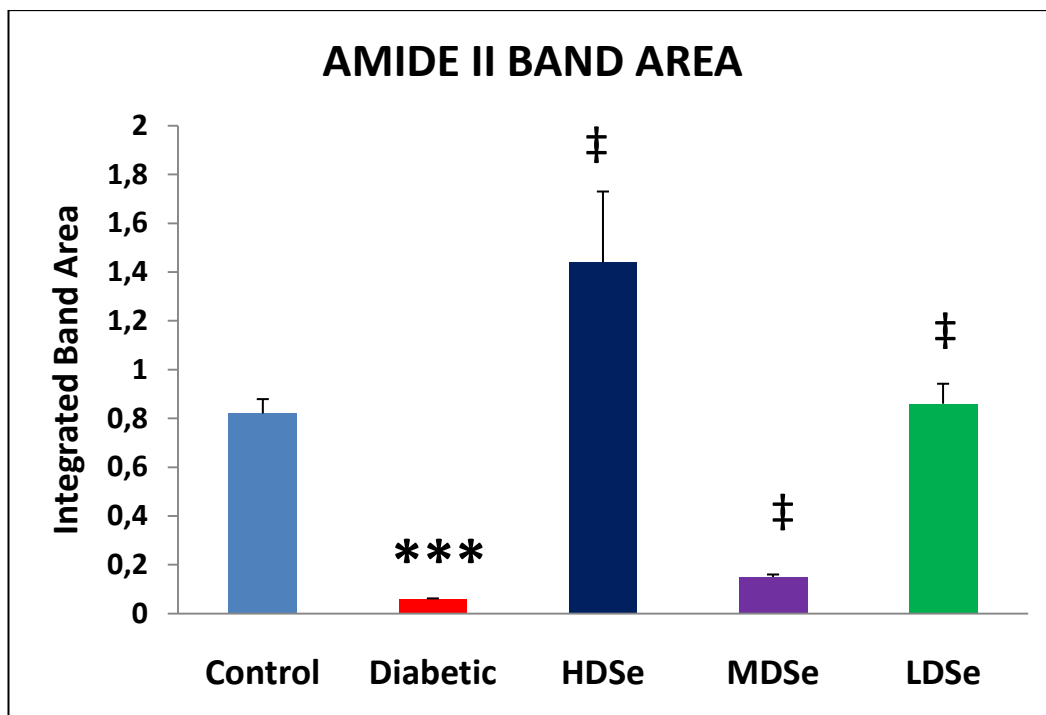
Figure 42.The comparison of band area values of amide II band among groups. The degree of significance were donated as *, ‡ P < 0.05 and ***, ‡‡‡ p < 0.001. The Selenium treated groups were compared with respect to the diabetic group.

As can be seen from the table 2, 3 and 4, the frequency of amide II band dramatically shifted to high values in both medium and low dose selenium-treated diabetic groups (p < 0.05 ‡). The area under amide II band significantly increased in all the selenium treated groups (p < 0.05 ‡) (see the Figure 42).

The band positioned at 1469. 47 ± 0.19 cm^{-1} in diabetic group significantly shifted to lower value in the high and medium dose selenium-treated diabetic groups (p < 0.05 ‡) . The area under this band significantly increased in all selenium treated groups (p < 0.05 ‡) (Table 2 and 3).

The band at 1455.06 ± 0.31 cm^{-1} significantly shifted to lower value for high dose selenium group, however, significantly shifted to higher value in medium dose selenium group (p < 0.05 ‡). The band area broadened significantly in all selenium treated groups (p < 0.05 ‡) (Table 2 and 3).

The band centered at 1398.92 ± 1.86 cm^{-1} in diabetic group insignificantly shifted to higher value in high dose selenium treated group and also shifted to higher value significantly for medium and low doses of selenium ($p < 0.05$ ‡) . The peak area significantly elevated in all selenium treated groups ($p < 0.05$ ‡) (Table 2 and 3).

The band at 1233.59 ± 1.17 cm^{-1} in diabetic group significantly shifted to lower value in selenium treated group at medium dose ($p < 0.05$ ‡) . The area under this band increased significantly for high and low doses of selenium, however we monitored significant decrease in medium dose group ($p < 0.05$ ‡) .

As seen from the table 2 and 3, the band at 1172.34 ± 0.43 cm^{-1} did not vary significantly, but this band shifted to higher value in medium dose selenium treated group, significantly ($p < 0.05$ ‡) . In addition we found that the frequency of this band significantly shifted to lower value in low dose selenium treated group, ($p < 0.05$ ‡) . We observed insignificant variations in the band area for all groups.

The band located at 1085.82 ± 0.96 cm^{-1} significantly shifted to lower value in high dose selenium group ($p < 0.05$ ‡). The area of this band increased dramatically in high and medium dose selenium treated groups ($p < 0.05$ ‡).

The band centered at $1045.78 \pm 0,18$ cm^{-1} was significantly shifted to lower value in high dose and medium dose selenium groups ($p < 0.05$ ‡) . In low dose group this observation was insignificant. The peak area of this band increased in high dose selenium group ($p < 0.05$ ‡). We found insignificant increase in other selenium treated groups (Table 2 and 3).

The band located at 972.45 ± 1.13 cm^{-1} did not change significantly in all groups. However, the area of this band significantly increased in high and medium dose selenium group ($p < 0.05$ ‡).

Based on these spectral differences cluster analysis was performed to see spectral differences of finger-print region of all groups as displayed in figure 43.
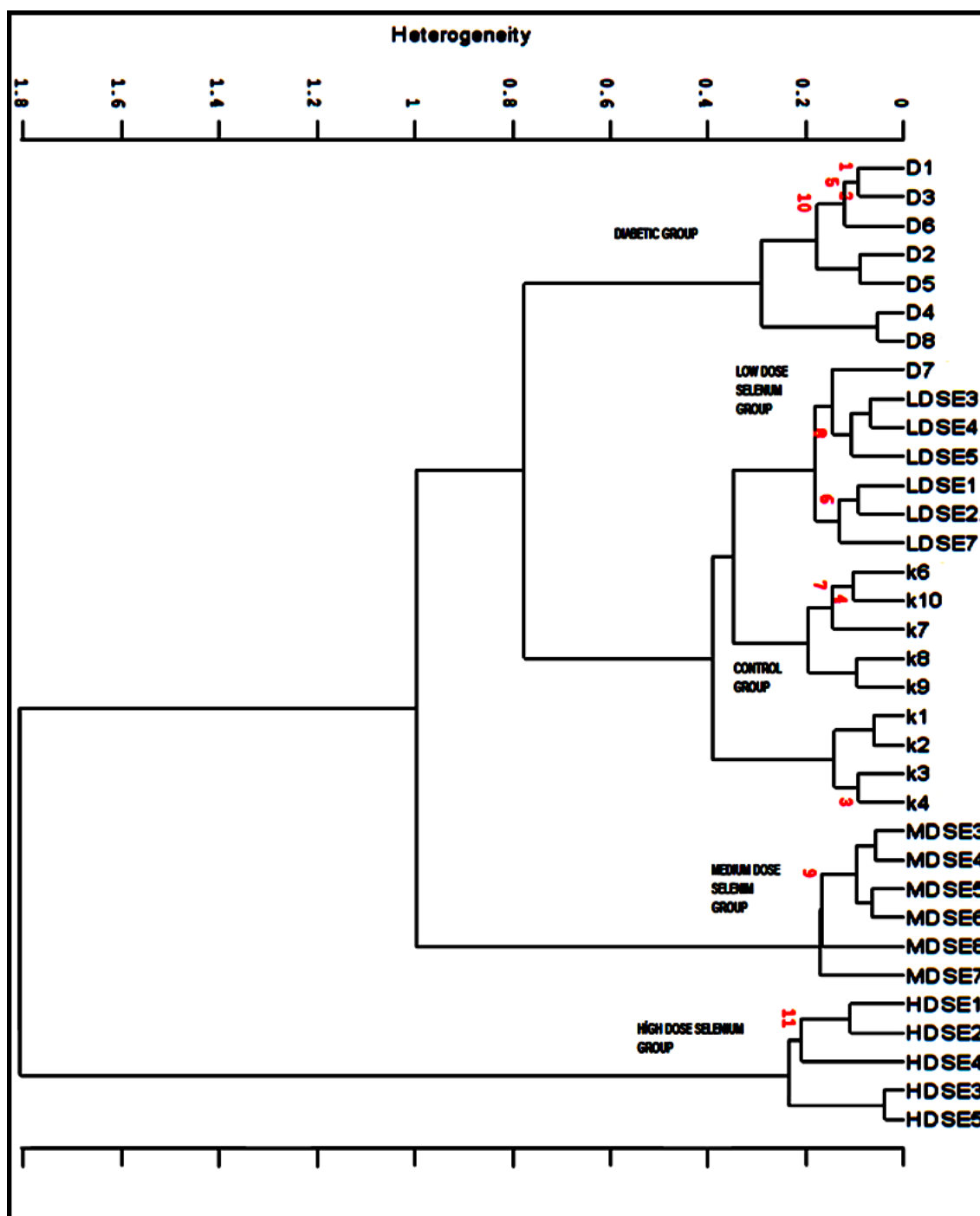
Figure 43.Hierarchical clustering of all groups of kidney cell membrane using second derivative spectra (spectral range: 1750-950 cm^{-1}).

As seen from this figure very succesful separation of all groups was obtained.

3.4 The Second Derivative Secondary Structure Analysis of Main Protein Band (Amide I band).

In order to identify the secondary structural changes of the rat brush-border kidney plasma membrane protein content, amide I was analyzed in detail in this part of the study. Table 7 summarizes the all data of related to the amide I band which includes assignment of the sub-bands and their intensityy values. As can be seen from Figure 44 also, the seven different types of secondary structures are identified.
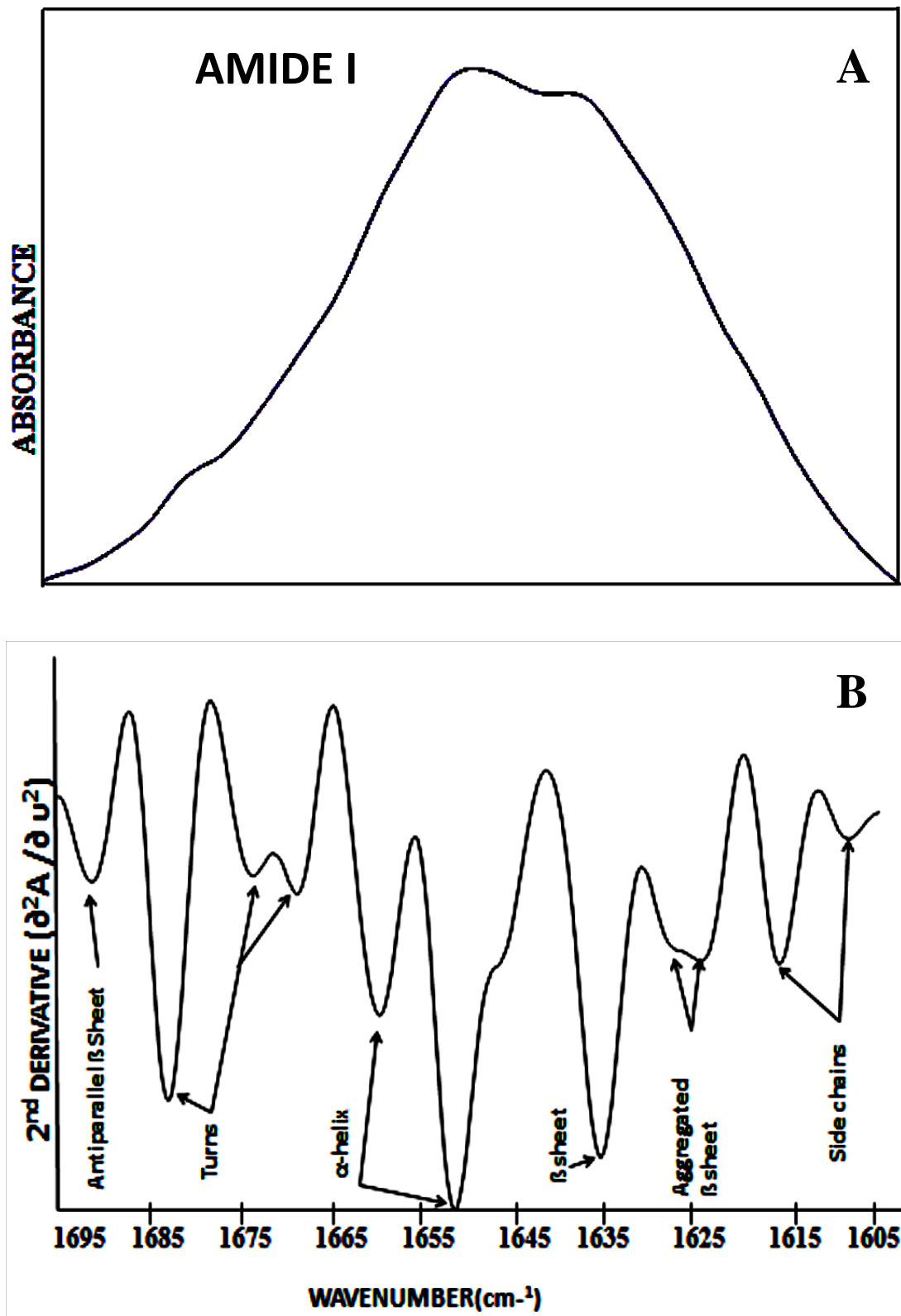
Figure 44.The representative second derivative infrared spectrum of amide I band of control brush-border plasma membrane at $1700^{-1}600$ cm $^{-1}$ region.
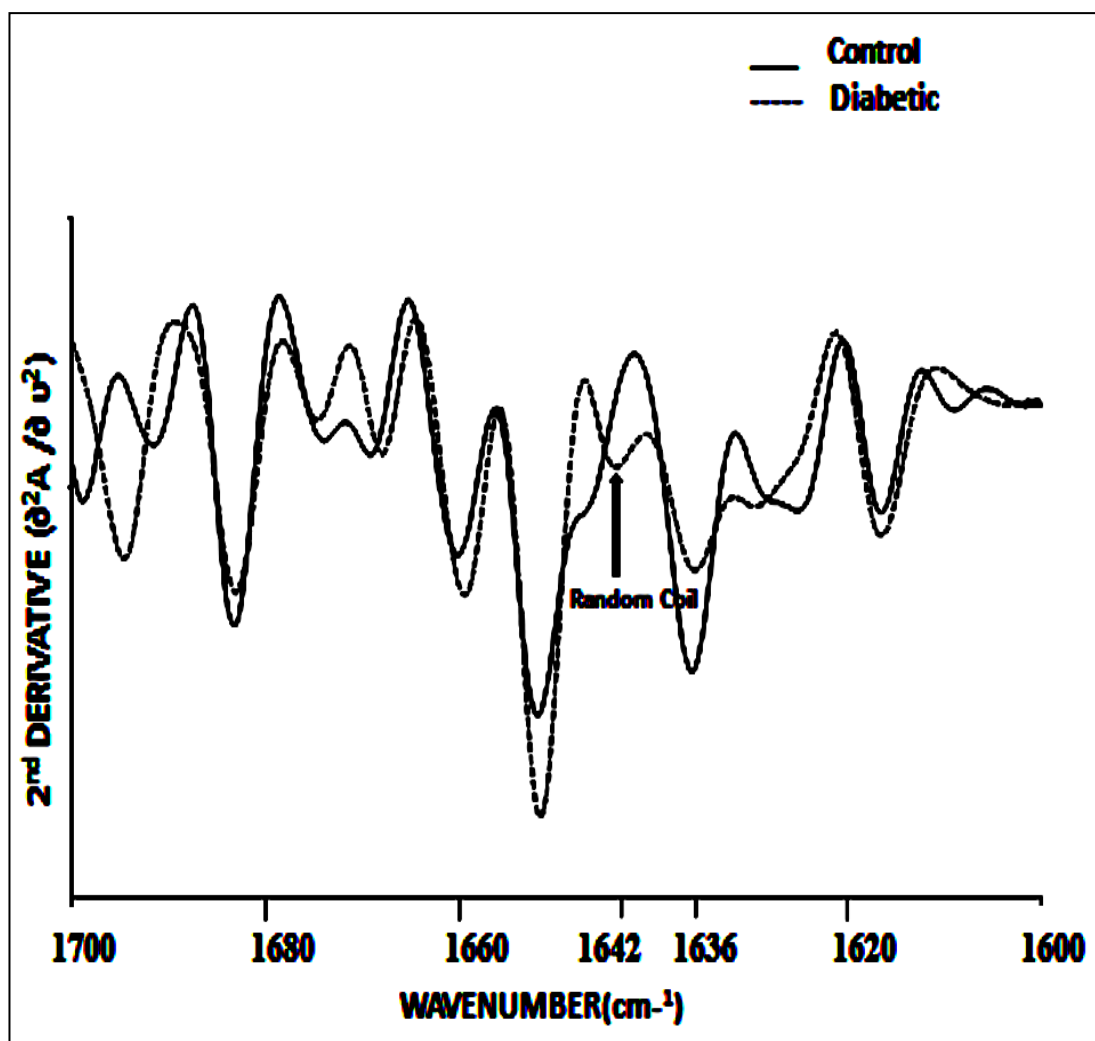
Figure 45.The comparison of second derivative of the amide I band in the average infrared spectraa of the control and diabetic group at 1700-1600 cm $^{-1}$ region.

As seen from the Table 7, the antiparallel ß sheet content of the diabetic samples drastically increased ($p < 0.01$) . In contrast, all selenium treated diabetic groups show dramatic decrease in this value toward the control group ($p < 0.001$). The area under the band of turns also increased significantly in diabetic group ($p < 0.001$) and decreased drastically in all selenium treated diabetic groups ($p < 0.01$) (Figure 45 and Table 7).

Futhermore, the α helix content significantly increased in diabetic group ($p < 0.001$) and decreased significantly in the other groups ($p < 0.01$). As shown in Figure 45

the random coil band was identified only in diabetic group at 1642 cm^{-1}. No significant variations were observed for all the other bands.

Table 7.Intensity changes of the main protein secondary structures between the control, diabetic and treated groups for kidney brush-border plasma membranes. The values are the means ± SEM for each group. Man-Whitney U-test was used to compare the groups. The degree of significance was donated as *, ‡ $P < 0.05$; **, ‡‡ $P < 0.01$ and ***, ‡‡‡ $P < 0.001$. The upward arrow indicates an increase and the downward arrow indicates a decrease. Diabetic group was compared with respect to the control group. The Selenium treated groups were compared with respect to the diabetic group.

Peak number	Secondary Structures	Peak centres (cm-1)	Secondary structure intensity (units)				
			Control (n=10)	Diabetic (n=8)	HDSE (n=5)	MDSE (n=8)	LDSE (n=8)
1	Antiparallel β-sheet	1695	0,04±0,03	0,1±0,03 ** ↑	0,04±0,03 ‡‡↓	0,05±0,03 ‡‡↓	0,05±0,03 ‡‡↓
2	Turns	1685	0,12±0,07	0,12±0,01	0,03±0,01 ‡‡↓	0,1±0,04 ↓	0,08±0,03 ↓
		1677	0,016±0,08	0,07±0,007 ‡‡‡↑	0,05±0,01 ↓	0,04±0,02 ‡‡↓	0,05±0,02 ‡‡↓
		1668	0,08±0,01	0,05±0,007 ‡‡‡↓	0,03±0,01 ↓	0,03±0,02 ‡‡↓	0,06±0,04 ↑
3	α-Helix	1652	0,2±0,08	0,4±0,02 ‡‡‡↑	0,18±0,06 ↓‡‡	0,3±0,1 ↓	0,3±0,1 ↓
4	Random coil	1642		0,03±0,02			
5	β-sheet	1636	0,15±0,09	0,13±0,02↓	0,16±0,05 ↑	0,1±0,06 ↓	0,14±0,09↑
6	Aggregated β-sheet	1626	0,07±0,015	0,04±0,002 ↓	0,1±0,08 ↑	0,1±0,04↑	0,1±0,07 ↑
7	Side Chain	1617	0,04±0,03	0,08±0,03 ↑	0,05±0,04 ↓	0,06±0,03 ↓	0,06±0,01↓
		1607	0,06±0,01	0,07±0,005↑	0,04±0,03↓	0,06±0,007↓	0,06±0,03↓

CHAPTER 4

DISCUSSION

Diabetes Mellitus is a metabolic disturbance affecting entire body, because of developed insulin resistance or autoimmune loss of insulin producing ß cells. Complications of this disease possess more harm than diabetes itself. These complications may damage eyes, nerves, heart, testes and kidneys. The dysfunction of above mentioned vital organs may lead to disability in diabetic patients or even to death. Among these organs the kidneys seriously harmed from diabetes. In developed countries the diabetic kidney disease is the major cause of renal insufficiency and leads to high financial cost. Up to now, very few studies were performed to investigate the diabetic nephropathy. Until recently, it was proposed there are several pathogenetic mechanisms related to diabetic complications. Unfortunately the exact molecular mechanisms explaining underlying causes of diabetic complications are still unknown.

The proposed mechanisms associated directly to diabetic complications include increased polyol pathway flux, increased hexosamine pathway, increased formation of advanced glycation end products (AGEs) and activation of protein kinase C (PKC) pathway. All these pathways are related to oxidative stress directly or indirectly. Oxidative stress is an important feature of diabetic complications. Free radicals can mediate the addition and subtraction of DNA nucleotide bases leading to DNA mutations. Consequently DNA cannot direct protein and fatty acid synthesis. In addition, increased ROS production as a consequence of diabetes oxidizes and inactivates enzymes and molecules of above mentioned pathways opening way to new diseases besides diabetes. These disorders are called diabetic complications. Many strategies have been used to target the disturbance in oxidative balance of the

body to treat diabetes and diabetic complications. The most common researches are focused on antioxidants and its components. The great majority of these studies reported that, selenium administration improved the antioxidant levels and protects the body from diabetes (Stachouse et al. , 1990; Douillet et al. ,1996 ; Stapleton , 2000 ; Turan et al. , 2007).

In our study FTIR spectroscopy was used to determine the structural and functional alterations of kidney plasma membrane resulted from diabetes mellitus and to monitor effect of selenium as an antioxidant on diabetes disease state. More precisely the changes caused by diabetes on kidney plasma membrane apical side (brush-border membrane) resulted from diabetes was monitored, in detail. The study can be divided into two parts. In the first part, we investigated the macromolecular alterations in the diabetic kidney plasma membrane. Alterations in membrane protein, lipid and carbohydrate content were monitored in this part. In the second part we studied the proposed therapeutic effects of selenium. Different doses of selenium were used to reveal the effects of selenium on stz-induced diabetic kidney disease using ATR- FTIR spectroscopy.

In infrared spectroscopic analysis, the intensity or band area of the bands in absorption spectra give information about the concentration of related functional groups (Freifelder, 1982; Toyran and Severcan, 2003; Toyran et al., 2004).

The C-H region at spectra (3050-2800 cm^{-1}) is composed of olefinic = CH, - CH_2 and CH_3 groups of C-H stretching vibrations which, originates from lipid molecules (Severcan et al., 2000; Severcan et al., 2003; Cakmak et al., 2006) . The C-H stretching vibrational modes of HC - CH groups give absorption at $3011 cm^{-1}$ position and called olefinic band. The band area of olefinic band gives information about the unsaturation state of acyl chains (Takahashi et al., 1991; Liu et al., 2002; Severcan et al., 2005). Increased lipid peroxidation may be caused by loss of unsaturation (Sills et al., 1994; Kinder et al., 1997). The area of olefinic band increased significantly in diabetic group showing that lipid peroxidation end products occurred during diabetes (Severcan et al., 2005).   Our results also revealed that low dose selenium treatment

restored lipid peroxidation in diabetes. In contrary, high dose and medium dose selenium administration increased lipid peroxidation in diabetes. Our experiments with low dose selenium treatment confirmed the previous studies reporting that selenite administration considerably lowered the extent of lipid peroxidation (Mukherjee et al., 1998). Lipid order parameter can be determined by the monitoring of frequency changes of CH_2 stretching vibrations (Liu et al., 2002; Mantsch, 1984; Severcan et al., 1997). In our study, CH2 stretching band frequency shifted to lower value indicating that the system became more ordered during diabetes. The ordered membrane lipids mean that there are increased dose of trans / gauche conformers that may cause more rigid membrane structure.

Free radicals may be responsible for membrane rigidity. In contrary, we monitored shifting of the CH_2 stretching band frequencies to higher values in all Selenium treated diabetic groups. This observation can be interpreted as decrease of order state and membrane rigidity during selenium treatment of diabetes.

The areas of CH_3 asymmetric (2962 cm^{-1}), CH_2 asymmetric (2923 cm^{-1}) and CH_2 symmetric (2853 cm^{-1}) bands can give information about membrane lipid content. In diabetic state the areas of these bands decreased significantly, suggesting that the lipid concentration decreased during diabetes. However, we found significant increase in band areas for selenium treated diabetic groups, which implies that the selenium has recovery effect on lipid content of diabetic kidney plasma membrane by approaching it to the control values. Supporting this, in addition, we revealed a decrease in the band areas of other bands related to lipids namely CH_2 scissoring band (1468 cm^{-1}) and CH_2 bending band (1455 cm^{-1}) in the diabetic group. However, in Selenium treated diabetic groups, the areas of these bands increased significantly towards the control values. It was previously reported that, treatment of diabetic animals or rat hepatocytes in culture with selenate restored the expression of FAS and G & PDH indicating that selenate is capable of stimulating lipogenesis in the liver (Ghosh et al., 1994; Shepherd et al., 1995). Our findings confirmed the referred studies because we also found that the selenium treatment stimulates lipogenesis.

The ratio of the areas of the CH_2 symmetric and asymmetric stretching bands and the sum of the areas of these bands to the area of the CH_3 symmetric stretching band lowered in diabetic group, indicating that the lipid concentration decreased more profoundly than protein content in diabetic condition. However, we observed dramatic increase of these ratios in low dose selenium treated diabetic group. In low dose selenium treated diabetic group the values were similar with the control values. These findings suggest that, in diabetic state, in order to restore lipid concentrations, the low doses of selenium can be used. In addition, the sum of the areas of CH_2 symmetric and asymmetric stretching bands to the area of the Amide I band lowered in diabetic group, however this value increased in all selenium treated groups. This indicates that, selenium treatment restored the lipid content in diabetic kidney brush-border plasma membrane. To sum up it can said that the low dose selenium treatment improved the lipid profile of renal brush-border plasma membrane.

Membrane dynamics can be determined by monitoring the bandwidths of CH_2 stretching bands (Mantsch, 1984 ; Lopez-Garcia et al. ,1993 ; Severcan et al. , 2003 ; Severcan et al. , 2005) . The increase in the bandwidths of these bands implies an increase in membrane dynamics (Levin et al., 1990; Severcan et al., 1999; Severcan et al., 2005; Korkmaz and Severcan, 2005). We have observed a decrease in the bandwidth of CH_2 symmetric band in diabetic group suggesting that membrane dynamics decreased in diabetic groups. In all selenium treated diabetic groups we found an increase in the CH_2 symmetric bandwidth values indicating that selenium restored diabetes-induced variations in membrane dynamics of diabetic kidney brush-border plasma membranes toward the normal values (see the Figure 37).

The band located at 1731 cm^{-1} belongs to carbonyl stretching vibrational modes of lipids. This band emerges from ester groups of phospholipids and cholesterol esters (Jackson, 1998; Dighton, 2001). According to our results the band frequency in diabetic group slightly shifted to higher values, indicating a decrease in the strength of hydrogen bonding (dehydration). We found significant shifting of this band frequency to the lower value in high dose selenium treated group, so we suggest that selenium administration in diabetes removes the excess amounts of hydrogen bonds

from the system. Band area of the C=O ester band increased dramatically in all selenium treated diabetic groups indicating that, the membrane phospholipids content elevated as a result of selenium treatment. The area of this band did not change during diabetes.

To support our results, the studies reported that, selenate treatment improved the plasma lipid levels, the cholesterol, triglycerides and free fatty acids of diabetic animals (Battell et al., 1998). Also selenium and selenium + L-arginine combination showed significant increase in plasma HDL-cholesterol level in diabetic rats (Nader et al., 2007).

Amide I and Amide II bands are very informative for monitoring proteins secondary structures (Haris and Severcan, 1999; Jackson and Smith, 1999; Lyman et al., 1999). The band located at 1652 cm^{-1} belongs to amide I band of proteins. In addition the band at 1546 cm^{-1} assigned to amide II protein band. Amide I band is mainly due to C=O stretching (%80) and C-N stretching. Amide II arises from N-H bending (%60) and C-N stretching (%40) of proteins (Haris and Severcan, 1999 ; Melin et al., 2000 ; Takahashi et al., 1991 ; Wong et al., 1991 ; Cakmak et al., 2006) . The band frequencies of Amide I and Amide II shifted to lower value in diabetic group indicating that the changes in protein conformation occurred during diabetes.

Amide II band assigned to α-helix structures of proteins and shifting to lower frequency value can be interpreted as elevated amounts of random coil structures (Melin et al. , 2000 ; Spassov et al. , 2006 ; Dousseau and Pezolet ,1990) . According to our findings, in diabetic state, the proteins native conformational structure changed with the increased formation of random coil. This indicates protein denaturation. Interestingly, we observed shifting to higher values of amide II band frequency in all selenium treated diabetic groups, demonstrating that, the process of denaturation in diabetic kidney plasma membrane proteins recovered with the selenium administration. In case of high dose selenium treated diabetic group we monitored significant increase of amide I band area, demonstrating that the protein content was normalized with the administration of selenium.

Amide II band area decreased in diabetic group. This result draw such a conclusion that, the protein degradation occurred in kidney plasma membranes during diabetes. However, selenium treatment as displayed with increased band areas improved the situation.

The bands at 1468 cm^{-1} and 1455 cm^{-1} originates from CH_2 scissoring and CH_2 bending vibrational modes of lipids respectively (Severcan et al, 2000 ; Severcan et al. , 2003 ; Cakmak et al. , 2006) . The frequency of CH_2 bending band shifted to lower value in all selenium treated diabetic groups. We observed that, the order parameter of these lipids decreased as a result of selenium treatment. The area of these bands increased which means the increased lipid content as a result of selenium treatment. Studies have shown that the tissue lipids, peroxides and fatty acids are normalized to in diabetic animals with the administration of selenium (Douillet et al., 1998).

The band positioned at 1400 cm^{-1} originates from the COO- symmetric stretching vibrations of amino acids side chains and fatty acids (Jackson et al., 1998; Cakmak et al., 2003). The band area decreased in diabetic group indicating the decreased amounts of amino acids and fatty acids on the diabetic kidney plasma membrane. In contrary, the area of this band was increased in all selenium treated diabetic groups. We suggest that the content of amino acids and fatty acids on the diabetic kidney plasma membrane increased with the administration of selenium.

It was demonstrated that selenate can act as a potent insulin-like agent (Ezaki et al., 1990). The healing effect of insulin on diabetes is well-known. Selenium and Vanadate mimics the insulin in regard to glycolysis, gluconeogenesis, fatty acid synthesis and pentose–phosphate pathway (Bosch et al, 1990; Miralpeix et al., 1991; Johnson et al., 1990).

Insulin plays a role in the facilitating the entry of amino acids into cells for protein synthesis, increases nucleic acid synthesis, stimulates Na+ /K+ ATPase, controls the expression of large number of genes and upregulates the glucose uptake via glucose

transporters. Selenium as an insulin mimetic translocates the glucose transporters (GLUT1 and GLUT2) to the membrane surface. At the same time, facilitation of aerobic and anaerobic glycolysis was observed (Furnsinn et al., 1996). As a result, an excess amount of glucose is taken away from the plasma into the cells. Insulin also regulates the transcription of genes for several key enzymes related to carbohydrate and fatty acid metabolism (O'Brien et al., 1996).

The PO_2^- asymmetric and symmetric stretching bands positioned at 1233 cm^{-1} and 1084 cm^{-1} respectively emerges from the phosphate stretching's of phospholipids head groups (Lyman et al. , 2001 ; Banyay et al. , 2003) . The phosphate stretching's deliver the information about the phospholipids head groups located on the non-polar interface of membrane (Mendelsohn and Mantsch, 1986). The frequency of the PO_2^- symmetric stretching's shifted to high value in diabetic group. This indicates that during the diabetes the PO_2 groups of phospholipids are dehydrated compared to healthy membranes. In contrary, we monitored that the PO_2 asymmetric and symmetric band frequencies in all selenium treated diabetic groups shifted to lower values. These results demonstrate that the selenium restored the situation by hydrating the system.

The area of PO_2 asymmetric stretching band increased in all selenium treated animals, indicating the elevation of the phospholipids content. We suppose that, as selenium treatment in diabetes can elevate the phospholipids concentrations so selenium positively affects the phospholipids content of diabetic kidney plasma membranes.

The bands located at 1171 cm^{-1} and 1045 cm^{-1} are emerged from glycogen, glycolipids and polysaccharides (Lyman et al. ,1999 ; Rigas et al. ,1990 ; Cakmak et al. , 2003 ; Cakmak et al., 2006). The band at 1171 cm^{-1} was assigned to C-O-O-C asymmetric stretching's of glycogen. The band at 1045 cm^{-1} was assigned to CO-stretching's of glycolipids and polysaccharides. The frequency of 1171 cm^{-1} band shifted to higher value significantly in medium dose selenium treated group indicating that the hydrogen bonds of glycogen are increased in plasma membranes

due to medium doses of selenium. So the medium doses of selenium negatively affected the glycogen levels in plasma membrane. However, the frequency of this band shifted to lower value significantly in low dose selenium treated group, indicating that the low doses of selenium restores the variation in the hydrogen bonds of glycogen in plasma membrane.

The increased area of 1045 cm^{-1} band in all selenium treated diabetic groups indicates increased amounts of glycolipids and polysaccharides in the system. However in diabetic group increased amounts of glycolipids and polysaccharides were also monitored. The frequency of this band shifted to lower values in selenium treated groups exhibiting that, the hydrogen bonds decreased in glycolipids and polysaccharides. Several studied demonstrated that, oral administration of selenite to diabetic animals partly reversed abnormal liver expression of glycogenic and glyconeogenic enzymes (Becker et al., 1996). Our findings are in agreement to some extent with previous studies.

The band at 972 cm^{-1} was considered to be arisen from the symmetric stretching modes of dianionic phosphate monoesters (Ci et al. , 1999 ; Chiriboga et al. , 2000 ; Cakmak et al. , 2003) and ribose-phosphate main chain vibrations of the RNA backbone (Banyay et al. , 2003 ; Tsuboi et al. , 1969) . The frequency of this band shifted to higher value in diabetic animals exhibiting conformational changes in these molecules. It was revealed that, in selenium treated groups the frequency shifted to lower values. We observed that structural variations in the phosphate monoesters and ribose-phosphates were restored with selenium treatment.

Area of this band was decreased in diabetic group demonstrating that the content of the phosphate monoesters and ribose-phosphate main chains decreased during diabetes. On the contrary, the area of this band increased in all selenium treated diabetic groups. We monitored that, selenium treatment elevated the concentration of phosphate monoesters and ribose-phosphate main chains.

In order to disclose the effect of diabetes and selenium on kidney plasma membranes, the Amide I main protein band was examined, in detail. We conducted the secondary structure analysis of amide I band for clarifying the structural conformational alterations of kidney plasma membrane proteins using FTIR spectroscopy. Antiparallel ß-sheet structure can be identified by the presence of band near 1670–1695 cm $^{-1}$. This component is normally weak and its precise assignment is often made difficult by the overlap of absorption from ß-turn and unordered structures (Hares et al. , 1999) .

Antiparallel ß sheet and α-helix content dramatically elevated in diabetic kidney plasma membranes. In addition, amide I band area located at 1652 cm^{-1} increased slightly confirming the elevation of contents of antiparallel ß sheet and α-helix. These results show that the proteins of diabetic kidney brush-border plasma membrane are predominantly α-helix.

We suggest that, the diabetes caused enormous increase in membrane proteins synthesis and folding properties. On the contrary, in all selenium treated diabetic plasma membranes we monitored drastically decrease of intensities of antiparallel ß sheet and α-helix. According to our results it is obvious that, selenium administration in diabetes has reversed enormous increased protein synthesis and folding toward the normal levels. The intensities of turns in diabetic group increased significantly supporting above mentioned abnormal increase in antiparallel ß sheet and α-helix secondary structures. In selenium treated diabetic plasma membranes the intensities of turns decreased significantly, proving that selenium restored the proteins secondary structures of diabetic membranes. We found that only in diabetic group the random coil band was apparent. However in control and in selenium treated groups this band was not observed. The manifestation of random coil band indicates the denaturation of membrane proteins. We observed that, the selenium treatment has completely reversed the denaturation process toward control values.

The ß sheet content was decreased slightly in diabetes; however, the intensities of these bands were increased in all selenium treated groups. This observation makes a sense that during diabetes the aggregated ß sheet and ß sheet was conversed to random coil structure, so we monitored decreased amounts of aggregated ß sheet and ß sheet. In addition, selenium treatment increased the aggregated ß sheet and ß sheet content indicating that the random coil structure has conversed to aggregated ß sheet and ß sheet.

Insulin has an important action on cell signaling pathway (Kahn et al., 1993). Also selenite as similar to insulin have been shown to activate the MAP kinase signaling pathway (Stapleton et al. , 1997 ; Stapleton et al. , 1998 ; Hei et al. , 1998) . To sum up, the altered protein synthesis and folding due to diabetes can be reversed as a result of antioxidant and insulin-like properties of selenium.

As our results supports the majority of previously reported studies, we can conclude that, during diabetes the protein content of membranes was enormously increased and proteins are severely denatured. However selenium administration in diabetes restored the protein content. It is obvious that the process of denaturation considerable reversed towards the control value as a result of selenium treatment.

Despite the fact that the selenium compounds can be used as antidiabetic agent in therapy, the administered dose should be handled carefully. In this study, we could not differentiate between three doses of selenium given to diabetic rats. Future investigations are necessary for selection of optimal doses of this trace element before it can safely be used in therapy for diabetes and diabetic nephropathy. In addition the detailed structural alterations caused by diabetes and selenium effect on diabetic structural alterations in the kidneys should be studied.

To sum up, the early alterations in the kidneys due to diabetes could be diagnosed with the help of spectroscopic techniques, which is difficult to determine with the usage of nowadays clinical data. Spectral changes such as lipid to protein ratio, protein secondary structure and lipid content can be used in this manner. In future, we hope, it will be possible to put a diagnosis of the early diabetes in the kidneys via the FTIR spectroscopy.

CHAPTER 5

CONCLUSION

The current study firstly demonstrated the significant changes happened in kidney brush-border plasma membranes due to STZ-induced type I Diabetes via ATR-FTIR spectroscopy. Equally, some protective and curable role of selenium in Diabetes was uncovered.

The detailed spectral analysis of ATR-FTIR spectroscopy was revealed the following remarks:
The protein and lipid content of diabetic kidney plasma membrane was prominently diminished. This shows that the lypolysis and lipid peroxidation occurred during diabetes. Nevertheless, the administration of selenium improved the condition by changing the lipid and protein content to normal values.

The lipids of diabetic plasma membrane were in more ordered structure than the lipids of healthy plasma membranes, whereas selenium treatment reversed this condition towards the normal structure.

The diabetes caused the decrease of membrane dynamics however; selenium treatment increased the dynamics of membrane.

The content of fatty acids and amino acids decreased in diabetic plasma membranes whereas with the selenium administration this content was elevated.

The glycogen, glycolipids and polysaccharides on the membrane displayed contradictory results. The hydrogen bonds of glycogen increased as a result of

medium doses of selenium, but decreased as a result of low doses of selenium. The glycolipids and polysaccharides content increased in selenium treated diabetic animals nevertheless, this content was increased in diabetic group also. In addition the hydrogen bonds of the glycolipids and polysaccharides in selenium treated diabetic plasma membranes decreased.

The diabetes caused critical secondary structural changes in plasma membranes. During the detailed analysis of proteins secondary structures, the aggregation and denaturation of proteins were observed, suggesting that, diabetes caused abnormal synthesis and folding of proteins. In contrary, the administration of selenium removed the denaturation and as a result, normal secondary structure of proteins was established.

The membrane phospholipids of diabetic kidney plasma membrane were found to be more ordered than normal ones. Nonetheless, the selenium therapy restored the ordered structural alterations. Also, membrane phospholipids content elevated as a result of selenium treatment.

To conclude, the kidney plasma membranes were severely deteriorated due to diabetes with respect to its lipid, protein and carbohydrate structure and content, which were restored after selenium treatment. The diabetes caused the diminishing of whole membrane fluidity, which was restored with the selenium administration. This the first study demonstrating the effect of stz-induced diabetes on kidney plasma membrane and the effect of selenium on stz-induced diabetic kidney plasma membranes using spectroscopic tools. The study revealed serious therapeutic capacities of selenium on diabetic kidney plasma membranes which needs confirmation of future researches. In future, the selenium treated control kidney brush-border plasma membrane samples will also be studied detailly, in order to see the effect of selenium on healthy kidney tissues.

REFERENCES

Atkinson MA, Eisenbarth GS. Type I diabetes: new perspectives on disease pathogenesis and treatment. Lancet 2001; 358: 221–229.

Akerblom HK, Knip M. Putative environmental factors in type 1 diabetes. Diabetes Metab Rev 1998; 14: 31–67.

Adler S. Structure-function relationships associated with extracellular matrix alterations in diabetic glomerulopathy. J Am Soc Nephrol 1994; 5: 1165–1172

Alberti K. G. M. M, P. Z. Zimmet. Definition, Diagnosis and Classification of Diabetes Mellitus and its Complications Part 1: Diagnosis and Classification of Diabetes Mellitus Provisional Report of a WHO Consultation. K. G. Diabet. Med. 15: 539–553 (1998)

Arthur RJ, Nicol F, Beckett GJ. Selenium deficiency, thyroid hormone metabolism and thyroid hormone deiodinases. Am J Clin Nutr. 1993; 57: 236S-239S

Arthur J.R., Nicol R., Beckett, G.J., 1993. Selenium deficiency, thyroid hormone metabolism, and thyroid hormone deiodinases. Am. J. Clin. Nutr. 57, 236S - 239S. Ujang Tinggi. Essentiality and toxicity of selenium and its status in Australia: a review Toxicology Letters 137 (2003) 103- 110

Aronson PS. Kinetic properties of the plasma membrane Na / H exchanger. Ann Rev Physio4l7: 545—560, 1985

Aronson PS. identifying secondary active solute transport in epithelia. Am J Pliysiol 240: Fl—F11, 1981

Arrondo J.R., Muga, A., Castresa, J., and Goni, R. M., (1993). "Quantative Studies of the Structure of Proteins in Solution by Fourier Transform Infrared Spectroscopy", Progress. Biophys. Acta. 468:63-72.

Armstrong AM, Chestnutt JE, Gormley MJ, Young IS. Theeffect of dietary treatment on lipid peroxidation and antioxidantstatus in new diagnosed non-insulin dependent diabetes. Free Radical Biol Med 1996; 21:719]726

Allander E.Kashin-Beck disease.An analysis of research and public health activities based on a bibliography 1849^{-1}992. Scand J Rheumatol.1994;23

AM van Rij, CD Thomson, JM McKenzie, and MF Robinson. Selenium deficiency in total parenteral nutrition J. Am. J. C/in. Nuir. 32 : 2076-2085, 1979.

Avissar N, Ornt DB, Yagil Y, Horowitz S, Watkins RH, KerlEA, Takahashi K, Palmer IS, Cohen HJ. Human Kidney Proximal Tubules Are the Main Source of Plasma Glutathione Peroxidase. Am. J. Physiol. 1994; 266: C367-75.

Barbu AR, Akusjarvi G, Welsh N. Adenoviral-mediated transduction of human pancreatic islets: importance of adenoviral genome for cell viability and association with a deficient antiviral response. Endocrinology 2005; 146: 2406–2414.

Bergman R. Non-esterified fatty acids and the liver: why is insulin secreted into the portal vein? Diabetologia 2000; 43: 946–952.

Brownlee M. Biochemistry and molecular cell biology of diabetic complications. Nature 2001; 414:813–820

Brownlee M. The pathobiology of diabetic complications: a unifying mechanism. Diabetes 2005; 54: 1615–1625

Brown DM, Andres GA, Hostetter TH, Mauer SM, Price R, Venkatachalam MA. Kidney Complications Diabetes 1982; Vol 31, Suppl 1.

Bell RH, Hye RJ. Animal Models of Diabetes Mellitus:Physiology and Pathology. Journal of surgical Research 1983; 35: 433-460

Belma Turan, Sevgi Bayari, Cenk Balcik, Feride Severcan, Nuri Akkas (2000).''A biomechanical and spectroscopic study of bone from rats with selenium deficiency and toxicity''. BioMetals 13: 113–121, 2000

Belma Turan, Esma Zeydanli, Evrim Tanriverdi, Aytac Seymen, Erkan Tuncay, Hakan Gurdal, Aslihan Koksoy. ''Beneficial effect of sodium selenate on vascular dysfunction in diabetic rats''. Journal of Molecular and Cellular Cardiology 42 (2007) S219–S233

Beck MA, Kolbeck PC, Rohr LH, Morris VC & Levander OA (1994a). Benign human enterovirus becomes virulent in selenium-deficient mice. Journal of Medical Virology 43, 166 $^{-1}$70.

Beck MA, Kolbeck PC, Shi Q, Rohr LH, Morris VC & Levander OA (1994b) Increased virulence of a human enterovirus (Coxsackievirus B3) in selenium-deficient mice. Journal of Infectious Diseases 170, 351 - 357.

Beck MA, Shi Q, Morris VC & Levander OA (1995). Rapid genomic evolution of a non-virulent Coxsackievirus B3 in selenium-deficient mice results in selection of identical virulent isolates. Nature Medicine 1, 433-436

Battell ML, Delgatty HL, McNeill JH. Sodium selenate corrects glucose tolerance and heart function in STZ diabetic rats. Mol Cell Biochem 1998; 179: 27–34.

Bevers E.M., P. Comfurius, J.L.M.L. van Rijn, H.C. Hemker, R.F.A. Zwaal. Generation of platelet prothrombin converting activity and the exposure of phosphatidylserine at the platelet outer surface. Eur. J. Biochem. 122 (1982) 429-436.

Bevers Edouard M. , Paul Comfurius, David W.C. Dekkers, Robert F.A. Zwaal. Lipid translocation across the plasma membrane of mammalian cells. Biochimica et Biophysica Acta 1439 (1999) 317-330

Bevers E.M., P. Comfurius, R.F.A. Zwaal. Changes in membrane phospholipid distribution during platelet activation. Biochim. Biophys. Acta 736 (1983) 57-66.

Matlin, K., Caplan, M., in: Seldin, D., Giebisch, G. (Eds.). The Kidney: Physiology and Pathophysiology, Lippincott Williams and Wilkins, Philadelphia, PA 2000

Bosch R., Hatzoglou M., Park E. A. and Hanson R. W. (1990). Vanadate inhibits expression of the gene for phosphoenolpyruvate carboxykinase (GTP) in rat hepatome cells. J. Biol. Chem. 265: 13677–13682

Banyay, M., Sarkar, M., Graslund, A., (2003). "A library of IR bands of nucleic acids in solution". Biophysical Chemistry, 104: 477–488.

Bizeau, M.E., Salano, J.M., and Jeffrey, R., (2000). "Menhaden oil feeding increases lypolysis without changing plasma membrane order in isolated rat adipocytes". Nutrition Research, 20(11): 1633^{-1}644.

Burk RF: Molecular biology of selenium with implications for its metabolism. FASEB J 5: 2274–2279, 1991

Burk RF, Hill KE. Regulation of Selenoproteins. Annual Review of Nutrition 1993; 13: 65-81.

Burk RF, Hill KE. Selenoprotein P: A selenium rich extra cellular glycoprotein. J. Nutr. 1994; 124(10): 1891-7.

Becker D. J., Reul B., Ozcelikay A. T., Buchet J. P., Henquin J. C. and Brichard S. M. (1996). Oral selenate improves glucose homeostasis and partly reverses abnormal expression of liver glycogenic and gluconeogenic enzymes in diabetic rats. Diabetologia 39: 3–11

Brinkkoetter PT, Holtgrefe S, van der Woude FJ, Yard BA. Angiotensin II type 1-receptor mediated changes in heparin sulfate proteoglycans in human SV40 transformed podocytes. J Am Soc Nephrol 2004; 15: 33–40.

Crouch R, Kimsey G, Priest DG, Sarda A, Buse MG. Effect of streptozotocin on erythrocyte and retinal superoxide dismutase. Diabetologia 1978; 15: 53

Cline G, Petersen K, Kreskas M, et al. Impaired glucose transport as a cause of decreased insulin-stimulated muscle glycogen synthesis in T2DM. The New England Journal of Medicine 1999; 341: 240–246.

Christelle Douillet, Alain Tabib, Muriel Bost, Michele Accominotti, Francoise Borson-Chazot, and Maryvonne Ciavatti1. Selenium in Diabetes: Effects of Selenium on Nephropathy in Type I Streptozotocin-induced Diabetic Rats the Journal of Trace Elements in Experimental Medicine 12:379–392 (1999)

Chen LK, Chou YC, Tsai ST, et al. Hepatitis C virus infection-related type 1 diabetes mellitus. Diabet Med 2005; 22: 340–343

Chen S, Kasama Y, Lee JS, et al. Podocytederivedvascular endothelial growth factor mediates the stimulation of alpha3 (IV) collagen production by transforming growth factor beta1in mouse podocytes. Diabetes 2004; 53:2939–2949.

Cooper ME, Vranes D, Youssef S, et al. Increased renal expression of vascular endothelial growth factor (VEGF) and its receptor VEGFR-2 in experimental diabetes. Diabetes 1999; 48: 2229–2239.

Chang, M.C., Tanaka, J., (2002). "FT-IR study for hydroxyapatite / collagen nanocomposite cross-linked by glutaraldehyde". Biomaterials, 23: 4811–4818.

Chiriboga, L., Yee, H., Diem, M., (2000). "Infrared spectroscopy of human cells and tissues. Part VI: A comparative study of histopathology and infrared micro spectroscopy of normal, cirrhotic, and cancerous liver tissue". Appl.Spectrosc. 54: 1-8.

Cakmak, G., Togan, I., Uguz, C., Severcan, F., (2003). "FT-IR spectroscopic analysis of rainbow trout liver exposed to nonylphenol". Appl. Spec. 57:835–841.

Cakmak, G., Togan, I., Severcan, F., (2006). "17-Estradiol induced compositional, structural and functional changes in rainbow trout liver. Aquatic Toxicology, 77: 53–63

Cakmak, G., Togan, I., Severcan, F., (2006). "17-Estradiol induced compositional, structural and functional changes in rainbow trout liver, revealed by FT-IR spectroscopy: A comparative study with nonylphenol", Aquatic Toxicology, 77: 53

Celik S., Yilmaz O, T. Asan, M. Naziroglu , M. Cay and M. Aksakal.'' Infuence of Dietary Selenium and Vitamin E on the Levels of Fatty Acids in Brain and Liver Tissues of Lambs''. Cell Biochem. Funct. 17, 115[-1]21 (1999)

Cser A, Sziklai-Laszlo I, Menzel H, Lombeck I. Selenium status and lipoproteins in healthy and diabetic children. J Trace Elem Electrolytes Heath Dis 1993; 7:205]210.

Contempre B,Dumont JE,Bebe N,Thilly CH,Diplock AT,Vanderpas J. Effect of selenium supplementation in hypothyroid subjects of an iodine and selenium deficient area. J Clin Endocrinol Metab.1991;73;213-215

Campbell, I. D. and Dwek, R. A. (1984). Biological spectroscopy, Benjamin / Cummings Publishing Company, USA, 1-60.

Ci, X. Y., Gao, T. Y., Feng, J. and Guo, Z. Q., (1999). "Fourier transforms infrared characterization of human breast tissue: Implications for breast cancer diagnosis", Applied Spectroscopy, 53:312-315.

Cuvin-Aralar ML, Furness RW. Mercury and selenium interaction: a review. Ecotoxicol Environ Health 1991; 21:348]364.

Dighton, J., Mascarenhas, M., and Arbuckle-Keil, G. (2001), "Changing Resources: Assessment of Leaf Litter Carbohydrate Resource Change at A Microbial Scale of Resolution", Soil Biology and Biochemistry. 33: 1429^{-1}432.

David Holben,Anne M.Smith. The diverse role of selenium within selenoproteins:a review.J Am Dietetic Assoc.1999;99-7

Ding G, Reddy K, Kapasi AA, et al. Angiotensin II induces apoptosis in rat glomerular epithelial cells. Am J Physiol Renal Physiol 2002; 283:F173–F180

Du XL, Edelstein D, Rossetti L, et al. Hyperglycemia-induced mitochondrial superoxide overproduction activates the hexosamine pathway and induces plasminogen activator inhibitor^{-1} expression by increasing Sp1 glycosylation. Proc Nat Acad Sci U S a 2000; 97: 12222–12226

Douillet C, Tabib A, Bost M, Accominotti M, Borson-Chazot F, Ciavatti M. A selenium supplement associated or not with vitamin E delays early renal lesions in experimental diabetes in rats. Proc Soc Exp Biol Med 1996; 211:323]331.

Douillet C, Bost M, Accominotti M, Borson-Chazot F, Ciavatti M. Effect of selenium and vitamin E supplements on tissue lipids, peroxides, and fatty acid distribution in experimental diabetes. Lipids 1998; 33:393–399

Douillet C, Bost M, Accominotti M, Borson-Chazot F, Ciavatti M. In vitro and in vivo effects of selenium and selenium with vitamin E on platelet functions in diabetic rats. Relationship to platelet sorbitol and fatty acid distribution. Biol Trace Elem Res 1996; 55:263–277.

Doublier S, Salvidio G, Lupia E, et al. Nephrin expression is reduced in human diabetic nephropathy: evidence for a distinct role for glycatedalbumin and angiotensin II. Diabetes 2003; 52:1023–1030.

Dousseau, F, and Pezolet, M., (1990). "Determination of the secondary structure content of proteins in aqueous solutions from their amide I and amide II infrared bands. Comparison between classical and partial least-squares methods?" Biochemistry, 29: 8771-8779.

The Diabetes Control and Complications (DCCT) Research group: Effect of intensive therapy on the development and progression of diabetic nephropathy in the Diabetes Control and Complications Trial. Kidney Int 47:1703[-1]720, 1995

Ezaki, O., 1990. The insulin like effects of selenate in rat adipocytes. J. Biol. Chem. 265, 1124–1130

Evers, C., Haase, W., Murer, H. and Kinne, R. (1978). Properties of Brush Border Vesicles Isolated from Rat Kidney Cortex by Calcium Precipitation. Molecular Membrane Biology, 1:3,203 — 219

Fan AM,Kizer KW. Selenium-nutritional,toxicological and clinical aspects. West J Med.1990;153;160[-1]67

Facchini FS, Humphreys MH, DoNascimento CA, et al. Relation between insulin resistance and plasma doses of lipid hydro peroxides, carotenoids, and tocopherols. Am J Clin Nutr 2000; 72:776–779?

Foster, L. H. and Sumar, S. (1997) Selenium in health and disease: a review. Crit Rev Food Sci Nutr 37:211-228.

Freifelder, D., (1982). Physical Chemistry. Applications to biochemistry and molecular biology, Freeman, W. H. (Ed), New York.

Friedman BI, Spray BJ, Tuttle AB, Buckalew VM Jr. The familial risk of end-stage renal disease in African Americans. Am J Kidney Dis 21: 387-393, 1993?

Francesco Piscean and Loreto Gesualdo. Pathogenetic Mechanisms of Diabetic Nephropathy. J Am Soc Nephrol 16:S30-S33, 2005

Furnsinn C., English R., Ebner K., Nowotny P., Vogle C. and Waldhausl W. (1996) Insulin-like vs. non-insulin stimulation of glucose metabolism by vanadium, tungsten and selenium compounds in rat muscle. Life Sci. 59: 1989–2000

Green J, Casabonne D, Newton R. Coxsackie B virus serology and type I diabetes mellitus: a systemic review of published case-control studies. Diabet Med 2004; 21: 507–514.

Guilherme A, Virbasius JV, Puri V, Czech MP. Adipocyte dysfunctions linking obesity to insulin resistance and T2DM. Nat Rev Mol Cell Biol 2008; 9 (5): 367–77.

Güvenc Görgülü,''The Effects of Antioxidants on Diabetic Rat Livet Microsomal Membranes and Antioxidant Enzyme Activities ''. PHD Thesis,2004.

Gordon G.Hammes. (2005) Spectroscopy of biological sciences, John Wiley & Sons, Inc

Gebre-Medhin M, Ewald U, Plantin LO, Tuvemo T. Elevated serum selenium in diabetic children. Acta Pediatr Scand 1984; 73:109]114

Greene HL, Hambridge KM, Schanler R, Tsang RC. Guidlines for the use of vitamins,trace elements ,calcium and phosphorus in infants and children receiving total parenteral nutrition. Am.J.Clin Nutr. 1988;48:1324^{-1}342

Ghosh R, Mukherjee B, Chatterjee M. A novel effect of selenium on streptozotocin-induced diabetic mice. Diabetes Res 1994; 25:165–171.

Hutton JC, Wenzlau JM, Juhl K, et al. The cation efflux transporter ZnT8 (Slc30A8) is a major autoantigen in human type 1 diabetes. PNAS 2007; 104: 17 040–17 045

Helzlsouer K, Jacobs R, Morris S. Acute selenium intoxication in the United States (abstract). Fed.Proc.1985; 44:1670

Hoekstra, W. G. 1975. Biochemical functions of selenium and its relation to vitamin E. Fed. Proc. 34:2083-89

Hafeman, D. G., Sunde, R. A., Hoekstra, W. G. 1974. Effect of dietary selenium on erythrocyte and liver glutathione peroxides in the rat. J. Nutr. 104: 580-87

Holovet P, Collen D. Oxidized lipoproteins in athereosclerosis and thrombosis. FASEB J.1994;8:1279^{-1}284

Hill KE, Lloyd RS, Yang JG, Read R & Burk RF (1991). The cDNA for rat selenoprotein P contains 10 TGA codons in the open reading frame. Journal Of Biological Chemistry 266, 10050±10053.

Hei Y., J., Farahbakhshian S., Chen X., Battell M. L. And McNeill J. H. (1998) Stimulation of MAP kinase and S6 kinase by vanadium and selenium in rat adipocytes. Mol. Cell. Biochem. 178: 367–375

Heini Murer and Piotr Gmaj. Transport studies in plasma membrane vesicles isolated from renal cortex. Kidney international, Vol. 30 (1986), pp. I/I—ISO

Hammes HP, Du X, Edelstein D, et al. Benfotiamine blocks three major pathways of Hyperglycemic damage and prevents experimental diabetic retinopathy. Nat Med 2003; 9:294–299

Ichinose K, Kawasaki E, Eguchi K. Recent advancement of understanding pathogenesis of type 1 diabetes and potential relevance to diabetic nephropathy. Am J Nephrol 2007; 27:554–564?

Idris I, Donnelly R. Protein kinase C beta inhibition: a novel therapeutic strategy for diabetic microangiopathy. Diab Vasc Dis Res 2006; 3: 172–178

Isogai S, Mogami K, Shiina N, Yoshino G. Initial ultra structural changes in pore size and anionic sites of the glomerular basement membrane in streptozotocin-induced diabetic rats and their prevention by insulin treatment. Nephron 1999; 83:53–58.

Jamin, N., Dumas, P., Moncuit, J., Friedman, W., Teillaud, J., Carr, L. G., and Williams, G. P., (1998). "Highly resolved chemical imaging of living cells by using synchrotron infrared micro spectroscopy", Applied Biological Sciences, 95(9): 4837-4840

Jackson, M., Ramjiawan, B., Hawk, M., and Mantsch, H. H., (1998). "Infrared microscopic functional group mapping and spectral clustering analysis of hypercholosterolomic rabbit liver", Cell. Mol. Biol., 44(1): 89-98.

Jenkins, Kemnitz, Tortora. (2007). Anatomy and Physiology, Wiley Inc.Textbook

John W. Hole (1993) Human anatomy and physiology, 6th edition.Wm.C.Brown Publishers, Dubuque. Textbook

Joseph W. DePierre and Manfred L. Karnovsky. Plasma Membranes of Mammalian Cells: A Review of Methods for Their Characterization and Isolation. The Journal of Cell Biology • Volume 56, 1973 • pages 275-303

Jun HS, Yoon JW. A new look at viruses in type 1 diabetes. Diabetes Metab Res Rev 2002; 19: 8–31.

Jackson, M., Ramjiawan, B., Hawk, M., and Mantsch, H. H., (1998). "Infrared microscopic functional group mapping and spectral clustering analysis of hypercholosterolomic rabbit liver", Cell. Mol. Biol., 44(1): 89-98.

Johnson T. M., Meisler M. H., Bennett M. I. and Willsky G. R. (1990) Vanadate induction of pancreatic amylase mRNA in diabetic rats. Diabetes 39: 757–762

Jun HS, Yoon JW. The role of viruses in type I diabetes: two distinct cellular and molecular pathogenic mechanisms of virus induced diabetes in animals. Diabetologia 2001; 44(3): 271-85.

Kahn C. R., White M. F., Shelson S. E., Backer J. M., Araki E., Cheatham B. et al. (1993). The insulin receptor and its substrate: molecular determinants of early events in insulin action. Recent Progress in Hormone Research 48: 291–360

Kawasaki E, Gill RG, Eisenbarth GS. Type 1 Diabetes Mellitus. Austin, TX: Landes Bioscience; 1999

Kelley D, Mintun M, Watkins S, et al. The effect of non-Insulin dependent diabetes mellitus and obesity on glucose transport and phosphorylation in skeletal muscle. J Clin Invest 1996; 97: 2705–2713.

Korkmaz, F., and Severcan, F., (2005). "Effect of progesterone on DPPC membrane: Evidence for lateral phase separation and inverse action in lipid dynamics", Arch. Biochem. Biophys. 440: 141–147.

Kanwar M, Chan PS, Kern TS, Kowluru RA. Oxidative damage in the retinal mitochondria ofdiabetic mice: possible protection by superoxide dismutase. Invest Ophthalmol Vis Sci 2007; 48:3805–3811

Kien CL and HE Ganther. Manifestations of chronic selenium deficiency in a child receiving total parenteral nutrition. American Journal of Clinical Nutrition, Vol 37, 319-328,1983

Klein R, Klein BE, Moss SE, Davis MD, DeMets DL. The Wisconsin Epidemiologic Study of Diabetic Retinopathy.IV.Diabetic macular edema. Ophthalmology 91:1464[-]474, 1984

Klapec T, Mandic ML, Grid J et al. Daily dietary intake of selenium in eastern Croatia. Sci Total Environ 1998; 217:127]136

Kinne Saffron E, Kinne R. The separation of apical from basal—lateral plasma membranes of epithelial cells: A tool to identify transport systems. Ann NYAcad SD 341:48—56, 1980

Kretzler M. Regulation of adhesive interaction between podocytes and glomerular basement membrane. Microsc Res Tech 2002; 57:247–25

Kinder, R., Ziegler, C., Wessels, J.M., (1997). "Irradiation and UV-C light induced Lipid peroxidation: A Fourier transform-infrared absorption spectroscopic study", Int. J. Radiat. Biol., 71(5): 561-571

Larsen PR, Berry MJ. Nutritional and hormonal regulation of thyroid hormone deiodinases. Annu Rev Nutr.1995; 15:323-352

Lockitch, G: Jacobson, B: Quigley, G: Dison, P: Pen dray, M. Selenium deficiency in low birth weight neonates: an unrecognized problem. J-Pediatr. 1989 May; 114(5): 865-70

Lee KU, Amano K, Yoon JW. Evidence for initial involvement of macrophages in development of insulitis in NOD mice. Diabetes 1988; 37: 989–991

Lee AY, Chung SS. Contributions of polyol pathway to oxidative stress in diabetic cataract. FASEB J 1999; 13: 23–30

Like AA, Rossini AA. Streptozotocin-induced pancreaticinitis: A new model of diabetes mellitus. Science 1976; 193: 415^{-1}7.

Lopez-Garcia, F., Villain, J., and Gomez-Fernandez, J.C., (1993). "Infrared spectroscopic studies of the interaction of diacylglycerols with phosphatidylcerol, phosphatidylserin in the presence of calcium". Biochim Biophys Acta, 1169: 264-272.

Lyman, D.J., and Murray-Wijelath, J., (1999). "Vacular graft healing: I.FTIR analysis of an implant model for studying the healing of a vascular graft". J.Biomed. Mater. Res. (Appl. Biomater.), 48; 172^{-1}86.

Liu, K.Z., Bose, R., Mantsch, H.H., (2002). "Infrared spectroscopic study of diabetic platelets", Vibrational Spectroscopy, 28: 131–136.

Mantsch, H.H., (1984). "Biological application of Fourier Transform Infrared Spectroscopy: A study of phase transitions in biomembranes". J. Mol.Strucutre, 113: 201-212

Mueller CF, Widder JD, McNally JS, et al. The role of the multidrug resistance protein^{-1} in modulation of endothelial cell oxidative stress. Circ Res 2005; 97: 637–644.

Melinda A. Beck, Orville A. Levander and Jean Handy. Selenium Deficiency and Viral Infection J. Nutr. 133: 1463S–1467S, 2003

Manoharan, R., Baraga, J.J., Rava, R.P., Dasari, R.R., Fitzmaurice, M. And Feld, M.S., (1993). "Biochemical analysis and mapping of atherosclerotic human artery using FTIR microspectroscopy". Atherosclerosis, 103:181[-1]93.

Melin, A., Perromat, A., and Deleris, G., (2000). "Pharmacologic Application of Fourier Transform IR Spectroscopy: In vivo Toxicity of Carbon tetrachloride on rat liver", Biopolymers (Biospectroscopy), 57:160[-1]68.

Mukherjee B, S Anbazhagan, a Roy, R Ghosh, M Chatterjee. Novel implications of the potential role of selenium on antioxidant status in streptozotocin-induced diabetic mice. Biomed & Pharmucothrr 1998; 52: 89-95

Mizutani M, Kern TS, Lorenzi M. Accelerated death of retinal micro vascular cells in human and experimental diabetic retinopathy. J Clin Invest 1996; 97:2883–2890

Miralpeix M., Decaux J.-F., Kahn A. and Bartrons R. (1991) Vanadate induction of L type pyrivate kinase mRNA in adult rat hepatocytes in primary culture. Diabetes 40: 462–467

Mikiya Fujieda & Keishi Naruse & Tadashi Hamauzu & Eriko Miyazaki & Yoshihiro Hayashi & Riyo Enomoto & Eibai Lee & Kazuhide Ohta & Yutaka Yamaguchi &Hiroshi Wakiguchi & Hideaki Enza. Effect of selenium-deficient diet on tubular epithelium in normal rats. Pediatr Nephrol (2007) 22:192–201

Mendelsohn, R. and Mantsch, H. H., (1986). Fourier transform infrared studies of lipid-protein interaction, Progress in Protein-Lipid Interactions, Volume 2, Elsevier Science Publishers, Netherlands, 103[-1]47.

Navarro-Alarcon M, Lopez-Ga de la Serrano H, Perez-Valero, Lopez-Martinez MC. Serum and urine selenium doses as indicators of body status in patients with diabetes mellitus. Sci Total Environ 1999b; 228:79]85

Navarro-Alarcon M, Lopez-Ga de la Serrano H, Perez-Valero, Lopez-Martinez MC. Serum selenium levels as indicators of body status in cancer patients and their relationship with other nutritional and biochemical markers. Sci Total Environ 1998; 212:195]202.

Navarro-Alarcon M, Lopez-Ga de la Serrano H, Perez-Valero, Lopez-Martinez MC. Serum and urine selenium doses in patients with cardiovascular diseases and relationship with other nutritional indexes. Ann Nutr Metab1999a; 43:30]36.

Nader Manar M., Laila A. Eissa, Nariman M. Gamil and El-Sayed M. Ammar. Effect of Nitric Oxide, Vitamin E and Selenium on streptozotocin induced Diabetic Rats. Saudi Pharmaceutical Journal, Vol. 15, No. 1, January 2007

Nepom, GT. Class II antigens and disease susceptibility. Annu Rev Med 1995; 46: 17–25.

Nihal Simsek Ozek, Yildirim Sara, Rustu Onur and Feride Severcan. Low dose simvastatin induces compositional, structural and dynamical changes in rat skeletal extensor digitorum longus muscle tissue. Biosci. Rep. (2009) Volume 29

O'Brien R. M. and Granner D. K. (1996). Regulation of gene expression by insulin. Physiol. Rev. 76: 1109–1161

Parvez I. Haris and Feride Severcan. FTIR spectroscopic characterization of protein structure in aqueous and non-aqueous media. Journal of Molecular Catalysis B: Enzymatic 7.1999. 207–221

Pagtalunan ME, Miller PL, Jumping-Eagle S, et al. Podocyte loss and progressive glomerular injury in type II diabetes. J Clin Invest 1997; 99: 342–348.

Patari A, Forsblom C, Havana M, et al. Nephrinuriain diabetic nephropathy of type 1 diabetes. Diabetes2003; 52: 2969–2974

Pavenstadt H, Kriz W, Kretzler M. Cell biology of the glomerular podocyte. Physiol Rev 2003; 83:253–307

Pietropaolo M, Barinas-Mitchell E, Kuller LH. Perspectives in diabetes heterogeneity of diabetes mellitus. Unraveling a dispute: is systemic inflammation related to islet autoimmunity? Diabetes 2007; 56: 1189–1197.

Pickup JC, Williams G. Textbook of Diabetes 2nded. Volume 1. Blackwell Science, Inc; 2002.

Pearl-Yafe M, Kaminitz A, Yolcu ES, et al. Pancreatic islets under attack: cellular and molecular effectors. Curr Pharm Des 2007; 13: 749–760.

Prasanth N. Surampudi, MD, Jennifer John-Kalarickal, MD, and Vivian A. Fonseca. Emerging Concepts in the Pathophysiology of Type 2 Diabetes Mellitus. MOUNT SINAI JOURNAL OF MEDICINE 76: 216–226, 2009

Rotruck, J.T., Pope, A.L., Ganther, H.E., Swanson, A.B., Hafeman, D.G., Hoekstra, W.G., 1973. Selenium: biochemical role as a component of glutathione peroxides. Science 179, 588- 590

Reddi, A. S. and Bollineni, J. S. Selenium deficient diet induces renal oxidative stress and injury via TGF- beta^{-1} in normal and diabetic rat's kidney. Kidney Int., 2001 59: 1342^{-1}353 Saudi Pharmaceutical

Rana, F.R., Sultany, C.M. and Blazyk, J., (1990). "Interactions between Salmonella typhimurium lipopolysaccharide and the antimicrobial peptide, magainin 2 amide", FEBS Letters, 261, 2, 464-467.

Rigas, B., Morgellot, S., Goldman, I.S., Wong, P.T.T., (1990). "Human colorectal cancers display abnormal Fourier-transform infrared spectra", Proc. Nati. Acad. Sci., 87: 8140-8144

Redondo MJ, Fain PR, Krischer P, et al. Expression of beta-cell autoimmunity does not differ between potential dizygotic twins of siblings of patients with type 1 diabetes. J Autoimmun 2004; 23: 275–279.

Seda V. Urer G.linnaz Alper. Experimental Models of Diabetes Mellitus Turk Klinik Biyokimya Derg 2004; 2(3): 127^{-1}36

Stern M. Strategies and prospects for finding insulin resistance genes. J Clin Invest 2000; 323–327

Shulman G. Cellular mechanisms of insulin resistance in humans. Am J Cardiol 1999; 83: 3J–10J

Seaquist ER, Goetz C, Rich S, Barbosa J: Familial clustering of diabetic nephropathy. N Eng J Med 320:1161^{-1}165, 1989

S. R. Stapleton Selenium: an insulin-mimetic CMLS, Cell. Mol. Life Sci. 57 (2000) 1874–1879.Bardsley JK, Want LL. Overview of diabetes. Crit Care Nurse Q 2004; 27: 106–112

Szkudelski T. The mechanism of alloxan and streptozotocin action in B cells of the rat pancreas. Physiol Res 2001; 50: 536-546.

Suri C, Jones PF, Patan S, et al. Requisite role of angiopoietin^{-1}, a ligand for the TIE2 receptor, during embryonic angiogenesis. Cell 1996; 87:1171–1180.

Spallohlz,J.E.,1994. On the nature of selenium toxicity and carcinostatic activity. Free Radic.Biol.Med.17,45-64

Stadtman TC. Selenocysteine.Annu Rev Biochem.1996;65:83[-1]00

Saleem MA, Ni L, Witherden I, et al. Colocalizationof nephrin, podocin, and the actin cytoskeleton: evidence for a role in podocyte foot process formation. Am J Pathol 2002; 161: 1459–1466?

Schrijvers BF, Flyvbjerg A, de Vriese AS. The role of vascular endothelial growth factor (VEGF) in renal pathophysiology. Kidney Int 2004; 65:2003–2017.

Severcan, F., Kaptan, N., Turan, B., (2003). "Fourier transform infrared spectroscopic studies of diabetic rat heart crude membranes", Spectroscopy, 17: 569–577 569.

Severcan, F., (1997). "Vitamin E decreases the order of the phospholipid model membranes in the gel phase: An FTIR study". Bioscience Reports, 17: 231-235.

Severcan, F., Kaptan, N., Turan, B., (2003). "Fourier transform infrared spectroscopic studies of diabetic rat heart crude membranes", Spectroscopy, 17: 569–577 569.

Severcan, F., Toyran, N., Kaptan, N. and Turan, B., (2000). "Fourier transform infrared study of diabetes on rat liver and heart tissues in the C-H region", Talanta, 53, 55-59.

Severcan, F., Yazıcı, Z., Guray, T., (1999). "Interaction of vitamin E-acetate with human erythrocyte membranes", Chem. Phys. Lipids 101:176[-1]77.

Shepherd P. R., Nave´ B. T. and Siddle K. (1995). Insulin stimulation of glycogen synthesis and glycogen synthase activity is blocked by wortmannin and rapamycin in 3T3-L1 adipocytes: evidence for the involvement of phosphoinositide-3 kinase and p70 ribosomal protein-S6 kinase. Biochem. J.305: 25–28

Stapleton S. R., Garlock G., Foellmi-Adams L., Kletzien R. F. (1997). Selenium: potent stimulator of tyrosyl phosphorylation and activator of MAP kinase. Biochem. Biophys. Acta 1355: 259–269

Stapleton S. R., Jivraj S. and Wagle A. (1998). Insulin and the insulin-mimetic selenium mediate the regulation of glucose-6- phosphate dehydrogenase gene expression via different signal proteins. FASEB J. 12: 1404

Spassov, S., Beekes M., Naumann, D., (2006). "Structural differences between TSEs strains investigated by FT-IR spectroscopy". Biochimica ET Biophysica Acta, 1760: 1138–1149.

Sills, R.H., Moore, D.J. and Mendelsohn, R., (1994). "Erythrocyte peroxidation: quantitation by Fourier transforms infrared spectroscopy". Analytical Biochemistry 218: 118^{-1}

Stapleton S.R. Selenium; An insulin-mimetic. CMLS, Cell .Mol. Life. Sci. 57 (2000) 1874^{-1}879

Stuart, B., (1997). Biological Applications of Infrared Spectroscopy. John Wiley and Sons, Ltd., England.

Stuart, B., (2004). Infrared Spectroscopy: Fundamentals and Applications. John Wiley and Sons, Ltd., England.

Schultz, C. and Naumann, D., (1991). "In vivo study of the state of order of the membranes of Gram-negative bacteria by Fourier-transform infrared spectroscopy (FT-IR)". FEBS Letters, 294, 43-46.

Stachouse S, Miller PL, Park SK, Meyer TW. Reversal glomerular hyperfiltration and renal hypertrophy by blood glucose normalization in diabetic rats. Diabetes 1990; 39:989–995

Schubert JR, Muth OH, Oldfield JE, Remmert LF. Experimental results with selenium in white muscle disease of abms and calves. Fed Proc 1961; 20: 689-692

Simonoff M, Simonoff G, editors. Le selenium ET la vie. Paris: Masson, 1991

Simonoff M, Sergeant C, Garnier N et al. Antioxidant status of selenium, vitamins A and E. and aging. In: Emerit I, Chance B, editors. Free radicals and aging. Basel: Birkhauser, 1992:3 68 - 396.

Schlienger JL, Grunenberger F, Maier EA, Simon C, Chabier G, Leroy MJF. Perturbation des oligoelements plasmatiques dans la diabetes. Relation avec lequilibre glycemique. Presse Med 1988; 17:1076]1079.

Smith, G.C.M., and Jackson, S.P., (1999). "The DNA dependant protein kinase", Genes Dev. 13, 916-934.

Szalontai, B., Nishiyama, Y., Gombos, Z., and Murata, N., (2000). "Membrane dynamics as seen by Fourier Transform Infrared Spectroscopy in a cyan bacterium, synechocystis PCC 6803. The effects of lipid unsaturation and the protein-to-lipid ratio", Biochim. Biophys. Acta, 1509; 409-419.

Simons, K., and E. Ikonen. 1997. Functional rafts in cell membranes. Nature. 387:569–572

Smith, G.C.M., and Jackson, S.P., (1999). "The DNA dependant protein kinase", Genes Dev. 13, 916

Tawardowska-Saucha K, Grzeszczak W, Lacka B, Froehlich J, Krywult D. Lipid peroxidation, antioxidant enzyme activity and trace element dose in II and III trimester of pregnancy in pregnant women with diabetes. Pol Arch MedWomen 1994; 92:313]321.

Takahashi K, Avissar JW, Cohen H. Purification and characterization of humna plasma glutathione peroxidase:a selenoglycoprotein distinct from the known cellular enzyme. Arch Biochem Biophys.1987; 256: 677-686

Takahashi, H., French, S. M., and Wong, P. T. T., (1991). "Alterations in hepatic lipids and proteins by chronic ethanol Intake: A highpressure Fourier transform Infrared spectroscopic study on alcoholic liver disease in the rat alcohol". Clin. Exp. Res., 15(2): 219-223.

Thomson, C.D., Robinson, M.F., 1996. The changing selenium status of New Zealand residents. Evr.J.Clin.Nutr.50, 107

Tsilibary EC. Microvascular basement membranes in diabetes mellitus. J Pathol 2003; 200:537–546.

Thomas JP, Maiorino M, Ursuni F, Girotti Aw. A protective action of phospholipids hydropexide glutathione peroxides against membrane-damaging lipid peroxidation: in situ reduction of phospholipids and cholesterol hydro peroxides. J Biol Chem.1990; 265:454-461

Thomas JP, Geiger PG, Maiorino M, Ursuni F, Girotti Aw. Enzymatic reduction of phospholipid and cholesterol hydro peroxides inartificial bilayers and lipoproteins. Biochim. Biophys Acta 1990: 1045: 252-276

Toyran, N., Lasch, P., Naumann, D., Turan, B., Severcan, F., (2006). "Early alterations in myocardia and vessels of the diabetic rat heart: an FTIR micro spectroscopic study", Biochem J., 397(3):427-36.

Toyran, N., and Severcan, F., (2003). "Competitive effect of vitamin D2 and Ca2+ on phospholipids model membranes: an FTIR study", Chem. Phys.Lipids, 123:165-176.

Toyran, N., Zorlu, F., Donmez, G., Oge, K., Severcan, F., (2004). "Chronic hypoperfusion alters the content and structure of proteins and lipids of rat brain homogenates: A Fourier transform infrared spectroscopy study", Eur. Biophys. J., 33: 549–554.

Toyran,N.,Turan,B.,Severcan,F.,.''Selenium alters the lipid content and protein profile of rat heart:An FTIR microspectroscopic study''.Archives of Biochemistry and Biophysics 458(2007) 184-193.

Tomlinson, K. C., Gardiner, S. M., Hebden, R. A. and Bennett, T., (1992). "Functional consequences of streptozotocin-induced diabetes mellitus, with particular reference to the cardiovascular system". Pharmacol Rev., 44:103-150.

Tsuboi, M., (1969). Application of infrared spectroscopy to structure studies of nucleic acids, Applied Spectroscopy Reviews, Dekker, New York, pp. 45–90

Ursini, F., Bindoli, A., 1987. The role of selenium peroxidasesin the protection against oxidative damage of membranes. Chem. Phys. Lipids 44, 255_ 276.

Ursuni F, Pelosi G, Tomassi G, Benassi A, Di elice M,Barsacchi R. Effect of dietary ats on hydro peroxide-induced chemiluni emission and eicosanoids release in the rat heart. Biochim Biophys Acta. 1987; 919:93-96

Ursini, F., Bindoli, A., 1987. The role of selenium peroxides in the protection against oxidative damage of membranes. Chem. Phys. Lipids 44, 255_ 276.

Varela-Calvino R, Peakman M. Enteroviruses and type 1 diabetes. Diabetes Metab Res Rev 2003; 19: 431–441

Vanderpas JB, Contempre B, Duale NL, Goossens W, Bebe N, horpe R ,Ntambue K, Dumont J, Thilly CH, Diplock AT. Iodine and selenium deficiency associated with cretinism in nortern Zaire. Am J Clin Nutr. 1990; 52: 1087 - 1093

Vendeland SC, Beilstein MA, Chen CL, kensen ON, Barofsky E, Whanger PD. Purification and properties of selenoprotein W rom rat muscle. J Biol Chem. 1993; 268: 17103-17107

Wagner L, Laczy B, Tamasko M. et al. Cigarette smoke-induced alterations in endothelial nitric oxide synthase phosphorylation: role of protein kinase C. Endothelium 2007; 14:245–255

Wells L, Hart GW. O-GlcNAc turns twenty: functional implications for post-translational modification of nuclear and cytosolic proteins with a sugar. FEBS Lett 2003; 546: 154–158

Wong, P.T.T., Wong, R.K., Caputo, T.A., Godwin, T.A., Rigas, B., (1991). "Infrared spectroscopy of exfoliated human cervical cells: Evidence of extensive structural changes during carcinogenesis", Proc. Nati. Acad. Sci., 88: 10988[-1]0992.

Wang WC, Makela AL, Nanto V, Makela P. Serum selenium levels in diabetic children. A follow-up study during selenium-enriched agricultural fertilization in Finland. Biol Trace Elem Res 1995; 47:335-364.

Wang, J., Chi, C., Lin, S., and Chern, Y., (1997). "Conformational changes in gastric carcinoma cell membrane protein correlated to cell viability after treatment with adamantyl maleimide", Anticancer Research, 17: 3473-3478.

Wendt TM, Tanji N, Guo J. et al. RAGE drives the development of glomerulosclerosis and implicates podocyte activation in the pathogenesis of diabetic nephropathy. Am J Pathol 2003; 162: 1123–1137?

Wolf G, Ziyadeh FN. Cellular and molecular mechanisms of proteinuria in diabetic nephropathy. Nephron Physiol 2007; 106:26–31.

Wolf G, Chen S, Ziyadeh FN. From the periphery of the glomerular capillary wall toward the center of disease: podocyte injury comes of age in diabetic nephropathy. Diabetes 2005; 54: 1626–1634

Wilson DS, Tappel AL .Subcellular fate of selenium from 75 S- labeled plasma selenoprotein P in selenium deficient dier. J Nutr Biochem.1993: 4:208-211

Yard BA, Kahlert S, Engelleiter R. et al. Decreased glomerular expression of agrin in diabetic nephropathy and podocytes, cultured in high glucose medium. Exp Nephrol 2001; 9:214–222

Yang, I.-G., Morrison-Plummer, J., Burk, R. F. 1987. l. Biol. Chern. 262: 13372-75

Yang,G.,Wang,S.,Zhou,R.,Sun,S.,1983. Endemic selenium intoxication of humans in China. Am.J.Clin.Nutr.37,872-881

Yilmaz O., Celik S., Cay M. and Naziroglu lu, M. (1997). Protective role of intraperitoneally administered vitamin E and selenium on the level of total lipid, total cholesterol and fatty acid composition of muscle and liver tissues in rats. J.Cell Biochem., 64, 233-241.

Yoon JW, Jun HS. Cellular and molecular pathogenic mechanisms of insulin-dependent diabetes mellitus. Ann N Y Acad Sci 2001; 928: 200–211

Zwaal R.F.A., A.J. Schroit, Pathophysiologic implications of membrane phospholipids asymmetry in blood cells, Blood 89 (1997) 1121.132